REMARKS

Claims 1-27 are pending in this case. Applicants note that there appears to be some confusion about the current claim set, as both original claims (claims 1-27) and claims submitted as "Amended Sheets" (claims 1-23) were provided at filing.[1] Because these claims differ beginning at claim 21, Applicants have canceled claims 21-27; the subject matter of claim 27 has been resubmitted as new claim 28.

The Office action is based on original claims 1-27. Of these, claim 27 stands rejected under 35 U.S.C. § 101. Claims 1-10 and 17-20 stand rejected under 35 U.S.C. § 102. And claims 1-27 stand rejected under 35 U.S.C. § 112, first and second paragraphs. In addition, claims 1-27 stand objected to because of formalities, and the Office has requested new inventor declarations. Each of these issues is addressed below.

Amendments

Claims 1-20 have been amended to correct formalities and for the purpose of clarification; support for these amendments is found within the original claims. Claim 28 has been newly added; this new claim finds support, for example, in original claim 27 and in the specification at page 24, lines 14-35.

In addition, the specification has been amended, at page 1, to provide Applicants' cross-reference to related priority applications. Foreign priority to International Application PCT/EP99/04288 (filed June 21, 1999) and its German parent application DE 198 27 457.2 (filed June 19, 1998) were recognized by the Office in the Form PCT/DO/EO/905 mailed July 13, 2001.[2]

---

[1] Applicants note that the Office has based the Office action on original claims 1-27. However, Applicants' Preliminary Amendment submitted with the application is based on claims 1-23.

[2] Due to what appears to be a Patent Office clerical error, the June 19, 1998 German priority date was later omitted in Form PCT/DO/EO/903 mailed July 2, 2002.

Priority Documents

The Office Action Summary indicates that acknowledgment of Applicants' claim to foreign priority under 35 U.S.C. § 119 has been made. The Summary, however, goes on to indicate both that (i) "None of" the certified copies of priority documents have been received by the Office and also that (ii) "Copies of the certified copies of the priority documents *have been received* in this National Stage application from the International Bureau (PCT Rule 17.2(a))." Applicants request clarification on this issue.

Oath Declaration

The Office has asserted that the declaration submitted October 15, 2001 is defective because the address of inventor Michael Hallek and the address and citizenship of inventor Anne Girod have been altered without initials or an indication of the date of alteration. These errors are regretted. A new declaration has been executed by these inventors and is submitted herewith.

Claim Objections

Claims 1-27 have been objected to as being informal for failing to begin with an article. These claims have been amended; all now begin with an article, and this objection may be withdrawn.

Rejection under 35 U.S.C. § 101

Claim 27 stands rejected under 35 U.S.C. § 101 because, according to the Office, the claim sets forth a use without setting forth any steps involved in the process. Claim 27 has been canceled, but the subject matter of this claim is now presented in new claim 28. Claim 28 sets forth the steps involved in altering the tropism of AAV, and this rejection may now be withdrawn.

Rejection under 35 U.S.C. § 102

Claims 1-10 and 17-20 stand rejected under 35 U.S.C. § 102 as being anticipated by Mamounas et al. (WO 97/38723). This rejection is respectfully traversed.

Independent claim 1 (from which claims 2-10 depend) recites:

> 1. A structural protein of adeno-associated virus (AAV), which comprises at least one mutation, *wherein the mutated structural protein is capable of particle formation*, and the mutation brings about an increase in the infectivity of the virus.

The other rejected claims, claims 17-20, specify an AAV particle which includes this mutated structural protein (claim 17), a nucleic acid which encodes the mutated structural protein (claim 18), a cell which includes the mutated structural protein-encoding nucleic acid (claim 19), and a process for the preparation of the mutated structural protein (claim 20). All of these claims therefore require a structural protein (or its coding sequence) that is mutated and that "is capable of [AAV] particle formation." Nowhere is this element of the claims disclosed by Mamounas.

The Office points to page 3, lines 9-15, page 4, lines 21-31, page 17, line 30 – page 19, line 10, and page 43, lines 28-30, as describing Applicants' claimed invention, but none of these passages discloses the successful production of a mutated AAV structural protein capable of supporting viral particle formation. The Office also cites a passage at page 67, lines 24-26. But this passage describes an scFv construct that Mamounas indicates at page 68, lines 13-14, "failed to produce any intact viral particles." It is these same structural proteins incapable of viral particle formation that are discussed at the final passage cited by the Office at page 69, lines 15-26 and Table 3.

Contrary to the Office's assertion, therefore, Mamounas does not disclose a presently claimed mutant structural protein capable of supporting viral particle formation. Neither does Mamounas provide any hint as to how production of such a mutated structural protein could be achieved. The subject matter of the present claims is clearly

novel over Mamounas, and this rejection may be withdrawn.

Rejections under 35 U.S.C. § 112, second paragraph

Claims 1-27 stand further rejected under 35 U.S.C. § 112, second paragraph, as being indefinite. This rejection has been overcome as follows.

Claims 1-27 have been asserted to be vague for reciting the structural protein "characterized by." This term has been replaced in all claims, and the rejection may be withdrawn.

Claim 1 is rejected on the basis that it recites the limitation "the virus" without sufficient antecedent basis. The claim has been amended to overcome this rejection.

Claim 2 is asserted to be unclear for reciting that the structural protein mutation is located on the virus surface. The Office requests that the claim be clarified as to whether the mutated structural protein coincidentally resides on the viral surface or whether the mutation must reside in a surface-exposed structural protein domain. The claim has been amended to specify that the mutation is in a surface-located region of the structural protein, and this basis for the rejection may be withdrawn. Claim 2 has also been amended to overcome the rejection related to antecedent basis.

Claim 3 stands rejected for reciting that a mutation is "located at the N terminus of the structural protein." This basis for the rejection is respectfully traversed. Those of skill in the art readily understand the term "N-terminus," which is used routinely by molecular biologists and has a well accepted meaning in the art. Indeed, the Office, in connection with the § 102 rejection discussed above, states (page 3; emphasis added):

> For example, VP-1, VP-2, and VP-3 were incorporated at their *N-terminus* with C4 (see e.g. page 43, lines 28-30) or were mutated to incorporate a single-chain fragment variable region of a monoclonal antibody against the CD34 molecule (sFv) at their *N-terminus* (see e.g. page 67, line 24-26).

Clearly, the Office as well recognizes this term's well-accepted meaning, and this basis

for the rejection should be withdrawn.

Claim 7 stands rejected as indefinite based on the recitation of the term "derived from." This term has been removed from the claim.

Claim 8 is asserted to be unclear based on the term "one or more deletions (insertions)" as the claim does not denote what is being deleted or inserted. The claim has been amended to specify that it is "amino acids" that are being deleted or inserted. Claim 8 has also been amended, as suggested by the Examiner, to recite "these mutations."

Claims 10-16 stand rejected on the basis that each includes a term that lacks antecedent basis. These claims have been amended to overcome these rejections.

Claim 17 has been rejected as being unclear in its recitation of a structural protein in the form of an AAV particle. This rejection is respectfully traversed because it would be clear to one skilled in the art that the claim covers a mutated structural protein having all of the characteristics set forth in claim 1 and in addition being present in a viral particle. This rejection may be withdrawn.

Claims 18-27 stand rejected based on their recitation of "according to." Claims 20-27 have been canceled, and the rejection as applied to these claims is moot. Claims 18-19 have been amended to remove this term. This basis for the rejection may be withdrawn.

Claim 20 has been further rejected based on the term "where appropriate, the expressed structural protein is isolated." This claim has been amended to remove the term "where appropriate," and this rejection may be withdrawn.

Claim 27 also stands rejected on the basis that the method is unclear because the claim fails to set forth the method steps. Claim 27 has been canceled, but the subject matter of this claim is now presented in new claim 28, which includes method steps. This final basis for the indefiniteness rejection may be withdrawn.

Rejections under 35 U.S.C. § 112, first paragraph

Claims 21-26 stand rejected under 35 U.S.C. § 112, first paragraph as lacking enablement. These claims have been canceled and will be pursued in a divisional application. For the record, Applicants do not agree with this rejection but wish to address it in a separately filed case.

Claims 1-27 also stand rejected under 35 U.S.C. § 112, first paragraph as lacking an adequate written description. This rejection is respectfully traversed.

As an initial matter, Applicants point out that this rejection is based on the statement in the Office action that (page 11):

> Applicants claim a genus of structural proteins with at least one mutation that is capable of particles formation that results in the increased infectivity of virus containing the mutated structural protein.

This, however, fairly characterizes the language of claim 1 only. The Office has supplied no explanation for why or how this rejection is being applied to the remaining claims, and withdrawal of the written description rejection as applied to claims 2-20 is therefore requested.

As applied to claim 1, the rejection is also traversed because the bases for the rejection are in error.[3] Applicants' claims cover AAV structural proteins that have been mutated to increase viral infectivity, while leaving intact the protein's ability to facilitate viral particle formation.

Contrary to the assertion in the Office action, production of such a mutated structural protein is not an "empirical" process, but rather is based on sound scientific methodologies set forth in Applicants' specification. As indicated by Applicants, selection of an AAV mutation site may be determined by structure and protein alignments of different parvoviruses, such as AAV2, CPV, and B19, as discovered by Applicants and as set forth in Applicants' specification at page 5, line 32 et al. and page 6, line 23 et al.

At these mutation sites, insertions may be made to target the virus to particular cell types. The insertion sequences chosen, far from being empirical, are typically sequences such as ligands known to target a cell type of interest. A number of preferred insertion sequences are provided by Applicants at page 8, line 4 – page 10, line 22.

Applicants demonstrate the effectiveness of this strategy using the P1 ligand as an exemplary targeting insertion. The P1 ligand was selected due to the presence of the RGD motif, a motif responsible for binding to the integrin receptor (see page 9, lines 32-34). This ligand was chosen because of its known cell targeting specificity. In the specification, for example, at Tables 1 and 2, Applicants demonstrate that mutated structural proteins that include the exemplary P1 ligand insertion (in either VP1 or VP3) support viral particle formation; this is shown unambiguously by the data in the columns denoted "Capsid titers," where ELISAs are performed using the antibody A20Mab, an antibody that *only* recognizes assembled viral capsids (as evidenced by the accompanying publication by Wistuba et al., J. Virol. 71:1341-1352, 1997, Appendix A). Similarly, at page 28, Applicants describe additional VP3 insertions of an unrelated sequence, the Z34C domain of protein A. The Office bases the present written description rejection, in part, on the assertion that, with respect to this VP3 insertion mutant, "no indication is given about the ability of the structural protein to form particles or the infectivity of a virus containing the mutated structural protein." In response to this rejection, Applicants submit, as Appendix B, Ried et al. (J. Virol. 76:4559-4566, 2002), a publication from the present inventors. This publication demonstrates that, like Applicants' other exemplary structural protein insertions, this AAV structural protein mutant does in fact support formation of viral particles and facilitates re-targeting of cell infectivity (see, e.g. the abstract).

In like manner, other AAV insertion mutations according to Applicants' claims have been successfully made. The accompanying publications by Grifman et al. (Mol.

[3] Applicants' arguments regarding claim 1 apply with equal force to the remaining claims 2-20 and 28.

Therapy 3:964-975, 2001, Appendix C) and Nicklin et al. (Mol. Therapy 4: 174-181, 2001, Abstract, Appendix D) demonstrate that ligands other than P1 can be inserted into AAV structural proteins, and result in mutated proteins that support viral particle formation and re-targeting of infectivity. In view of this evidence, it is clear that a number of mutant AAV structural proteins falling under Applicants' claims can be – and indeed have been – generated. This fact demonstrates that, contrary to the Office's asserted basis for the written description rejection, the production of such structural protein mutants is neither empirical nor unpredictable. Moreover, again contrary to the Office's assertion, Applicants have disclosed not one, but many, species falling under the present claims. These species differ in the structural protein mutated, the mutation site, and the ligand used to accomplish re-targeting of infectivity. A genus claim is appropriate in the present case, and Applicants request reconsideration on this issue.

CONCLUSION

Applicant submits that the claims are now in condition for allowance, and such action is respectfully requested.

Enclosed are a Petition to extend the period for replying to the Office action for one month, to and including February 17, 2004 (as February 16th is a national holiday), and a check in payment of the required extension fee.

If there are any additional charges or any credits, please apply them to Deposit Account No. 03-2095.

Respectfully submitted,

Date: 17 February 2004

Karen L. Elbing, Ph.D.
Reg. No. 35,238

Clark & Elbing LLP
101 Federal Street
Boston, MA 02110
Telephone: 617-428-0200
Facsimile: 617-428-7045

APPENDIX A

JOURNAL OF VIROLOGY, Feb. 1997, p. 1341–1352 Vol. 71, No. 2
0022-538X/97/$04.00+0

Subcellular Compartmentalization of Adeno-Associated Virus Type 2 Assembly

ANDREAS WISTUBA, ANDREA KERN, STEFAN WEGER, DIRK GRIMM, AND JÜRGEN A. KLEINSCHMIDT*

Deutsches Krebsforschungszentrum, Forschungsschwerpunkt Angewandte Tumorvirologie, D-69120 Heidelberg, Germany

Received 12 July 1996/Accepted 28 October 1996

Using immunofluorescence and in situ hybridization techniques, we studied the intracellular localization of adeno-associated virus type 2 (AAV-2) Rep proteins, VP proteins, and DNA during the course of an AAV-2/adenovirus type 2 coinfection. In an early stage, the Rep proteins showed a punctate distribution pattern over the nuclei of infected cells, reminiscent of replication foci. At this stage, no capsid proteins were detectable. At later stages, the Rep proteins were distributed more homogeneously over the nuclear interior and finally became redistributed into clusters slightly enriched at the nuclear periphery. During an intermediate stage, they also appeared at an interior part of the nucleolus for a short period, whereas most of the time the nucleoli were Rep negative. AAV-2 DNA colocalized with the Rep proteins. All three capsid proteins were strongly enriched in the nucleolus in a transient stage of infection, when the Rep proteins homogeneously filled the nucleoplasm. Thereafter, they became distributed over the whole nucleus and colocalized in nucleoplasmic clusters with the Rep proteins and AAV-2 DNA. While VP1 and VP2 strongly accumulated in the nucleus, VP3 was almost equally distributed between the nucleus and cytoplasm. Capsids, visualized by a conformation-specific antibody, were first detectable in the nucleoli and then spread over the whole nucleoplasm. This suggests that nucleolar components are involved in initiation of capsid assembly whereas DNA packaging occurs in the nucleoplasm. Expression of a transfected full-length AAV-2 genome followed by adenovirus infection showed all stages of an AAV-2/adenovirus coinfection, whereas after expression of the cap gene alone, capsids were restricted to the nucleoli and did not follow the nuclear redistribution observed in the presence of the whole AAV-2 genome. Coexpression of Rep proteins released the restriction of capsids to the nucleolus, suggesting that the Rep proteins are involved in nuclear redistribution of AAV capsids during viral infection. Capsid formation was dependent on the concentration of expressed capsid protein.

The nucleus, commonly referred to as the control center of the eucaryotic cell, is highly organized into subcompartments to perform a number of essential functions such as DNA replication, RNA transcription, processing, and transport (6, 13, 58, 68). Development of protein and nucleic acid localization techniques allowed the visualization of many nuclear components and processes at discrete subnuclear sites, which suggests that they are part of an underlying structure involved in the functional organisation of the nucleus. These structures are highly dynamic and change in the cell cycle as a function of cellular activity (36, 39, 40, 43, 44, 54). Viral infections often are associated not only with a functional reprogramming of host cell gene expression but also with a reorganization of the cellular architecture, in particular of the nucleus (4, 9, 10, 14, 19, 20, 46, 56, 59, 64). Although several viral components possibly involved in formation and reorganization of this nuclear architecture are being investigated, they still are not well understood.

The life cycle of the adeno-associated virus (AAV) strongly depends on helper virus functions provided by either adenovirus or herpesvirus families (for reviews, see references 8 and 41). These helper viruses themselves show a profound influence on the host cells and a characteristic subcellular compartmentalization of viral products during infection (10, 46, 47, 49, 66). Coinfection of AAV-2 with adenovirus leads to induction of AAV-2 gene expression and to changes of the cellular milieu which are necessary for replication and production of infectious virus (3, 7, 11, 12, 15, 16, 31, 51). Accumulation of viral transcripts is controlled by a set of nonstructural AAV-2 proteins which are also required for DNA replication (5, 35, 38, 63). They are encoded by an overlapping reading frame located on the left half of the AAV-2 genome and are transcribed from either the p5 or the p19 promoter at map units 5 and 19, respectively. The transcripts from both promoters are translated from spliced and unspliced mRNAs, resulting in four proteins designated Rep78, Rep68, Rep52 and Rep40 according to their apparent molecular weight. Rep78 and Rep68 play key roles in AAV DNA replication (25, 62) by binding to the inverted terminal repeats and catalyzing the terminal resolution reaction (2, 29, 57). Several influences of these proteins on AAV gene expression have been documented, without delineating a comprehensive model for AAV gene regulation by these proteins (5, 27, 34, 35, 38, 63). Mutations that prevent the synthesis of the small Rep proteins Rep52 and Rep40 lead to a strongly reduced level of single-stranded DNA (ssDNA) accumulation, suggesting that they play a role in DNA packaging (17, 26). The AAV cap gene located in the right half of the AAV genome codes for three capsid proteins, VP1, VP2, and VP3, which are present in the virion in a 1:1:10 stoichiometry (32, 33, 52). Pulse-chase experiments support the view that the single-stranded AAV genomes are packaged into preformed capsids (42). In a time course of AAV-2/adenovirus type 2 coinfection, the synthesis of Rep and Cap proteins follows similar kinetics, reaching a maximum level around 20 h postin-

* Corresponding author. Mailing address: Deutsches Krebsforschungszentrum, Forschungsschwerpunkt Angewandte Tumorvirologie, Abteilung Tumorvirologie, Im Neuenheimer Feld 242, D-69120 Heidelberg, Germany. Phone: 49-6221-424978. Fax: 49-6221-424962. E-mail: j.kleinschmidt@dkfz-heidelberg.de.

fection together with bulk duplex DNA synthesis, whereas maximum ssDNA accumulation appears to occur about 4 h later (50). Immunoprecipitation experiments showed that Rep proteins were detected in complexes with capsid proteins possibly representing intermediates of the AAV-2 DNA packaging process (48, 67). The observation that the four Rep proteins colocalize in intranuclear centers together with the capsid proteins (28) was interpreted in terms of replication and packaging centers of AAV-2 DNA. Recently, it could be shown by in situ hybridization that AAV-2 DNA and Rep proteins colocalize with adenovirus DNA in common foci, which were interpreted as replication centers (65).

In this study, the dynamics of the subcellular distribution of AAV proteins, capsids, and DNA was monitored over the time course of an AAV-2/adenovirus type 2 coinfection to define the possible sites of AAV capsid assembly and DNA packaging. In early phases of infection, Rep proteins and AAV DNA are colocalized in typical replication centers, but at that time no capsid proteins were detectable, showing that these centers are not the sites of DNA packaging. By using a conformation-specific capsid antibody, it was possible to show that capsids accumulated first in the nucleoli and later also in intranuclear areas outside the nucleoli. Rep proteins and AAV DNA also colocalized in these extranucleolar zones, suggesting that DNA packaging could occur at these sites. DNA and Rep could hardly be detected in the nucleoli. Free capsid proteins, capsids, and Rep proteins underwent a number of redistributions during later stages of infection and showed mainly a separate nuclear localization. Expression of the *cap* and *rep* genes by transient transfection showed that capsid formation was strongly dependent on capsid protein concentration and that the Rep proteins have an influence on the subnuclear compartmentalization of AAV capsids.

MATERIALS AND METHODS

Cell culture and virus infections. HeLa cells were grown in Dulbecco's modified Eagle's medium (DMEM) supplemented with 10% fetal calf serum and penicillin-streptomycin at 37°C and 5% CO_2. For generation of AAV-2, cells were grown to 80% confluency, the medium was removed, and the cells were incubated with AAV-2 (multiplicity of infection [MOI] = 20) and adenovirus type 2 (MOI = 2) for 2 h in 2 to 3 ml of DMEM per 175-cm^2 flask. After the incubation period, DMEM was added and the cells were incubated at 37°C and 5% CO_2 for 3 days. Then the flasks containing cells and medium were frozen and thawed three times at −70 and 37°C, respectively. Debris was removed by centrifugation at 5,000 × g_{av}, and the clear supernatant was collected. Adenovirus was inactivated by heating to 56°C for 30 min. For generation of adenovirus stocks, HeLa cells were infected solely with adenovirus (MOI = 2) and supernatants were harvested as described above. AAV and adenovirus stocks were subjected to titer determination by immunofluorescence staining of cells which had been infected for 3 days either with serial dilutions of AAV to which adenovirus was added at an MOI of 2 or serial dilutions of adenovirus alone. Cells were grown to 70% confluency in 96-well plates prior to infection. AAV infections were monitored with monoclonal antibody 76/3 (67), which reacts with the nonspliced Rep proteins of AAV, and adenovirus infections were monitored with monoclonal antibody A30 (see below). Immunofluorescence staining was performed as described below, except that cells in 96-well plates were fixed with methanol alone before the staining procedure. The titers were calculated from the average numbers of fluorescence-positive cells infected with limiting dilutions of virus stocks.

For analysis of different stages of infection by immunofluorescence staining, cells were grown on coverslips and were infected in 10-cm petri dishes for 2 h in 1 ml of medium with the same MOIs as described for the preparation of virus stocks. After infection, 9 ml of medium was added and the dishes were incubated at 37°C and 5% CO_2 for the time intervals indicated at the respective experiments. Transfections of HeLa cells were performed in 10-cm petri dishes by following published protocols (18).

Plasmids. The plasmid containing the full-length AAV2 genome (pTAV-2) was derived from pAV-2 (37) as described previously (24). Plasmids designated pCMV-Rep78, pCMV-Rep68, pCMV-Rep52, and pCMV-Rep40 are identical to the respective plasmids pKEX-Rep78, pKEX-Rep68, pKEX-Rep52, and pKEX-Rep40 described elsewhere (27). The cap gene expression plasmid (pCMV-VP) was generated by insertion of a 650-bp *Bam*HI human cytomegalovirus (CMV) promoter fragment from pHCMV-Luci (kindly provided by K. Butz, German Cancer Research Center, Heidelberg, Germany) into the *Bam*HI site of BluescriptII SK+ (Stratagene) and ligation of the *Fsp*I-*Sna*BI cap gene fragment from pTAV-2 into the *Sma*I site of the same plasmid. pHCMV-Luci was constructed by cloning the *Hin*cII-*Ava*II fragment of the CMV promoter into the *Sma*I site of pUC19. An *Eco*RI-*Hin*dIII fragment containing the CMV promoter was subcloned into the *Eco*RI-*Hin*dIII site of plasmid pBL (21).

Gel electrophoresis, immunoblotting, and immunoprecipitation. Protein samples were analyzed on 15% polyacrylamide gels in the presence of sodium dodecyl sulfate (SDS-PAGE) (61). Total-cell lysates were prepared by sonification of cells in protein sample buffer followed by heating to 100°C for 5 min. For immunoblotting, proteins were electrophoretically transferred to nitrocellulose membranes by using a semidry blotting equipment and stained with Ponceau S. Incubations with monoclonal antibodies or polyclonal antisera were performed by following published protocols (23). Rep and Cap proteins were visualized by alkaline phosphatase-coupled secondary antibodies as described in standard protocols (23) or by peroxidase-coupled secondary antibodies and enhanced chemoluminescence detection (Amersham, Little Chalfont, United Kingdom), as described by the supplier.

For immunoprecipitation experiments, either sucrose gradient fractions from soluble nuclear extracts (500 μl) (67), purified, nonassembled, baculovirus-expressed capsid proteins (14 μl, 100 μg/ml) (60), AAV virus stock (100 μl of 10^9 IU/ml), or purified recombinant VP2/VP3-containing virus-like particles (28 μl, 50 μg/ml) (53) were incubated overnight at 4°C in the presence of 0.5% Nonidet P-40 (NP-40) with 200 μl of hybridoma supernatant of monoclonal antibody A1, A69, B1, or A20 (see below) or 2 μl of a polyclonal capsid protein antiserum raised in a rabbit (VP-S) (53). For control precipitations, we used monoclonal antibody IVA7 (see below), which is directed against the 33-kDa protein of *Onchocerca volvulus*. After this incubation, 2 μl of affinity-purified polyclonal goat anti-mouse immunoglobulins was added to the samples with the monoclonal antibodies as a sandwich for binding to protein A, and the mixtures were incubated for 1 h. To remove nonspecific protein precipitates, the samples were centrifuged for 5 min at 17,600 × g_{av} at 4°C. The immune complexes were precipitated by addition of 30 μl of protein A-Sepharose (10% [wt/vol] in NETN buffer, where NETN buffer consists of 0.1 M NaCl, 1 mM EDTA, 20 mM Tris/HCl [pH 7.5], and 0.5% NP-40). The samples were agitated for 1 h, and the Sepharose beads were washed three times with 1 ml of NETN buffer, boiled in protein-loading buffer, and analyzed by SDS-PAGE and Western blotting. All incubations were done at 4°C. For immunoprecipitation of metabolically labeled proteins, 5 × 10^5 cells were infected as described above either with AAV-2 and adenovirus type 2 or with adenovirus alone. After 20-h, the cells were incubated for 1 h in DMEM free of methionine and cystine and then for 3 h in the same medium containing 100 μCi of ^{35}S-translabeling mix (ICN Biochemicals). The cells were washed twice with phosphate-buffered saline (PBS; 18 mM Na_2HPO_4, 10 mM KH_2PO_4, 125 mM NaCl [pH 7.2]) and lysed directly in the dish with 1 ml of RIPA buffer (150 mM NaCl, 1% NP-40, 0.5% deoxycholate, 0.1% SDS, 50 mM Tris/HCl [pH 8.0]) for 15 min at 4°C. The lysates were centrifuged for 15 minutes at 17,600 × g_{av} at 4°C, and the supernatants were immunoprecipitated as described above.

Generation of monoclonal antibodies. Monoclonal antibodies against AAV-2 capsid proteins (A1, A69, B1, and A20), replication proteins (76/3), and an adenovirus protein (A30) were generated as described previously (67). The nucleolus-specific antibodies were obtained commercially (Paesel & Lorei, Hanau, Germany), and antibody IVA7, directed against the 33-kDa protein of *O. volvulus*, was kindly provided by R. Lucius, University of Heidelberg.

Immunofluorescent staining. Cells were grown on coverslips and were transfected and infected as described above. Before fixation, the cells were washed for 5 min in PBS and fixed in methanol (5 min at 4°C) and then in acetone (5 min at 4°C). Then the coverslips were air dried and either stored dry at −20°C or used directly for immunofluorescence staining. Alternatively, cells were fixed in 2% paraformaldehyde (PFA) in PBS for 20 min. After incubation in PFA, the coverslips were incubated for 3 min in 50 mM $(NH)_4Cl$ in PBS and for 5 min in 0.5% Triton X-100 in PBS. Then they were washed in PBS. All steps of the PFA fixation were performed at room temperature. PFA-fixed cells were directly used without air drying for immunofluorescence staining. The first antibody was applied to the coverslips for 1 h at 20°C or 15 h at 4°C in a moist chamber. Hybridoma supernatants were applied undiluted, and polyclonal antisera were diluted 1:50 in PBS containing 1% bovine serum albumin (BSA) prior to application. After incubation with the first antibody, the samples were washed three times in PBS for 5 min each at 20°C. The samples were incubated for 1 h at 20°C with either fluorescein- or rhodamine-coupled anti-mouse or anti-rabbit secondary antibodies (Dianova, Hamburg, Germany) diluted 1:50 or 1:100 in PBS–1% BSA. After incubation, the samples were washed as described above and then given short rinses in distilled water and in 100% ethanol. Then the coverslips were air dried, embedded in Elvanol, visualized, and photographed with a Leitz Dialux 22-Microscope, using Kodak T-Max 400 films. For counting fluorescence-positive cells, 5 to 10 randomly chosen image fields each displaying between 100 and 400 cells were evaluated.

Fluorescent in situ hybridization. Coverslips with adherent cells were washed three times in PBS and fixed with 4% PFA in PBS for 20 min. Then the cells were permeabilized by incubation for 20 min in PBS containing 0.5% (vol/vol) Triton X-100 and 0.5% (vol/vol) saponin. After permeabilization, they were washed again in PBS three times, placed in 0.1 M HCl for 5 min, and incubated for 30

minutes at room temperature in PBS containing 20% glycerol. Then the samples were immersed in liquid nitrogen for 2 min and thawed slowly at room temperature. This freeze-thaw step was repeated three times. The coverslips were either stored at −70°C or directly used for in situ hybridization. A *ClaI-BsaI* fragment of pTAV-2 which covers the first 286 nontranscribed nucleotides of AAV was used for in situ hybridization. It was labeled with Bio-16 dCTP (Sigma, Munich, Germany) by using Ready-To-Go DNA-labeling beads (Pharmacia, Uppsala, Sweden) as specified by the manufacturers. The hybridization mixture was prepared by dissolving 36 ng of the labeled fragment and 8 μg of competitor tRNA in 4 μl of formamide per coverslip. The probe was denatured via incubation at 70°C for 10 min and immediately chilled on ice. Then dextran sulfate and 10× SSC (1.5 M NaCl plus 0.15 M sodium citrate [pH 7.0]) were added to final concentrations of 4 ng of labeled probe per ml, 1 μg of tRNA per μl 2× SSC, 10% dextran sulfate, and 50% formamide. Prior to hybridization, the frozen samples were thawed and washed twice with 2× SSC, incubated with 2× SSC (in 50% formamide) at 90°C for 10 min and washed with ice-cold 2× SSC. Then the samples were incubated with the hybridization mixture for 1 h at 37°C in a moist chamber. After hybridization, they were successively washed in 2× SSC (in 50% formamide) for 15 min at 37°C, 2× SSC for 30 min at room temperature, and 1× SSC for 15 min at room temperature. The coverslips were then rinsed in buffer W (20 mM HEPES [pH 7.2], 150 mM KCl, 0.05% Tween 20) and incubated with fluorescein isothiocyanate-coupled ExtrAvidin (Sigma) for 15 h at 4°C (2 μg of ExtrAvidin per ml in 20 mM HEPES [pH 7.2]–250 mM KCl–0.5 mM dithiothreitol–1% BSA). After two washing steps in buffer W (5 min at 20°C each), the samples were immunolabeled for double staining as described above.

Preparation of AAV proteins and particles. Recombinant AAV proteins and VP2/VP3 particles were prepared by infection of SF9 cells with recombinant baculoviruses expressing VP1, VP2, and VP3 (53, 60). For preparation of AAV-2 capsids for electron microscopy, 5×10^7 HeLa cells were transfected with pCMV-VP, infected with adenovirus (MOI = 10), harvested, and sedimented by centrifugation for 5 min at 200 × g_{av} and 4°C. The pellet was resuspended in 50 ml of PBS and centrifuged again for 5 min at 200 × g_{av} and 4°C. The supernatant was discarded, and the pellet was resuspended in 1 ml of PBS containing 1 mM phenylmethylsulfonyl fluoride, 1 μg of pepstatin per ml, and 3 μg of leupeptin per ml and sonified three times for 10 s on ice (Branson sonifier, level 4). The extract was centrifuged (16,500 × g_{av} for 10 min at 4°C), and the pellet was resuspended in 1 ml of digestion buffer (150 mM NaCl, 50 mM Tris/HCl [pH 8.0], 1 mM EDTA, 5 mM $MgCl_2$). DNase and RNase were added to final concentrations of 50 and 25 μg/ml, respectively, and the extracts were incubated for 3 h at 12°C. After digestion, NaCl was added to a final concentration of 0.5 M. Dithiothreitol and EDTA were added to final concentrations of 10 and 2 mM, respectively. Then the samples were sonified again three times for 10 s each and subjected to agitation for 30 min at room temperature. After the agitation, the extracts were centrifuged for 20 min at 3,500 × g_{av} and 4°C. The supernatant was loaded onto a two-step sucrose cushion, with the lower layer consisting of 200 μl of 50% sucrose in TE buffer (10 mM Tris [pH 7.5], 1 mM EDTA) and the upper layer consisting of 200 μl of 30% sucrose in TE, and the extracts were centrifuged for 2.5 h at 42,000 rpm and 4°C in a Beckman TLS55 rotor. The pellet was resuspended in 300 μl of TE buffer with 0.1 M NaCl and incubated at room temperature for 30 min. Then the samples were centrifuged for 1.5 h at 80,000 rpm and 4°C in a Beckman TLA100.3 rotor, and the sediment was resuspended in 200 μl of 0.3 M NaCl in TE buffer and subjected by agitation for 15 h at 4°C. The samples were cleared by centrifugation for 10 min at 16,500 × g_{av} and 4°C, and the supernatant was stained for electron microscopy with 2% uranyl acetate and examined in a Zeiss EM 10 electron microscope.

RESULTS

Characterization of AAV-2 capsid protein antibodies. To study the intracellular localization of AAV-2 capsid proteins in comparison to the localization of Rep proteins and AAV-2 DNA during AAV-2/adenovirus type 2 coinfections, we raised a number of monoclonal antibodies directed against AAV-2 capsid proteins. Western blot analysis of extracts of AAV-2/adenovirus type 2-infected HeLa cells showed that the hybridoma clone A1 produced antibodies which specifically recognize VP1, antibodies of clone A69 recognize VP1 and VP2, and antibodies of clone B1 react with all three capsid proteins (Fig. 1). The immunoreactive polypeptides exactly comigrated with polypeptides detected with a polyclonal capsid protein antiserum (Fig. 1, VP-S) (53). None of the antibodies tested showed cross-reaction with proteins extracted from HeLa cells infected with adenovirus alone under the conditions tested. Antibodies of clone A20 did not react with capsid proteins in Western blot analyses. Based on the overlapping reading frames of VP1, VP2, and VP3 in the AAV-2 cap gene, these findings indicate that A1 detects an epitope within N-terminal

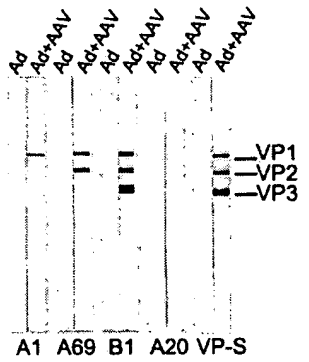

FIG. 1. Immunoblot analysis of monoclonal antibodies raised against AAV capsid proteins. Extracts of HeLa cells infected with adenovirus type 2 (Ad) or AAV-2 plus adenovirus type 2 (AAV+AD) were prepared 24 h postinfection, separated by SDS-PAGE, and blotted. Monoclonal antibodies A1, A69, B1, and A20 were applied to these Western blots and compared with a polyclonal antiserum (VP-S) described previously (53). The antibody reaction was visualized by reaction with an alkaline phosphatase-coupled secondary antibody. Note that A20 does not detect AAV proteins after SDS-PAGE.

amino acids 1 to 137 of VP1, A69 detects an epitope between amino acids 138 and 203 of VP1, corresponding to amino acids 1 to 65 of VP2, and B1 detects an epitope of the VP3 sequence which completely overlaps with VP1 and VP2.

To investigate the specificity of the antibodies toward nondenatured proteins, we immunoprecipitated capsid proteins from extracts of [^{35}S]methionine-labeled HeLa cells infected with AAV-2 and adenovirus type 2 (Fig. 2a) or adenovirus alone (Fig. 2b). Monoclonal antibodies A1, A69, B1, and A20 immunoprecipitated AAV capsid proteins as confirmed by comparison with polypeptides precipitated with the VP-S antiserum. In some precipitations, we recovered a non-AAV-specific polypeptide (Fig. 2a, b, asterisks), but this polypeptide was not specific for a particular antibody and probably represented material nonspecifically adsorbed to protein A-Sepharose. The fact that VP3 was also found in precipitates obtained with antibodies A1 and A69, which do not recognize epitopes of VP3, suggests that VP1 and VP2 are also detected in capsids, capsid precursors, or other complexes involving VP3 (Fig. 2a). To distinguish between these possibilities, we tested the antibodies on more clearly defined substrates, such as recombinant nonassembled capsid proteins purified from baculovirus-infected SF9 cells, assembled capsids present in AAV-2 virus stocks, and recombinant VP2/3 containing empty virus-like particles prepared from baculovirus-infected SF9 cells (Fig. 2c to e). While A1, A69, B1, and VP-S precipitated the recombinant, nonassembled, but partially oligomerized AAV-2 capsid proteins (60), A20 failed to precipitate these proteins, although they were renatured and soluble in buffers of physiological ionic strength (Fig. 2c). A1 and A69 coprecipitated some VP3, probably reflecting complex formation between the capsid proteins. Interestingly, all antibodies except B1 recognized and precipitated capsids from AAV virus stocks (Fig. 2d). Obviously, the epitope which is recognized by B1 becomes masked during capsid assembly. In contrast, A20 antibodies, which failed to detect nonassembled or denatured capsid proteins, precipitated assembled capsids, suggesting that they recognize an epitope which is formed during capsid assembly. These properties of the capsid protein antibodies were confirmed by precipitation of VP2/3 containing virus-like particles (Fig. 2e). In addition it was confirmed that A1 specifically detects VP1, since VP2/3 particles were not precipi-

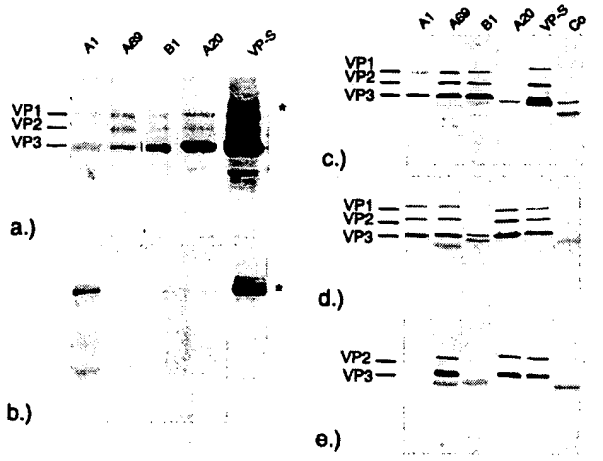

FIG. 2. Immunoprecipitations with monoclonal capsid protein antibodies. (a) Monoclonal antibodies A1, A69, B1, and A20 were used to immunoprecipitate capsid proteins from extracts of [^{35}S]methionine-labeled HeLa cells infected with AAV-2 and adenovirus type 2. (b) Control precipitations were performed with extracts of adenovirus type 2-infected cells. The asterisks denote a nonspecific precipitate in some lanes. (c) Capsid proteins precipitated from a pool of soluble, nonassembled capsid proteins. (d) Capsids precipitated from virus stocks. (e) Precipitation of VP2/VP3 containing capsid-like particles (53). For controls, precipitations with the polyclonal capsid protein antiserum (VP-S) and a nonspecific antibody (Co) were performed. Precipitated capsid proteins were detected by Western blotting with B1 and developing the detected bands with alkaline phosphatase-coupled secondary antibodies.

tated by this antibody. B1 also did not precipitate these virus-like particles. The weakly stained bands migrating below VP3 in Fig. 2c to e are immunoglobulin G molecules of the antibodies. To further clarify the specificity and selectivity of these antibodies for capsid protein populations present in AAV-2/adenovirus type 2-infected HeLa cells, we fractionated nuclear extracts of AAV-2/adenovirus type 2-infected HeLa cells on sucrose gradients and immunoprecipitated the capsid proteins from each fraction (Fig. 3). A1, A69, B1, and VP-S preferentially precipitated VP proteins sedimenting below 20S, representing monomeric or oligomeric capsid proteins. A20 did not precipitate capsid proteins sedimenting in this range. Instead, A20 antibodies selectively precipitated capsid proteins sedimenting around 60S and above (see also reference 67), representing the sedimentation range of empty and full AAV capsids (42). However, it is not clear whether empty and full capsids are recognized with the same affinity. This confirms and extends the conclusion drawn from Fig. 1 and 2 that the A20 antibody specifically recognizes an epitope of assembled capsids which is not present in denatured capsid proteins and native but nonassembled capsid proteins. A1, A69, and VP-S precipitated capsids with lower efficiency than did free capsid proteins. Nevertheless, the specific epitopes for A1, A69, and VP-S are accessible on capsids at least to some extent. Although B1 was highly efficient in precipitating free VP proteins, it precipitated only trace amounts of capsids, which were close to background levels. Taken together with the results of Fig. 2d and e, this antibody can be characterized by a high preference for free capsid proteins; however, a slight reaction with capsids cannot be completely ruled out.

As such, these antibodies, in particular A20 and B1 in combination with polyclonal anticapsid antibodies, e.g., VP-S, are interesting tools for investigating capsid assembly on the cellular level, since they distinguish between free capsid proteins and assembled AAV-2 capsids within infected cells.

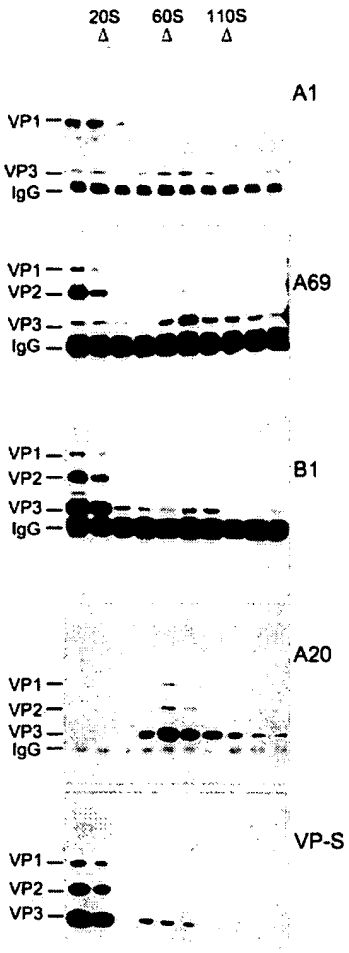

FIG. 3. Immunoprecipitation of size-fractionated capsid proteins obtained from AAV-2/adenovirus type 2-infected HeLa cells with monoclonal capsid protein antibodies. Nuclear extracts of AAV-2/adenovirus type 2-infected HeLa cells were fractionated on sucrose density gradients, and monoclonal antibodies A1, A69, B1, and A20 were used to immunoprecipitate capsid proteins from the fractions obtained. The immunoprecipitates were analyzed by SDS-PAGE and Western blotting with monoclonal antibody B1. The immunoreaction was visualized by incubation with a peroxidase-coupled secondary antibody followed by enhanced chemiluminescence detection. Immunoprecipitations were compared with those obtained by precipitation with a polyclonal capsid protein antiserum (VP-S). Sedimentation positions were determined in parallel gradients with thyroglobulin (20S), empty VP2/3 capsid-like particles (60S), and infectious AAV particles (110S).

Stages of AAV-2/adenovirus type 2 coinfection characterized by the intracellular localization of Rep and Cap proteins. After staining of HeLa cells infected with AAV-2 and adenovirus type 2 (MOI_{AAV} = 20, MOI_{Ad} = 2) by double immunofluorescence with the polyclonal antiserum VP-S, recognizing all capsid proteins, and monoclonal antibody 76-3, recognizing the nonspliced Rep proteins Rep78 and Rep52 (67), we observed a number of different phenotypes regarding the spatial intracellular distribution of Rep and Cap proteins. We classified them into five groups defined by typical patterns of intracellular Rep and Cap protein distribution (Fig. 4a) and counted their frequencies at consecutive time points after infection. As shown in Fig. 4b, different phenotypes, defined as stages 2 to 5, exhibited their peaks of relative frequency at

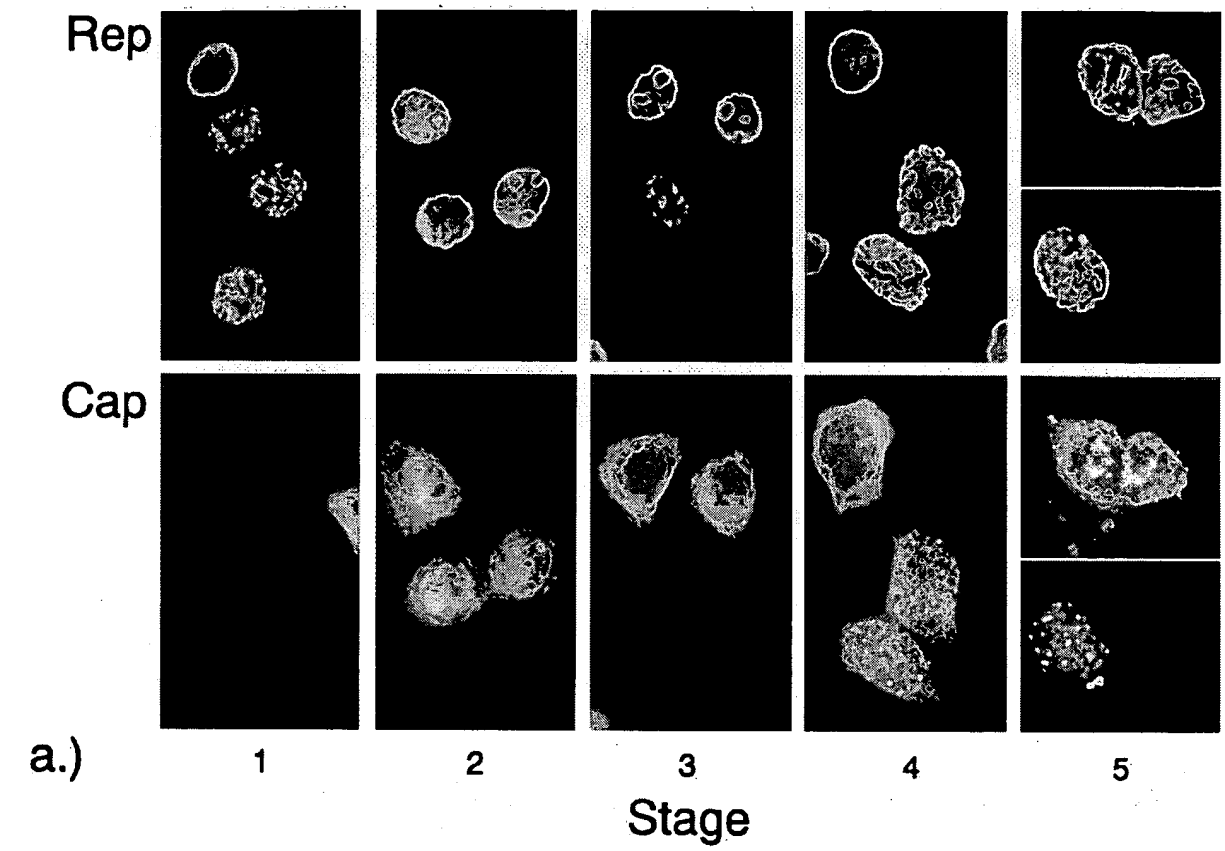

FIG. 4. Characterization of stages of a productive AAV-2/adenovirus type 2 coinfection in HeLa cells by double immunofluorescence with Rep and Cap antibodies. (a) The subcellular localization of replication proteins (Rep) and capsid proteins (Cap) was visualized with the polyclonal VP antiserum and monoclonal antibody 76/3, recognizing Rep78 and Rep52 (67), in samples prepared during the time course of infection by double immunofluorescence staining. (b) The succession of five stages shown in panel a was analyzed by determining the frequency of defined subcellular Rep and Cap distributions in a population of coinfected cells at various time points postinfection. Stage 1 was omitted from the graph, since its frequency remained constant throughout the infection, although it appeared before the other stages.

different time points postinfection. This allowed us to postulate a sequence of stages representing the progression of an AAV-2/adenovirus type 2 coinfection.

Stage 1 clearly appeared at earlier time points than stage 2, between 10 and 14 h after infection, but did not decline in frequency when the following stages appeared. This made it difficult to include the frequency distribution of stage 1 in the graph shown in Fig. 4b. Between 70 and 80% of the cells showed this distribution of the Rep proteins. The observation that a higher proportion of cells, up to 90% and more, appeared in stages 2 to 5 when the MOI of adenovirus was enhanced suggests that at low MOI of adenovirus relative to the MOI of AAV-2 there is a block of progression to the following stages in some cells (data not shown). The dotted distribution pattern of Rep proteins probably represents sites of AAV DNA replication (65), since AAV-2 DNA colocalized in the same spots (see Fig. 7). At this stage, no capsid proteins which could be used for packaging of the replicated DNA were expressed, whereas cells in stage 2 expressed both Rep and Cap proteins. In stage 2, Rep proteins were detectable all over the nucleoplasm and occasionally were also visible in the nucleoli as a group of small fluorescence-positive clusters. We interpret this as a short transient nucleolar state of Rep (e.g., Fig. 4, stage 2), since Rep was not detectable in nucleoli in the preceding or following stages. Capsid proteins were detectable in the nucleus and in the cytoplasm and were clearly enriched in the nucleoli. The identity of the nucleoli was confirmed with a commercially available nucleolus specific antibody (data not shown). In stage 3, large amounts of Rep and capsid proteins

were present in the nucleoplasm; however, capsid proteins were also detectable in the cytoplasm and the nucleoli. The nucleoli, if detectable, were strongly enlarged or fragmented and began to disappear. In this stage, the most extensive colocalization of replication and capsid proteins in broad zones of the nucleoplasm was observed. The colocalization of Rep and Cap proteins of some of the samples shown here by conventional immunofluorescence microscopy was verified by laser scanning microscopy of doubly stained samples (data not shown). In stages 4 and 5, Rep proteins concentrated in some clusters of the nucleus, often along the nuclear periphery, and the capsid proteins were no longer codistributed in these stages. Some of these redistributions might be due to adenovirus-induced changes of the nuclear structure. Furthermore, an increasing amount of strongly capsid protein-positive dots became visible both in the nucleus and in the cytoplasm. These stages describe the most frequent images and omit intermediates and rare patterns of Rep and Cap distribution. The localization pattern of replication and capsid proteins was confirmed after fixation of cells with PFA (data not shown).

VP1 and VP2 accumulate in the nucleus, in contrast to VP3. Comparison of the distribution patterns of VP1 alone (determined by antibody A1), VP1 plus VP2 (determined by antibody A69), and nonassembled VP1 plus VP2 plus VP3 (determined by antibody B1) with those of total capsid proteins (detected by the VP-S serum) showed some interesting details (Fig. 5). VP1 and VP2 were highly enriched in the nucleus, while nonassembled VP3 detected with B1 was evenly distributed over the nucleus and cytoplasm. This result suggests that the stoichiometry of capsid proteins is different in the nuclear and cytoplasmic compartments. As B1, in contrast to VP-S, does not detect assembled capsids, it seems likely that the higher proportion of the VP-S-positive material in the nucleoplasm accounts for assembled capsids. All three monoclonal antibodies, A1, A69, and B1, showed similar rearrangements of nuclear compartmentalization of capsid proteins during the time course of infection, as shown in Fig. 4 with the VP antiserum (data not shown).

Localization of AAV-2 capsids during the time course of infection. To localize the cellular compartment of capsid formation, we used the capsid-specific antibody A20 in double-immunofluorescence stainings with the polyclonal capsid protein antiserum (VP-S) to visualize AAV-2 capsids in AAV-2/adenovirus type 2-coinfected HeLa cells at various time points postinfection. Between 10 and 14 h after infection (transition of stage 1 to stage 2), VP proteins were distributed over the cytoplasm and the nucleoplasm while the nucleoli were negative. At this time, no AAV-2 capsids were detectable (Fig. 6a). Before 10 h postinfection, no immunofluorescence was seen, demonstrating that the VP-S antiserum detected newly synthesized capsid proteins. At later time points (stage 2 and the transition between stage 2 and stage 3), capsid proteins accumulated in the nucleoli, which increased in size and intensity of staining for capsid proteins (Fig. 6b to d). Coincidentally with the nucleolar localization of capsid proteins, AAV-2 capsids were detectable with the A20 antibody. Counting the frequencies of various A20-positive images at early time points after infection suggested that the nucleoli were the sites in infected cells where capsids were first detected (Fig. 6i), although at the earliest stages a significant number of cells also showed some nucleoplasmic staining. The nucleoli gradually increased in size during infection (Fig. 6b to d) and finally seemed to become fragmented (Fig. 6e) or completely dissolved (Fig. 6f). At intermediate stages (stage 3 and 4), capsids colocalized with capsid proteins in the nucleoli and the nucleoplasm; however, they were never detectable in the cytoplasm at these stages

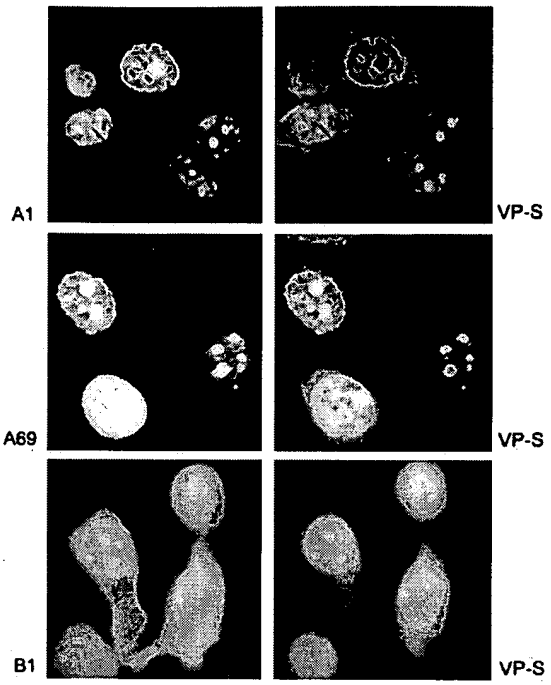

FIG. 5. Subcellular localization of VP1, VP1/2, or VP1/2/3 in AAV-2/adenovirus type 2-infected HeLa cells. Double immunofluorescence with monoclonal antibodies A1, A69, B1, and the VP antiserum (VP-S) at stages 2 to 3 is shown. B1 (reacting with VP1, VP2 and VP3) detected nuclear and cytoplasmic capsid proteins with similar intensity, whereas A1 (reacting with VP1) and A69 (reacting with VP1 and VP2) exclusively stained nuclear capsid proteins.

(Fig. 6d to f). Only very late in the progression of the infection were capsids released to the cytoplasm. They did not colocalize with the bulk of capsid proteins (Fig. 6g and h). These results clearly indicate that capsid assembly is confined to nuclei of infected cells and that the nucleoli or nucleolar components may play a role in the assembly process.

Localization of AAV-2 DNA in relation to Rep and Cap proteins. To define potential sites for AAV DNA packaging, we performed fluorescent in situ hybridization experiments in combination with immunofluorescent stainings to compare the distribution patterns of Rep and Cap proteins with the localization of AAV-2 DNA (Fig. 7). In cells of stage 1, Rep and AAV-2 DNA colocalized in the finely dotted pattern already described for Rep localization in Fig. 4, an observation which recently was also made by others (65). As mentioned above, capsid proteins were not detectable at this stage. In stages 2 and 3, Rep and DNA still colocalized over large areas of the nucleoplasm and weak signals inside the nucleoli could sometimes be observed. During these stages, localization of the capsid proteins visualized with the B1 antibody overlapped with DNA in the nucleoplasmic areas, but DNA was either absent from the nucleoli or present in only very small amounts, although the nucleoli were the sites of strongest capsid protein fluorescence. Double staining of AAV DNA and capsids with the capsid-recognizing antibody (A20) was not successful because a denaturation step was necessary for DNA hybridization and the A20 antibodies did not react with denatured capsid proteins. We were unable to detect AAV-2 DNA in cells harvested 30 h postinfection (stages 4 and 5 [data not shown]), suggesting that the amount of DNA accessible for hybridization was too small at late stages of infection because

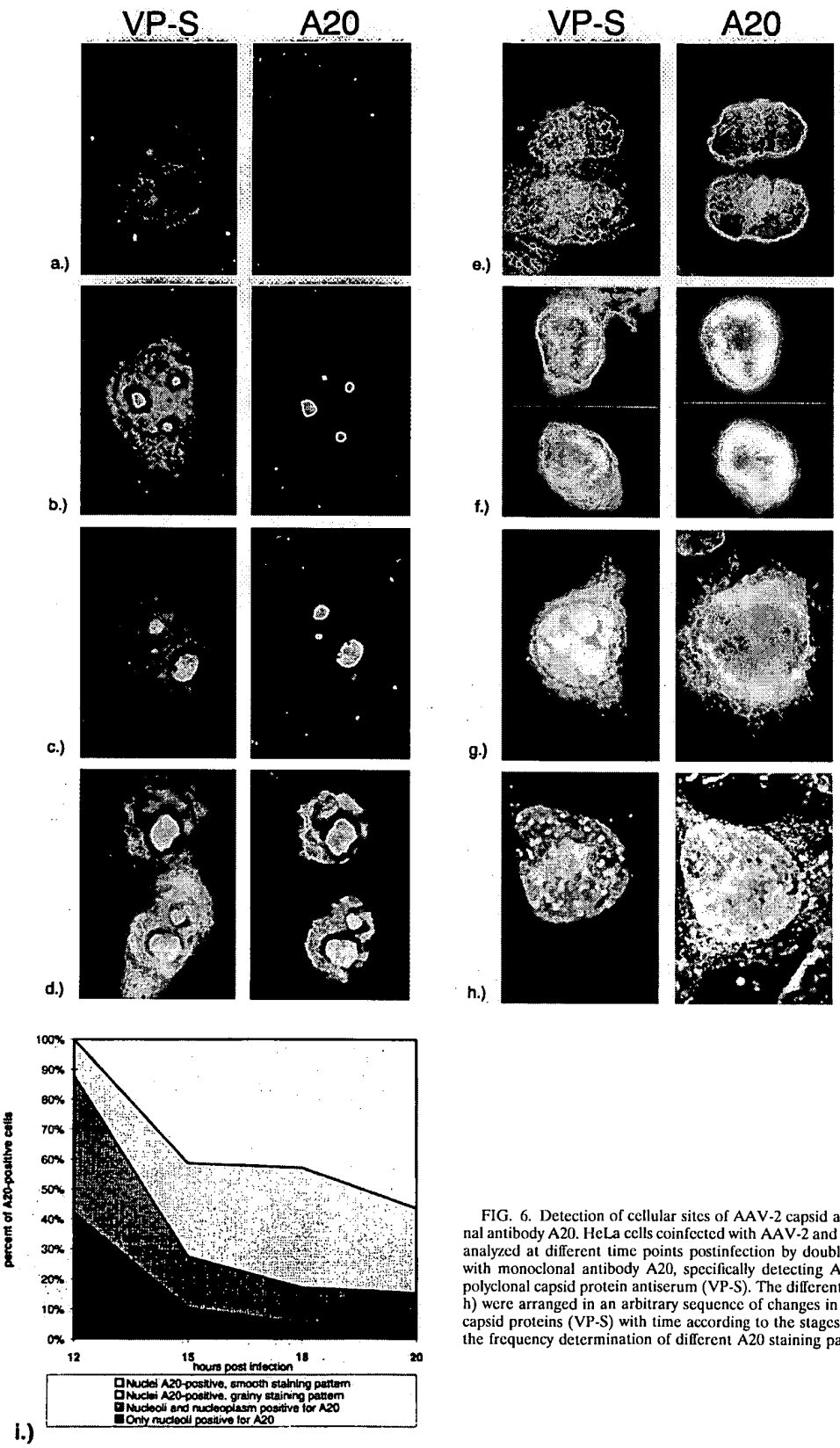

FIG. 6. Detection of cellular sites of AAV-2 capsid assembly with monoclonal antibody A20. HeLa cells coinfected with AAV-2 and adenovirus type 2 were analyzed at different time points postinfection by double immunofluorescence with monoclonal antibody A20, specifically detecting AAV-2 capsids and the polyclonal capsid protein antiserum (VP-S). The different staining patterns (a to h) were arranged in an arbitrary sequence of changes in cellular localization of capsid proteins (VP-S) with time according to the stages depicted in Fig. 4 and the frequency determination of different A20 staining patterns (i).

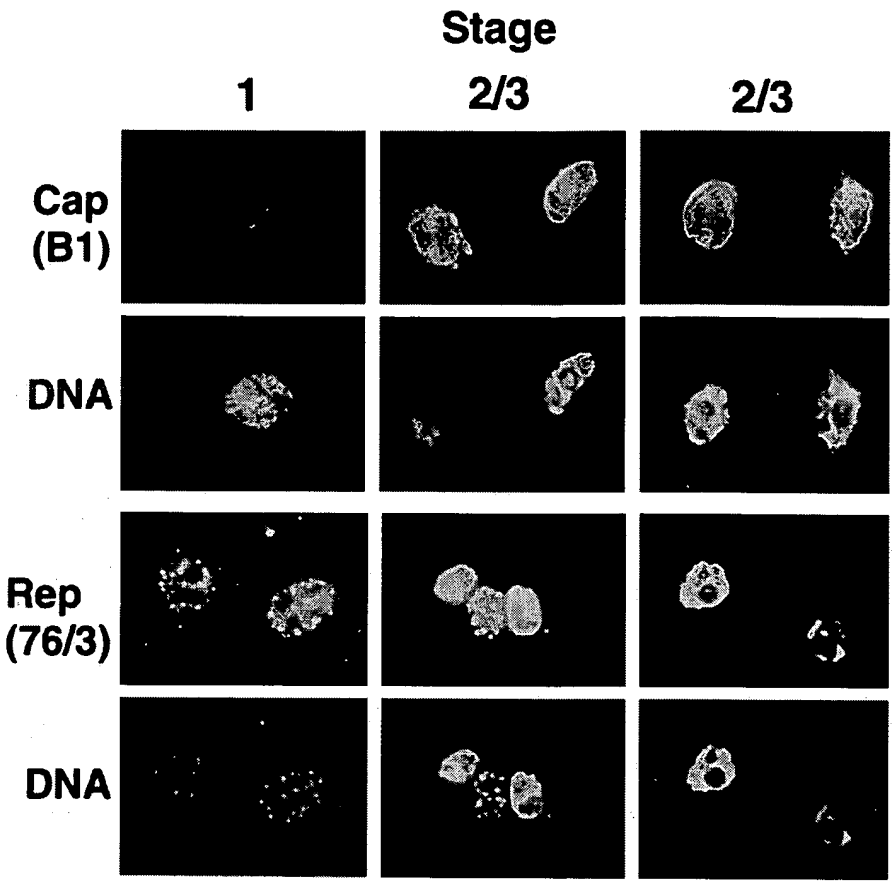

FIG. 7. Subcellular localization of AAV-2 DNA in comparison to Rep and Cap proteins in AAV-2/adenovirus type 2-infected HeLa cells. Double staining of AAV-2/adenovirus type 2-coinfected HeLa cells was performed using indirect immunofluorescence and in situ hybridization techniques. The localization of AAV-2 DNA was shown in comparison to capsid proteins by detection with monoclonal antibody B1 and in comparison to the nonspliced Rep proteins visualized with monoclonal antibody 76/3 for stage 1 and stages 2 and 3 of an AAV-2/adenovirus type 2 coinfection. Note the complete colocalization of AAV-2 DNA and Rep proteins and the only partial colocalization of AAV-2 DNA and capsid proteins in the nuclei of infected cells.

most of the AAV-2 DNA had already been packaged. As such, the nucleoplasm is an area where replication proteins, capsid proteins, and DNA colocalize and where DNA packaging might occur.

Genetic elements of AAV-2 involved in capsid formation. Detection of capsids by the A20 antibody allowed us to investigate which AAV-2 genes are involved in capsid formation. HeLa cells were transiently transfected with a plasmid containing the complete AAV genome (pTAV-2) and infected with adenovirus, and capsid formation was monitored by A20 immunofluorescence in comparison to cells transfected with a construct expressing the cap gene alone (pCMV-VP) (Fig. 8). Transfection of pTAV-2 and infection with adenovirus led to the formation of capsids in about 90% of capsid protein-expressing cells (equivalent to AAV-2/adenovirus type 2-coinfected cells), and the cells proceeded through the same stages as in a coinfection experiment (data not shown). Only the cells showing nucleolus-localized capsid proteins also showed capsid formation (Fig. 8a, pTAV-2). This correlation also held true for cells expressing solely the cap gene, regardless of whether they were infected with adenovirus (Fig. 8a, pCMV-VP +Ad, pCMV-VP −Ad). Preparative isolation of capsids from such transfected cells and analysis by negative staining and electron microscopy confirmed that capsids were indeed assembled (data not shown). However, two differences were obvious when cells transfected with pCMV-VP were compared with cells transfected with pTAV-2: first, the capsids accumulated in the enlarged nucleoli and did not proceed through the following stages of infection, and second, only about 40% of the capsid protein-expressing cells also formed capsids as quantitated by comparison of VP-S- and A20-positive cells. Therefore, we tried to determine which components of the AAV genome enhance the efficiency of capsid formation and which factors have an influence on the subcellular distribution of capsids.

Transfection of increasing amounts of the AAV cap gene expression plasmids (CMV-VP) resulted in a nearly exponential increase in the percentage of capsid-producing cells (Fig. 8b), showing that capsid formation is strongly dependent on cellular capsid protein concentration.

When we studied the influence of different Rep proteins or of replication-competent plasmids with terminal repeats on the efficiency of capsid formation, we were not able to detect a direct and reproducible stimulation of capsid assembly by these components (data not shown). An indirect effect due to changes of the intracellular capsid protein concentration could not be excluded. However, when we analyzed the subcellular distribution of capsids, we observed an altered pattern of cap-

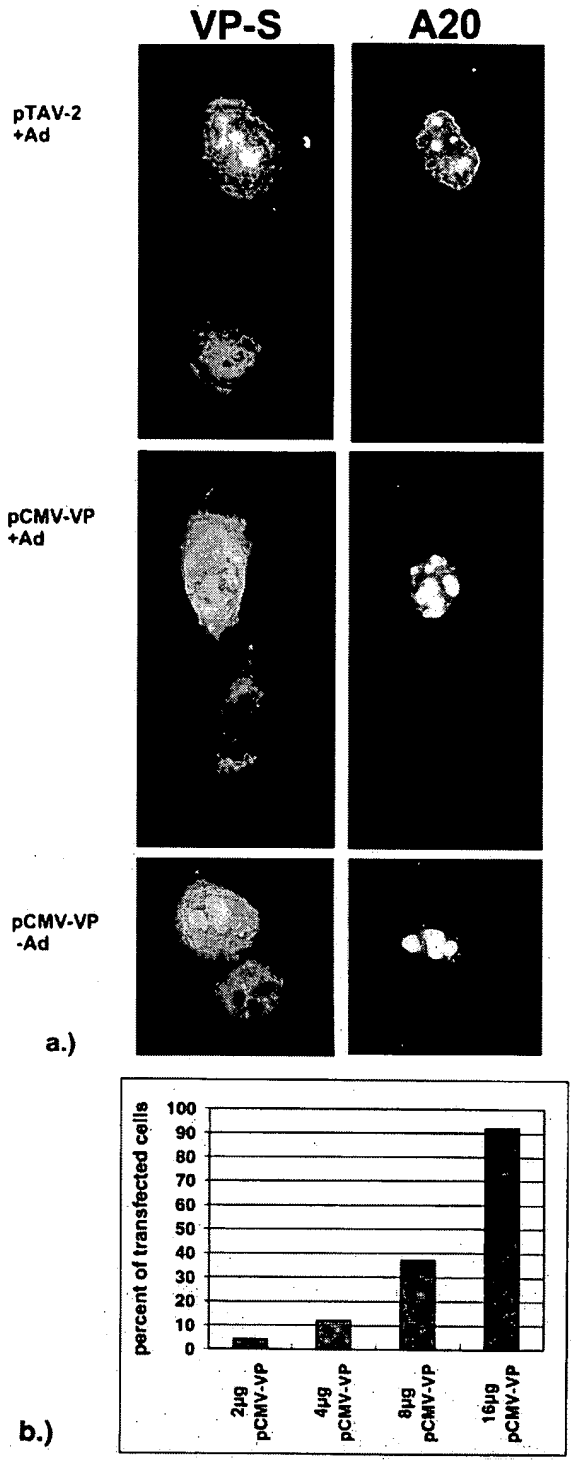

FIG. 8. Capsid assembly in HeLa cells transfected with a full-length AAV-2 genome or the cap gene alone. (a) HeLa cells were transfected with plasmids containing a full-length AAV-2 genome (pTAV-2) or the cap gene expressed under the control of the CMV promoter (CMV-VP) in the presence or absence of adenovirus type 2 (Ad) and analyzed for capsid formation by double immunofluorescence with the polyclonal capsid protein antiserum (VP-S) and monoclonal antibody A20 for detection of capsid formation. (b) The percentage of capsid protein-expressing cells which formed capsids was determined by the same assay after transfection of increasing quantities of CMV-VP plasmid.

sid distribution when Rep proteins were coexpressed (Fig. 9). As mentioned above, expression of the cap gene alone led to the formation of capsids which were restricted to the nucleoli, in contrast to the accumulation of capsids throughout the nucleoplasm in the presence of the whole AAV genome (Fig. 9, pTAV2 and pCMV-VP + pKEX). Coexpression of the small Rep proteins in most cells resulted in a punctate distribution pattern of assembled capsids (Fig. 9). This was accompanied by a significantly reduced capsid protein expression level and reduced capsid formation efficiency (data not shown). Coexpression of Rep78 or Rep 68 seemed to permit the release of assembled capsids from the nucleoli or stimulated capsid assembly outside the nucleoli also, leading to a capsid distribution rather similar to the situation in AAV-2/adenovirus type 2-coinfected cells (Fig. 9). This effect was capsid protein concentration independent, and cotransfection of a plasmid with AAV terminal repeats did not change this pattern. This result clearly showed an influence of the Rep proteins on the subcellular distribution of assembled AAV capsids.

DISCUSSION

Analysis of cellular compartmentalization of AAV-2 DNA, Rep, and Cap proteins during the course of a productive infection provided evidence for temporal and spatial regulations of DNA replication, capsid assembly, and DNA packaging. The whole process could be described in a number of characteristic stages of infection. The spatial distribution of capsid protein subgroups, including the distribution of assembled and nonassembled capsid proteins by specific monoclonal antibodies, allowed us to determine the cellular sites of capsid assembly and packaging and finally to identify AAV genes involved in capsid assembly and localization. These data provide a framework for the interpretation of biochemical and genetic data describing the process of AAV reproduction.

An important tool for the analysis of subcellular capsid protein localization was a set of monoclonal antibodies which allowed us to distinguish between proteins VP1 (A1), VP1 plus VP2 (A69), and VP1 plus VP2 plus VP3 (B1) and between nonassembled capsid proteins (B1) and assembled capsids (A20). The specificity of these antibodies was established by Western blotting and immunoprecipitations with a number of different substrates. Only the A1 antibody occasionally reacted with a non-AAV-derived protein in immunoprecipitations, whereas the other antibodies showed cross-reactions only at very high concentrations of antibodies and protein and after prolonged exposure. The cross-reaction of A1 was variable and of low affinity compared to the reaction with the VP1 polypeptide, since, for example is was not detectable when VP1 was precipitated from extracts of AAV-2/adenovirus type 2-infected HeLa cells. Immunoprecipitations with the VP1- or VP1/VP2-specific antibodies A1 and A69, respectively, resulted in a weak precipitation not only of assembled capsids but also of nonassembled VP3, suggesting that the epitopes for VP1 and VP2 are accessible both in assembled capsids and in nonassembled capsid precursor complexes containing VP1 and VP3. In contrast, the antibody reacting with all three capsid proteins (B1) did not significantly precipitate assembled capsids according to several criteria. It is more difficult to interpret the characteristics of the A20 antibody. This antibody certainly has a high affinity for assembled capsids, and the Western blotting and immunoprecipitation experiments suggest that it recognizes a conformational epitope which is absent in denatured or nonassembled native capsid protein. The epitope is also present in recombinant virus-like particles made up of VP2 and VP3. It is, however, difficult to exclude the possibility

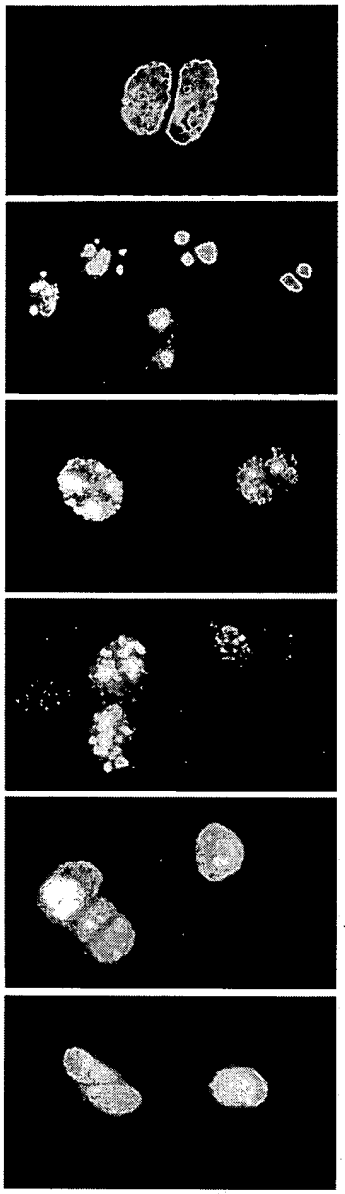

FIG. 9. Rep proteins influence the subcellular distribution of assembled AAV capsids. HeLa cells were transfected with a plasmid containing the complete AAV genome (pTAV-2) or the AAV-2 cap gene alone (pCMV-VP) or the cap gene in combination with single Rep protein expression constructs (pCMV-Rep40, pCMV-Rep52, pCMV-Rep68, and pCMV-Rep78) and infected with adenovirus type 2 18 h after transfection. Cells were fixed 20 h after infection and stained with monoclonal antibody A20 to detect AAV-2 capsids. Note the different subcellular distribution patterns of AAV capsids.

that this antibody also reacts with capsid precursors which possibly already have acquired the specific conformational epitope. Keeping this precaution in mind, this antibody is a very useful tool for the analysis of the AAV assembly process.

The immunofluorescence data obtained with the A20 antibody clearly showed that capsid assembly is a nuclear process. The antibody characteristics of A1 and A69 allowed us to show that VP1 and VP2, unassembled and assembled, are highly enriched in the nucleus whereas unassembled VP3 is equally distributed between both compartments or somewhat enriched in the cytoplasm. This observation already implies that the stoichiometry of VP1 and VP2 to VP3 must be different in the nucleus and in the cytoplasm. This conclusion seems to contradict the analysis of capsid proteins obtained by preparation of nuclear and cytoplasmic fractions of infected cells (67). Such fractionation data, however, often lead to a mislocalization of highly soluble proteins, such as, e.g., the small Rep proteins, due to the leakiness of prepared nuclei. Expression of single capsid proteins also showed that VP1 and VP2 efficiently entered the nucleus whereas VP3 only equilibrated between both compartments (53). Coexpression of VP1 or VP2 with VP3 increased the nuclear accumulation of VP3, suggesting that VP1 and VP2 are able to cotransport VP3 to the nucleus as has also been shown for capsid proteins of other viruses (30). Such a heterotypic complex formation for nuclear transport of a particular capsid constituent could be a mechanism to enrich the capsid proteins in the correct stoichiometry for capsid assembly in the nucleus. Assembly experiments with single capsid proteins expressed by infections with recombinant baculoviruses are in line with these speculations, since capsid-like structures could be detected in VP3-expressing SF9 cells only when VP2 was coexpressed (53). Recently, the expression of single capsid proteins in HeLa cells also showed that VP3 alone was incapable of assembling into capsids as analyzed by immunofluorescence with the A20 antibody (60).

Strikingly, the capsid proteins accumulated in the nucleoli of HeLa cells in early stages of infection or when expressed by transfection of the cap gene. We observed capsid formation only in cells in which the capsid proteins had entered the nucleoli. Exceptions were cells in which nucleoli could no longer be detected, either due to progression of the infection or to the disassembly of the nucleoli during the cell cycle (e.g., Fig. 6e to h). Cells which expressed the capsid proteins but in which the nucleoli were clearly capsid protein negative never showed any signs of capsid formation. This suggests that nucleolar components are involved in the capsid assembly process. In kinetic studies, capsids clearly were first detected in the nucleoli of a large proportion of infected cells; however, at the same time, smaller amounts of capsids in addition to the ones localized in the nucleoli were also detectable at some nucleoplasmic sites in a similar proportion of infected cells. Since A20 fluorescence is an indicator for capsids but not for the assembly process itself and the capsid localization pattern changes with time, this could reflect capsids which had already been released or exported from the nucleoli. Alternatively, initiation of capsid assembly could also occur at these nucleoplasmic positions. The transfection studies support the first interpretation, since in the presence of the cap gene alone, capsids were detectable almost exclusively in highly enlarged nucleoli. The fact that coexpression of the large Rep proteins leads to a significant increase of extranucleolar capsids can be interpreted as an influence of the Rep proteins on relocalization of the assembled capsids from the nucleoli to the nucleoplasm. The alternative interpretation, i.e., that Rep stimulates capsid assembly outside the nucleoli, possibly by recruitment of assembly factors at these sites, cannot be excluded. Although the presented data do not allow us to postulate an assembly pathway which obligatorily goes through the nucleolus in infected cells, the nucleolar localization of capsids during AAV infection is strikingly prominent. A high concentration of empty parvovirus H-1 particles in the nucleolus was also observed in early electron microscopic studies (1, 56). Capsid assembly undoubtedly depends on the capsid protein concentration, and since capsid proteins accumulate in the nucleoli, they might represent just the cellular sites where the critical concentration for capsid

assembly is first reached. This simple interpretation, however, is questionable, since capsid proteins did not continuously concentrate in the nucleolus. In transfection and infection experiments, one could observe many cells which showed a strong capsid protein fluorescence while the nucleoli were empty of capsid proteins, giving the impression that a switch for nucleolar uptake of VP proteins had not yet occurred. The nucleoli are the cellular sites of ribosome biogenesis and harbor many proteins involved in assembly processes. It is therefore tempting to speculate that nucleolar chaperones may also be used for AAV capsid assembly.

According to the model of AAV packaging established by Myers and Carter (42), ssDNA resulting from displacement synthesis is introduced into preformed empty AAV capsids. Genetic evidence showed that in addition to the capsid proteins (25), Rep40 and Rep52 significantly stimulated ssDNA accumulation (17). This means that during AAV-2 DNA packaging, colocalization of Rep proteins, DNA, and capsids should be expected. Rep proteins 78 and 52 and AAV-2 DNA showed a perfect colocalization pattern (see also reference 65). A direct comparison of the localization of capsids and DNA was not possible because denaturation steps required for in situ hybridization of the DNA destroyed the epitope recognized by the A20 antibody. However, comparison of the localization of free capsid proteins by the B1 antibody with AAV-2 DNA and correlation of B1 fluorescence and A20 fluorescence by comparison of the fluorescence obtained with the VP-S antiserum clearly demonstrate that the predominant sites of capsid and DNA colocalization are nucleoplasmic areas at a certain distance from the nucleolus. This means that at the site of the highest capsid concentration and probably the most intensive capsid production, namely, the nucleolus, little or no DNA packaging occurs. Only trace amounts of AAV-2 DNA were detectable in the nucleolus, in contrast to reports of nucleolar localization of minute virus of mice DNA in mouse cells (22, 64). Coinfection with adenovirus also redirected minute virus of mice DNA to multiple intranuclear foci in HeLa cells, similar to the distribution of AAV-2 DNA. Ultrastructural studies of the autonomous H-1 parvovirus replication suggest that DNA synthesis begins at clusters of fibrillar centers released from nucleoli (55), suggesting that destruction of the nucleolus is part of the viral replication and asembly process. This view urges the interpretation that the assembled capsids are released from the nucleoli to the sites of DNA packaging, possible with the aid of the large Rep proteins in the course of nucleolar destruction. Hunter and Samulski (28) observed that AAV Rep and capsid proteins colocalize in the nuclei of infected cells. However, they also observed densely fluorescent capsid regions where they did not see an increase in Rep fluorescence. These regions may correspond to the nucleoli. It is not clear why these authors found a colocalization of Rep and Cap proteins in the foci where Rep proteins and AAV-2 DNA already colocalized, i.e., at a stage when we could not detect capsid protein expression. In the course of the present experiments, colocalization of Rep and capsid proteins could be observed only at stage 2, with a peak at stage 3 when Rep was already distributed in rather broad areas of the nucleoplasm. One possibility is that infections with a higher MOI of adenovirus led to an earlier onset of capsid protein expression than was observed in this study, which could result in an overlap of Rep and Cap localization at an earlier stage of infection than reported here. A close spatial association of replication proteins and DNA but a rather distinct localization of the capsid proteins was also observed for the Aleutian mink disease virus (45), although at different nuclear sites from those observed in this study. The segregation of replicating DNA and replication proteins from capsid proteins and capsids at certain time points postinfection to separate compartments might reflect necessary regulatory events in DNA replication and packaging.

The interpretation of different localization patterns as a process is difficult, because several different images can be observed at a certain time point after infection, and often the tools for revealing the underlying processes are not available. The five stages described above are more or less arbitrarily defined and omit rare images which could not be arranged into an order of events. Several studies have interpreted the distribution pattern of Rep proteins and DNA in a number of foci typically observed in stage 1 as replication centers which increase in size with the duration of infection (28, 65; see above). The strong nucleolar accumulation of capsid proteins in stage 2 could be interpreted as an expression of an intense capsid assembly activity. The nucleoli also increase in size during infection, and capsids finally spread over the nuclear interior, possibly indicating relocation of capsids for packaging. The broad nucleoplasmic zones outside the nucleoli and not directly associated with the nuclear envelope harboring AAV DNA, Rep proteins, and capsid proteins are probably the areas of DNA packaging. They are formed in stage 2 and 3 and last for about 2 h. Interpretation of clusters of Rep proteins or the speckles of capsid proteins where no capsids are detectable at later stages (stages 4 and 5) is not possible at present. The fine network of capsid fluorescence emerging from the nuclei of AAV-producing cells which often ends at the surface of not yet infected cells might depict the path of virion release and attachment at cells for a new round of infection.

ACKNOWLEDGMENTS

A. Wistuba is supported by a fellowship of the German-Israeli Cooperation in Cancer Research.

We are grateful to B. Hub and U. Ackermann for expert technical assistance in electron microscopy and photography. We thank H. zur Hausen for continuous support and M. Pawlita and H. Zentgraf for critical reading of the manuscript.

REFERENCES

1. **Al-Lami, F., N. Ledinko, and H. Toolan.** 1969. Electron microscope study of human NB and SMH cells infected with the parvovirus, H-1: involvement of the nucleolus. J. Gen. Virol. **5**:485–492.
2. **Ashktorab, H., and A. Srivastava.** 1989. Identification of nuclear proteins that specifically interact with adeno-associated virus type 2 inverted terminal repeat hairpin DNA. J. Virol. **63**:3034–3039.
3. **Atchinson, R. W., B. C. Castro, and W. M. Hammon.** 1965. Adeno-associated defective particles. Science **149**:754–756.
4. **Baines, J. D., R. J. Jacob, L. Simmermann, and B. Roizman.** 1995. The herpes simplex virus 1 UL11 proteins are associated with cytoplasmic and nuclear membranes and with nuclear bodies of infected cells. J. Virol. **69**: 825–833.
5. **Beaton, A., P. Palumbo, and K. I. Berns.** 1989. Expression from the adeno-associated virus p5 and p19 promoters is negatively regulated in *trans* by the rep protein. J. Virol. **63**:4450–4454.
6. **Berezney, R.** 1991. The nuclear matrix: a heuristic model for investigating genomic organization and function in the cell nucleus. J. Cell. Biochem. **47**:109–123.
7. **Berns, K. I.** 1990. Parvovirus replication. Microbiol. Rev. **54**:316–329.
8. **Berns, K. I., and R. A. Bohenzky.** 1987. Adeno-associated viruses: an update. Adv. Virus Res. **32**:243–306.
9. **Bosher, J., A. Dawson, and R. T. Hay.** 1992. Nuclear factor I is specifically targeted to discrete subnuclear sites in adenovirus type 2-infected cells. J. Virol. **66**:3140–3150.
10. **Bridge, E., D. X. Xia, M. Carmo-Fonseca, B. Cardinali, A. I. Lamond, and U. Pettersson.** 1995. Dynamic organization of splicing factors in adenovirus-infected cells. J. Virol. **69**:281–290.
11. **Buller, R. M. L., J. Janik, E. D. Sebring, and J. A. Rose.** 1981. Herpes simplex virus types 1 and 2 completely help adeno-associated virus replication. J. Virol. **40**:241–247.

12. **Carter, B. J.** 1990. Adeno-associated virus helper functions, p. 255–282. *In* P. Tijssen (ed.), Handbook of parvoviruses. CRC Press, Inc., Boca Raton, Fla.
13. **Carter, K. C., D. Bowman, W. Carrington, K. Fogarty, J. A. McNeil, F. S. Fay, and J. B. Lawrence.** 1993. A Three-dimensional view of precursor messenger RNA metabolism within the mammalian nucleus. Science **259:** 1330–1335.
14. **Carvalho, T., J. S. Seeler, K. Ohman, P. Jordan, U. Pettersson, G. Akusjarvi, M. Carmo-Fonseca, and A. Dejean.** 1995. Targeting of adenovirus E1Aand E4-ORF3 proteins to nuclear matrix-associated PML bodies. J. Cell Biol. **131:**45–56.
15. **Chang, L. S., and T. Shenk.** 1990. The adenovirus DNA-binding protein stimulates the rate of transcription directed by adenovirus and adeno-associated virus promoters. J. Virol. **64:**2103–2109.
16. **Chang, L. S., Y. Shi, and T. Shenk.** 1989. Adeno-associated virus p5 promoter contains an adenovirus E1A-inducible element and a binding site for the major late transcription factor. J. Virol. **63:**3479–3488.
17. **Chejanovsky, N., and B. J. Carter.** 1989. Mutagenesis of an AUG codon in the adeno-associated virus rep gene: effects on viral DNA replication. Virology **173:**120–128.
18. **Chen, C., and H. Okayama.** 1987. High-efficiency transformation of mammalian cells by plasmid DNA. Mol. Cell. Biol. **7:**2745–2752.
19. **DeBruyn Kops, A., and D. M. Knipe.** 1988. Formation of DNA replication structures in herpes virus-infected cells requires a viral DNA binding protein. Cell **55:**857–868.
20. **DeBruyn Kops, A., and D. M. Knipe.** 1994. Preexisting nuclear architecture defines the intranuclear location of herpesvirus DNA replication structures. J. Virol. **68:**3512–3526.
21. **DeWet, J. R., K. V. Wood, M. DeLuca, D. R. Helinski, and S. Subramani.** 1987. Firefly luciferase gene: structure and expression in mammalian cells. Mol. Cell. Biol. **7:**725–737.
22. **Fox, E., P. T. Moen, Jr., and J. W. Bodnar.** 1990. Replication of minute virus of mice DNA in adenovirus-infected or adenovirus-transformed cells. Virology **176:**403–412.
23. **Harlow, E., and D. Lane.** 1988. Antibodies: a laboratory manual. Cold Spring Harbor Laboratory, Cold Spring Harbor, N.Y.
24. **Heilbronn, R., A. Bürkle, S. Stephan, and H. zur-Hausen.** 1990. The adeno-associated virus *rep* gene suppresses herpes simplex virus-induced DNA amplification. J. Virol. **64:**3012–3018.
25. **Hermonat, P. L., M. A. Labow, R. Wright, K. I. Berns, and N. Muzyczka.** 1984. Genetics of adeno-associated virus: isolation and preliminary characterization of adeno-associated virus type 2 mutants. J. Virol. **51:**329–339.
26. **Hölscher, C., J. A. Kleinschmidt, and A. Bürkle.** 1995. High level expression of adeno-associated virus (AAV) Rep78 and Rep68 protein is sufficient for infectious-particle formation by a *rep*-negative AAV mutant. J. Virol. **69:** 6880–6885.
27. **Hörer, M., S. Weger, K. Butz, F. Hoppe-Seyler, C. Geisen, and J. A. Kleinschmidt.** 1995. Mutational analysis of adeno-associated virus Rep protein-mediated inhibition of heterologous and homologous promoters. J. Virol. **69:**5485–5496.
28. **Hunter, L. A., and R. J. Samulski.** 1992. Colocalization of adeno-associated virus rep and capsid proteins in the nuclei of infected cells. J. Virol. **66:**317–324.
29. **Im, D. S., and N. Muzyczka.** 1989. Factors that bind to adeno-associated virus terminal repeats. J. Virol. **63:**3095–3104.
30. **Ishii, N., A. Nakanishi, M. Yamada, M. H. Macalalad, and H. Kasamatsu.** 1994. Functional complementation of nuclear targeting-defective mutants of simean virus 40 structural proteins. J. Virol. **68:**8209–8216.
31. **Janik, J. E., M. M. Huston, K. Cho, and J. A. Rose.** 1989. Efficient synthesis of adeno-associated virus structural proteins requires both adenovirus DNA binding protein and VA I RNA. Virology **168:**320–329.
32. **Johnson, F. B.** 1984. Parvovirus proteins, p. 259–295. *In* K. I. Berns (ed.), The parvoviruses. Plenum Publishing Corp., New York, N.Y.
33. **Johnson, F. B., H. L. Ozer, and M. D. Hoggan.** 1971. Structural proteins of adenovirus-associated virus type 3. J. Virol. **8:**860–863.
34. **Kyöstiö, S. R., R. A. Owens, M. D. Weitzmann, B. A. Antoni, N. Chejanovsky, and B. J. Carter.** 1994. Analysis of adeno-associated virus (AAV) wild-type and mutant Rep proteins for their abilities to negatively regulate AAV p5 and p19 mRNA levels. J. Virol. **68:**2947–2957.
35. **Labow, M. A., P. L. Hermonat, and K. I. Berns.** 1986. Positive and negative autoregulation of the adeno-associated virus type 2 genome. J. Virol. **60:** 251–258.
36. **Laskey, R. A., M. P. Fairman, and J. J. Blow.** 1989. S phase of the cell cycle. Science **246:**609–614.
37. **Laughlin, C. A., J.-D. Tratschin, H. Coon, and J. B. Carter.** 1983. Cloning of infectious adeno-associated virus genomes in bacterial plasmids. Gene **23:** 65–73.
38. **McCarty, D. M., M. Christensen, and N. Muzyczka.** 1991. Sequences required for coordinate induction of adeno-associated virus p19 and p40 promoters by Rep protein. J. Virol. **65:**2936–2945.
39. **McIntosh, J. R., and M. P. Koonce.** 1989. Mitosis. Science **246:**622–628.
40. **Mittnacht, S., and R. A. Weinberg.** 1991. G1/S phosphorylation of the retinoblastoma protein is associated with an altered affinity for the nuclear compartment. Cell **65:**381–393.
41. **Muzyczka, N.** 1992. Use of adeno-associated virus as a general transduction vector for mammalian cells. Curr. Top. Microbiol. Immunol. **158:**97–129.
42. **Myers, M. W., and B. J. Carter.** 1980. Assembly of adeno-associated virus. Virology **102:**71–82.
43. **Nakamura, H., T. Morita, and C. Sato.** 1986. Structural organizations of replicon domains during DNA synthetic phase in the mammalian nucleus. Exp. Cell Res. **165:**291–297.
44. **Nakayasu, H., and R. Berezney.** 1989. Mapping replicational sites in the eucaryotic cell nucleus. J. Cell Biol. **108:**1–11.
45. **Oleksiewicz, M. B., F. Costello, M. Huhtanen, J. B. Wolfinbarger, S. Alexandersen, and M. E. Bloom.** 1996. Subcellular localization of aleutian mink disease parvovirus proteins and DNA during permissive infection of Crandell feline kidney cells. J. Virol. **70:**3242–3247.
46. **Ornelles, D. A., and T. Shenk.** 1991. Localization of the adenovirus early region 1B 55-kilodalton protein during lytic infection: association with nuclear viral inclusions requires the early region 4 34-kilodalton protein. J. Virol. **65:**424–429.
47. **Pombo, A., J. Ferreira, E. Bridge, and M. Carmo-Fonseca.** 1994. Adenovirus replication and transcription sites are spatially separated in the nucleus of infected cells. EMBO J. **13:**5075–5085.
48. **Prasad, K. M., and J. P. Trempe.** 1995. The adeno-associated virus Rep78 protein is covalently linked to viral DNA in a preformed virion. Virology **214:**360–370.
49. **Quinlan, M. P., L. B. Chen, and D. M. Knipe.** 1984. The intranuclear localization of a herpes simplex virus DNA-binding protein is determined by the status of viral DNA replication. Cell **36:**857–868.
50. **Redemann, B. E., E. Mendelson, and B. J. Carter.** 1989. Adeno-associated virus rep protein synthesis during productive infection. J. Virol. **63:**873–882.
51. **Richardson, W. D., and H. Westphal.** 1981. A cascade of adenovirus early functions is required for expression of adeno-associated virus. Cell **27:**133–141.
52. **Rose, J. A., J. V. Maizel, J. K. Inman, and A. J. Shatkin.** 1971. Structural proteins of adeno-associated viruses. J. Virol. **8:**766–770.
53. **Ruffing, M., H. Zentgraf, and J. A. Kleinschmidt.** 1992. Assembly of viruslike particles by recombinant structural proteins of adeno-associated virus type 2 in insect cells. J. Virol. **66:**6922–6930.
54. **Shaw, P. J., and E. G. Jordan.** 1995. The nucleolus. Annu. Rev. Cell Dev. Biol. **11:**93–121.
55. **Singer, I.I., and S. L. Rhode.** 1978. Ultrastructural studies of H-1 parvovirus replication. VI. simultaneous audioradiographic and immunochemical intranuclear localization of viral DNA synthesis and protein accumulation. J. Virol. **25:**349–360.
56. **Singer, I.I., and H. W. Toolan.** 1975. Ultrastructural studies of H-1 parvovirus replication. I. Cytopathology produced in human NB epithelial cells and hamster embryo fibroblasts. Virology **65:**40–54.
57. **Snyder, R. O., R. J. Samulski, and N. Muzyczka.** 1990. In vitro resolution of covalently joined AAV chromosome ends. Cell **60:**105–113.
58. **Spector, D. L.** 1993. Macromolecular domains within the cell nucleus. Annu. Rev. Cell Biol. **9:**265–315.
59. **Staufenbiel, M., W. Deppert.** 1983. Different structural systems of the nucleus are targets for SV40 large T antigen. Cell **33:**173–181.
60. **Steinbach, S., A. Wistuba, T. Bock, and J. A. Kleinschmidt.** Assembly of adeno-associated virus type 2 (AAV-2) capsids in vitro. Submitted for publication.
61. **Thomas, J. O., and R. D. Kornberg.** 1975. An octamer of histones in chromatin and free in solution. Proc. Natl. Acad. Sci. USA **72:**2626–2630.
62. **Tratschin, J. D., I. L. Miller, and B. J. Carter.** 1984. Genetic analysis of adeno-associated virus: properties of deletion mutants constructed in vitro and evidence for an adeno-associated virus replication function. J. Virol. **51:**611–619.
63. **Tratschin, J. D., J. Tal, and B. J. Carter.** 1986. Negative and positive regulation in trans of gene expression from adeno-associated virus vectors in mammalian cells by a viral *rep* gene product. Mol. Cell. Biol. **6:**2884–2894.
64. **Walton, T. H., P. T. Moen, E. Fox, and J. W. Bodnar.** 1989. Interactions of minute virus of mice and adenovirus with host nucleoli. J. Virol. **63:**3651–3660.
65. **Weitzman, M. D., K. J. Fisher, and J. M. Wilson.** 1996. Recruitment of wild-type and recombinant adeno-associated virus into adenovirus replication centers. J. Virol. **70:**1845–1854.
66. **Wilcock, D., and D. P. Lane.** 1991. Localization of p53, retinoblastoma and host replication proteins at sites of viral replication in herpes-infected cells. Nature **349:**429–431.
67. **Wistuba, A., S. Weger, A. Kern, and J. A. Kleinschmidt.** 1995. Intermediates of adeno-associated virus type 2 assembly: identification of soluble complexes containing Rep and Cap proteins. J. Virol. **69:**5311–5319.
68. **Xing, Y., C. V. Johnson, P. R. Dobner, and J. B. Lawrence.** 1993. Higher level organization of individual gene transcription and RNA splicing. Science **259:**1326–1330.

JOURNAL OF VIROLOGY, May 2002, p. 4559–4566 Vol. 76, No. 9
0022-538X/02/$04.00+0 DOI: 10.1128/JVI.76.9.4559–4566.2002

Adeno-Associated Virus Capsids Displaying Immunoglobulin-Binding Domains Permit Antibody-Mediated Vector Retargeting to Specific Cell Surface Receptors

Martin U. Ried,[1] Anne Girod,[1] Kristin Leike,[1] Hildegard Büning,[1] and Michael Hallek[1,2,3]*

Laboratorium für Molekulare Biologie, Genzentrum,[1] and Medizinische Klinik III, Klinikum Grosshadern,[2] Ludwig-Maximilians-Universitaet Muenchen, and GSF-National Center for Research and Environment, KKG Gentherapie,[3] 81377 Munich, Germany

Received 10 September 2001/Accepted 18 January 2002

Recombinant adeno-associated virus type 2 (rAAV2) is a promising vector for human somatic gene therapy. However, its broad host range is a disadvantage for some applications, because it reduces the specificity of the gene transfer. To overcome this limitation, we sought to create a versatile rAAV vector targeting system which would allow us to redirect rAAV binding to specific cell surface receptors by simple coupling of different ligands to its capsid. For this purpose, an immunoglobulin G (IgG) binding domain of protein A, Z34C, was inserted into the AAV2 capsid at amino acid position 587. The resulting AAV2-Z34C mutants could be packaged and purified to high titers and bound to IgG molecules. rAAV2-Z34C vectors coupled to antibodies against CD29 (β_1-integrin), CD117 (c-kit receptor), and CXCR4 specifically transduced distinct human hematopoietic cell lines. In marked contrast, no transduction was seen in the absence of antibodies or in the presence of specific blocking reagents. These results demonstrate for the first time that an immunoglobulin binding domain can be inserted into the AAV2 capsid and coupled to various antibodies, which mediate the retargeting of rAAV vectors to specific cell surface receptors.

The human parvovirus adeno-associated virus type 2 (AAV2) has many features that make it attractive as a vector for human somatic gene therapy (9, 11). However, its broad host range might represent a limitation for some applications, because recombinant AAV (rAAV)-mediated gene transfer would not be specific for the tissue or cell type of interest. The host range is determined by the interaction of the AAV2 capsid with specific cellular receptors and coreceptors (18, 26, 27).

Recently, a hypothetical model of the AAV capsid was generated, and several regions which were exposed on the viral capsid accepted the insertion of an integrin-specific 14-amino-acid (aa) RGD ligand (L14) and bound to target cells expressing the corresponding receptor (6). Moreover, AAV2 vectors with a ligand insertion at site 587 infected wild-type AAV-resistant B16F10 melanoma cells with infectious targeting titers of 5×10^4 LacZ expression-forming units (EFU) per ml (multiplicity of infection, 1), indicating that the susceptibility of these cells to AAV2 infection was increased by at least 4 orders of magnitude (6).

However, with this approach it remained difficult and laborious to generate targeting vectors, because the design and optimization of new AAV capsid mutants were required for each specific receptor and cell type. Thus, it seemed desirable to generate a universal AAV targeting capsid on which different ligands could bind and redirect the virus to specific cell surface receptors (Fig. 1A). Such a vector would allow rapid screening of appropriate receptors mediating virus binding, uptake, and correct intracellular processing, which are all prerequisites for successful retargeting of AAV-based vectors.

For this purpose, an immunoglobulin G (IgG) binding domain was introduced into the capsid to enable AAV to bind different antibodies via their Fc regions. In these virus-antibody conjugates, the variable domain of the respective antibodies would function as a ligand directed against a specific cell surface receptor. A similar strategy has already been used for the retargeting of Sindbis virus vectors (15, 16). The IgG binding molecule chosen for our experiments was a minimized and optimized domain of protein A from *Staphylococcus aureus*, Z34C (25). Z34C is a 34-aa two-helix domain which shows only a twofold-reduced binding affinity in comparison to the natural B domain.

By use of Z34C insertion mutants, rAAV was retargeted to hematopoietic cell lines which were poorly transduced by rAAV carrying the wild-type capsid (10, 17) via a specific interaction with the cell surface receptor CD29 (β_1-integrin), CD117 (c-kit), or CXCR4 (13, 32).

MATERIALS AND METHODS

Plasmids. Plasmid pUC-AV2 was constructed by subcloning the 4.8-kb *Bgl*II fragment of pAV2 (12) (ATCC 37216) into the *Bam*HI site of pUC19 (New England Biolabs) by blunt-end ligation. It contained the full-length AAV2 genome and served as the parental plasmid for all constructs described in this report.

Plasmid pCap was obtained by blunt-end subcloning of the 2.2-kb *Eco*RI-*Bsp*MI fragment of pUC-AV2 into the *Eco*RI site of pUC19; therefore, it contained only the *cap* gene. It served as a template for all PCRs.

The mutated plasmids contained the full-length AAV2 genome; the Z34C-encoding sequence was inserted in the *cap* gene of the AAV2 genome after the sequence for amino acid 587 (p587Z34C) or in combination with a deletion of amino acids 581 to 589 after the sequence for amino acid 580 (p587Δ9Z34C). Mutagenesis was achieved by using an ExSite PCR-based site-directed mutagenesis kit as described by the supplier (Stratagene). For the two mutants, a PCR

* Corresponding author. Mailing address: Genzentrum, Universitaet Muenchen, Feodor-Lynen-Str. 25, D-81377 Munich, Germany. Phone: 49-89-2180-6774. Fax: 49-89-2180-6797. E-mail: mhallek@med3.med.uni-muenchen.de.

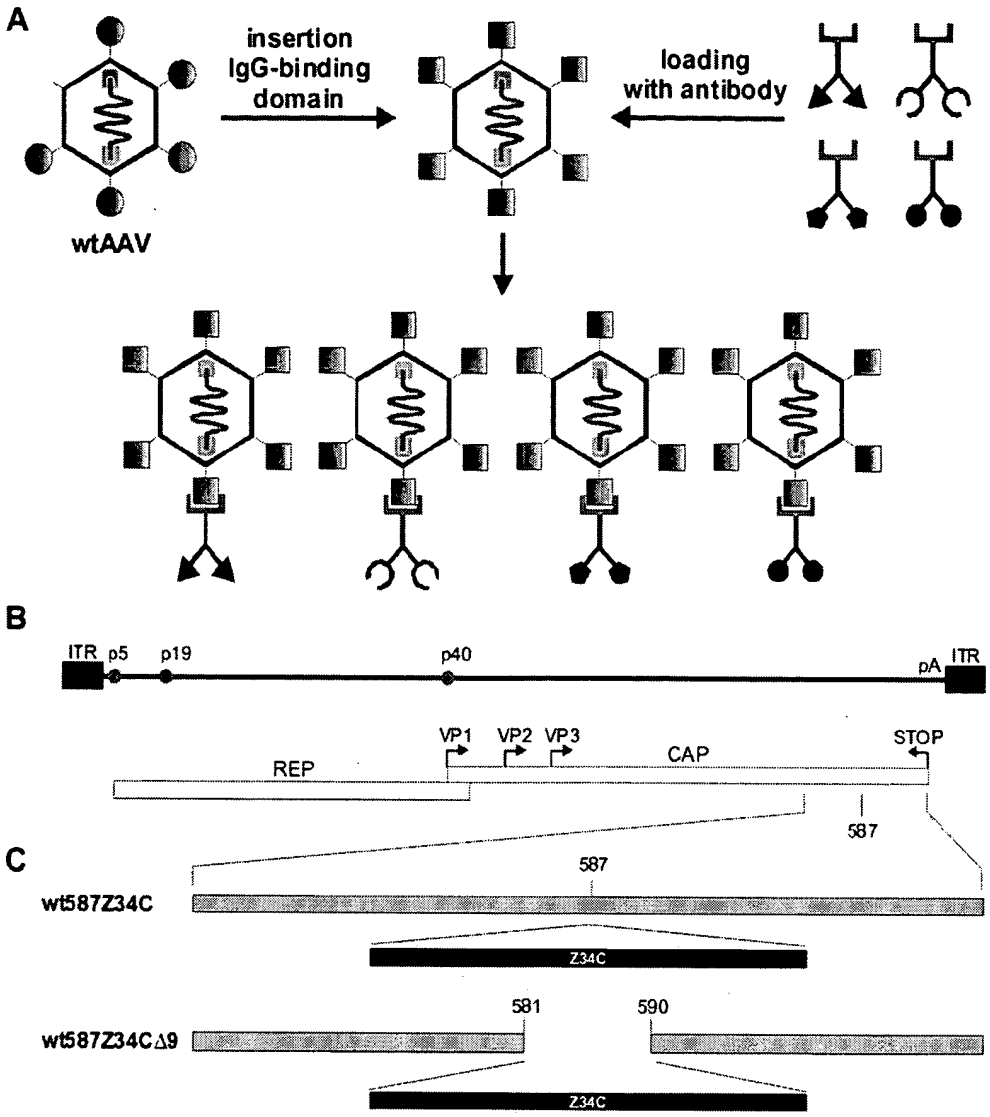

FIG. 1. (A) Strategy for retargeting AAV2 vectors with immunoglobulin-binding domains. The wild-type AAV2 (wtAAV) capsid is modified by insertion of the Z34C immunoglobulin binding domain. The mutated virus capsid is loaded with targeting antibodies against specific cell surface receptors. (B) Genomic structure of wild-type AAV2. The positions of the p5, p19, and p40 viral promoters and the polyadenylation signal (pA) are indicated. Symbols show ITRs, *rep* and *cap* coding regions, and initiation and stop codons for the VP1, VP2, and VP3 viral capsid proteins. (C) Schematic diagram of the generated Z34C capsid mutants. The insertion site at position 587, the deleted amino acids (positions 581 to 589), and the Z34C ligand are indicated.

fragment was generated by using plasmid pCap as the template and two primers: one (FOR) containing nucleotides belonging to the *cap* gene immediately upstream of the insertion site and some nucleotides coding for the 5′ portion of the Z34C ligand and the other (BACK) containing nucleotides belonging to the *cap* gene immediately downstream of the insertion site and some nucleotides coding for the 3′ portion of the Z34C peptide.

The following primers were used: 580Z34C-BACK (5′-ATTAGGATCGTGG AGGGCTTCGTAAAAGCGTGCGTTGACATTGCATATTAAAAGATACA GAACCATA-3′), 587Z34C-BACK (5′-ATTAGGATCGTGGAGGGCTTCGT AAAAGCGGCGTTGACATTGCATATTAAAGTTGCCTCTCTGGAG-3′), 587Z34C-FOR (5′-TTAAATGAAGAACAACGCAATGCCAAGATTAAGA GTATTCGCGATGATTGTAGACAAGCAGCTACC-3′), and 590Z34C-FOR (5′-TTAAATGAAGAACAACGCAATGCCAAGATTAAGAGTATTCGC GATGATTGTGCACTCCGCAGAT-3′).

The PCR products were amplified in bacteria and sequenced. The 1.4-kb *Eco*NI-*Xcm*I fragment containing the Z34-encoding sequence was then subcloned into pUC-AV2 from which the corresponding fragment encoding the wild-type *cap* sequence had been removed.

Plasmid pRC was constructed by blunt-end subcloning of the 4.5-kb *Xba*I-*Xba*I fragment of psub201(+) (22) (plasmid obtained from R. J. Samulski) into the *Pst*I-*Bam*HI sites of pSV40oriAAV (3).

Plasmids pRC587Z34C and pRC587Δ9Z34C were derived from plasmid pRC by subcloning of the *Eco*NI-*Xcm*I fragments of p587Z34C and p587Δ9Z34C into pRC from which the corresponding fragment had been removed. The plasmids contained the AAV2 *rep* and *cap* coding regions but lacked the viral inverted terminal repeats (ITRs); therefore, they allowed the production of helper-free AAV2-based vectors either with a wild-type AAV2 capsid (pRC) or with a capsid presenting the Z34C peptide.

Plasmid pGFP is an AAV2-based vector plasmid in which the AAV2 ITR sequences flank the hygromycin selectable marker gene controlled by the thy-

midine kinase promoter and the *Aequorea victoria* green fluorescence protein (GFP) gene promoted by the cytomegalovirus promoter. pGFP was generated by inserting the *Asp*718-*Not*I fragment of pEGFP-N1 (Clontech) into the *Asp*718-*Not*I sites of psub/CEP4(Sal inverse). psub/CEP4(Sal inverse) was a derivative of psub201(+) (22) that had been digested with *Xba*I, blunt ended, and ligated to a blunt-ended 3,923-bp *Sal*I-*Nru*I fragment of pCEP4(Sal inverse). pCEP4(Sal inverse) differs from pCEP4 (Invitrogen) by inversion of the *Sal*I-*Sal*I fragment from positions 8 to 1316.

Cell cultures. Cell lines HeLa (ATCC CCL-2), 293 (ATCC CRL-1573), and Jurkat (ATCC CRL-1990) were provided by the American Type Culture Collection. M-07e and Mec1 cells were described previously (1, 24) and were obtained from J. Griffin (Boston) and F. Caligaris-Cappio (Turin), respectively. They were maintained at 37°C in 5% CO_2 as monolayer cultures in Dulbecco's modified Eagle's medium (HeLa and 293) or as suspension cultures in RPMI 1640 medium (Jurkat, M-07e, and Mec1). The medium was supplemented with 10% fetal calf serum, 100 U of penicillin/ml, 100 μg of streptomycin/ml, 2 mM L-glutamine, and 10 ng of interleukin 3/ml (M-07e).

Production of AAV2 particles. 293 cells were seeded in 20 culture dishes (150-mm diameter, each containing 7.5×10^6 293 cells) and cotransfected by the calcium phosphate method with a total of 37.5 μg of vector plasmid (pGFP), packaging plasmid pRC, and adenovirus plasmid pXX6-80 (obtained from J. Samulski) at a 1:1:1 molar ratio. For viruses containing AAV *rep* and *cap* genes, plasmid pUC-AV2 or a mutated plasmid was transfected with pXX6-80 at a 1:1 molar ratio. After 24 h, the transfection medium was replaced with fresh Dulbecco's modified Eagle's medium containing 2% fetal calf serum, and the cells were incubated for 24 h at 37°C in 5% CO_2. Thereafter, cells were harvested and pelleted by low-speed centrifugation at 3,000 × *g*. Cells were resuspended in 150 mM NaCl–50 mM Tris-HCl (pH 8.5)–1 mM $MgCl_2$ and sonicated. Cell debris was spun down at 3,700 × *g* for 20 min at 4°C. The supernatant was purified by ammonium sulfate precipitation. Contaminants were precipitated with 35% ammonium sulfate. After centrifugation, the viral particles in the supernatant were precipitated in 55% ammonium sulfate. The pellet was resuspended in PBS-MK buffer (phosphate-buffered saline [PBS], 1 mM $MgCl_2$, 2.5 mM KCl) and loaded onto an iodixanol gradient (4, 31, 34). Briefly, the solution containing the resuspended virus was transferred into an Optiseal centrifuge tube (26 × 77 mm; Beckman) by layering in the following order: 7 ml of 15% iodixanol and 1 M NaCl in PBS-MK buffer, 5 ml of 25% iodixanol in PBS-MK buffer, 5 ml of 40% iodixanol in PBS-MK buffer and, finally, 6 ml of 60% iodixanol in PBS-MK buffer. All the iodixanol buffers, with the exception of the 40% buffer, contained phenol red. The tube was centrifuged in a type 70 Ti rotor (Beckman) at 69,000 rpm for 1 h at 18°C. The 40% iodixanol phase containing the virus was collected and dialyzed against PBS-MK buffer.

Titer determinations. The concentration of DNA containing viral particles was determined by DNA dot blot hybridization. AAV2 preparations were first incubated with 500 μg of DNase I/ml to remove DNA including putatively free viral genomes that could be subsequently hybridized with the probe. The viral preparations were then blotted in serial dilutions and finally hybridized with a random-primer *rep* or *gfp* probe by standard methods. Particle titers were determined by comparing the intensity of the hybridization signal with that obtained for a plasmid standard of a known concentration blotted on the same membrane.

The titer was also tested by an enzyme-linked immunosorbent assay (ELISA) with murine monoclonal antibody (MAb) A20, which recognizes only assembled capsids of AAV2 (7, 28). Purified MAb A20 (200 ng) was attached to Costar microtiter plates by overnight incubation at 4°C. After blocking with PBS containing 10% bovine serum albumin (BSA) and 0.05% Tween 20, serial dilutions of AAV2 preparations were added to the wells and incubated for 3 h at room temperature. After a wash with PBS, the wells were incubated with biotin-conjugated MAb A20 for 1 h at room temperature. After a second wash, the wells were incubated with peroxidase-conjugated streptavidin (Dianova) for 1 h at room temperature. After a wash, 100 μl of substrate solution (0.1 M sodium citrate buffer [pH 6.0] containing 0.1 μg of 3,3′,5,5′-tetramethylbenzidine and 0.003% H_2O_2) was added to each well. After 10 min, the reaction was stopped with 50 μl of 1 M H_2SO_4, and the light absorbance at 450 nm was measured with an automated microplate reader (MWG). Particle titers were determined by comparing the absorbance with that obtained for a viral preparation of a known titer (measured by electron microscopy) added to the same plate.

Electron microscopy. Electron microscopy was done at DKFZ, Heidelberg, Germany. Iodixanol gradient-purified and PBS-MK-dialyzed viral particles were adsorbed onto Formvar-carbon-coated copper grids and negatively stained with uranyl acetate. Empty capsids could be recognized as black viral particles, and full capsids were recognized as bright particles. Titers were calculated in comparison to a known viral standard.

TABLE 1. Capsid formation and natural tropism of the AAV2-Z34 capsid mutant virions

Virus	No. of genomic particles/ml	Infectious titer on HeLa cells[a]	No. of particles/ml	
			A20+ epitope[b]	EM capsid[c]
wtAAV2[d]	5×10^{13}	5×10^{9}	1×10^{12}	6×10^{13}
wt587Z34C[d]	2×10^{12}	3×10^{5}	1×10^{10}	3×10^{12}
wt587Δ9Z34C[d]	5×10^{13}	1×10^{6}	1×10^{11}	7×10^{13}
rAAV-GFP[e]	1×10^{12}	5×10^{7}	ND	ND
rAAV-GFP587Z34C[e]	5×10^{10}	2×10^{4}	ND	ND
rAAV-GFP587Δ9Z34C[e]	5×10^{10}	2×10^{4}	ND	ND

[a] Expressed as Rep EFU/ml for preparations with the viral *rep* gene or as GFP EFU/ml for preparations with the GFP transgene.
[b] Detection of A20-positive ($A20^+$) epitopes by an ELISA. ND, not done.
[c] Detection of capsid particles by electron microscopy (EM).
[d] Containing the wild-type AAV2 genome.
[e] Containing the GFP transgene.

IgG binding ELISA. The surface expression and functionality of the Z34C ligand on viral capsids was measured by an IgG binding ELISA. Serial dilutions of viral preparations were used to coat 96-well plates (Costar) overnight at 4°C and were blocked with PBS containing 2% BSA and 0.05% Tween. After a wash with PBS, biotinylated rabbit antibody (Dianova) was added (2.5 μg/ml in PBS, 100 μl/well), and the plates were incubated at room temperature for 1 h. Detection of Z34C-bound biotinylated antibody was performed as described above.

Infection assays and infectious titer determinations. For retargeting infection assays, 2×10^5 cells were seeded in 48-well plates and irradiated with 70 Gy from a ^{137}Cs gamma irradiation source (GSF, Grosshadern, Germany). Genomic viral particles (5×10^8) were incubated with 1 μg of targeting antibody, protein A (final concentration, 10 μg/ml), rabbit IgG (final concentration, 2 μg/ml), or heparin (final concentration, 100 μg/ml) for 30 min at room temperature. Cells were incubated with virus solution in 300 μl of serum-free medium for 60 min at 37°C in 5% CO_2 and then supplemented with 35 μl of serum. After 24 h, the infection solution was replaced with 1 ml of serum-containing medium. Titers were determined 48 h after infection by counting infected cells by fluorescence microscopy. The optimum of 1 μg of targeting antibody was determined in separate dilution experiments (data not shown). Infectious titers of virus stocks with the wild-type gene (Rep EFU) were determined by in situ detection of Rep protein synthesis in an immunofluorescence assay with anti-Rep antibody or by microscopic detection of virus containing a GFP transgene as described before (6, 8).

All transduction experiments were carried out at least three times.

RESULTS

Generation of AAV2-Z34C mutants. To retarget AAV2, the minimized Z34C protein A binding domain (25) was inserted into the *cap* gene at site 587. Site 587 was shown to accept the insertion of a targeting ligand, to express this ligand at the capsid surface, and to allow retargeting of AAV2 or rAAV vectors (6). The minimized Z34C domain was chosen because the size of the insertion at site 587 was limited to approximately 30 aa (unpublished data). One insertion at site 587 and one insertion in combination with a deletion of 9 aa were used in order to reduce the length of the loop predicted at this position by a hypothetical AAV surface model (6) (Fig. 1C).

AAV2-Z34C mutants package the viral genome, express Z34C at the capsid surface, and bind immunoglobulins. The two AAV2-Z34C mutants (wt587Z34C and wt587Δ9Z34C) were analyzed for their ability to package the viral genome. Each mutant could be efficiently packaged (Table 1). When analyzed by electron microscopy, both mutants showed a normal capsid morphology. However, two to three times more empty particles were detected with the mutants than with wild-type AAV2 (Fig. 2 and Table 1). To determine whether the

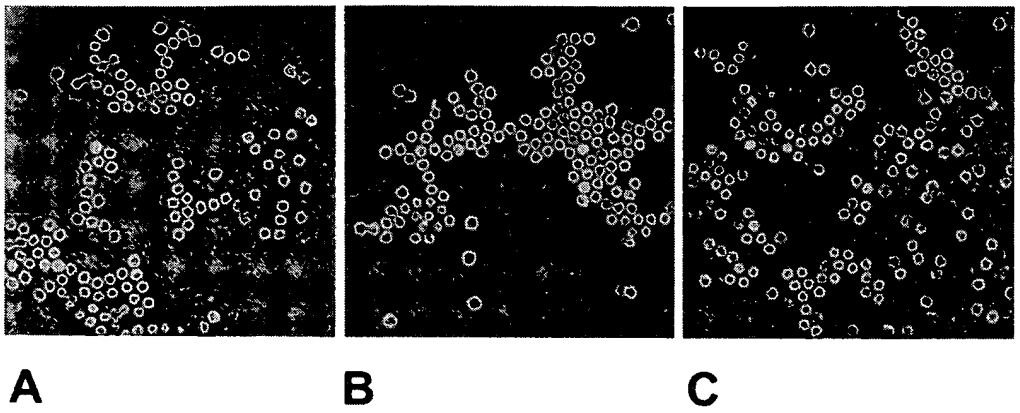

FIG. 2. Electron microscopy analysis of AAV2 and AAV2-Z34C mutants. (A) Wild-type AAV2. (B) wt587Z34C. (C) wt587Δ9Z34C. Empty capsids can be recognized as viral capsids with black centers. Titers were calculated in comparison to a known viral standard.

structures of wt587Z34C and wt587Δ9Z34C were similar to that of wild-type AAV2, we performed an ELISA with MAB A20, which specifically reacts with completely assembled AAV2 capsids and allows the calculation of wild-type analog AAV2 particles (28). A20 reacted with both mutants. Capsid titers of $>10^{11}$ particles/ml were achieved, a value which represented only a 5- to 11-fold reduction in the EM:$A20^+$ titer ratio compared to that for wild-type AAV2 (Table 1). Because the binding of the murine IgG1 constant region of A20 to Z34C is orders of magnitude less efficient than A20 variable region binding to specific viral surface epitopes, a disturbance of the A20-positive titer determination could be excluded (data not shown). In Western blot analysis, the distribution of VP1, VP2, and VP3 proteins in viral capsids was identical to that in wild-type AAV2, i.e., 1:1:10 (data not shown).

The infectivity of AAV2-Z34C mutants for HeLa cells, which were used as indicator cells for natural tropism, was reduced from 5×10^9 Rep EFU/ml (wild-type AAV2) to 3×10^5 Rep EFU/ml (wt587Z34C) and 1×10^6 Rep EFU/ml (wt587Δ9Z34C). Analogous results were achieved with recombinant vectors and with GFP as a transgene (Table 1).

Next, we wished to determine whether Z34C was expressed on the capsid surface and whether it was functional. Using an ELISA, wild-type AAV2 or AAV2-Z34C particles were directly attached to microtiter plates, and the binding of biotinylated antibodies from different species (human, rabbit, and mouse) was measured. With both mutants, specific immunoglobulin binding was observed, whereas wild-type AAV2 showed only weak, nonspecific binding. Figure 3 shows the binding of rabbit IgG in a representative experiment. The optical density was elevated at least three- to fivefold compared to that of the controls. Mutant wt587Z34C reacted considerably stronger with antibodies than wt587Δ9Z34C, suggesting that the combination of a 9-aa deletion with the insertion of Z34C was not advantageous in terms of immunoglobulin binding. Antibodies from other species (human and mouse IgG2a-IgG2b and rabbit IgG) bound with comparable affinities to both AAV2-Z34C mutants. The same differences in binding affinities were observed for the two mutants (data not shown).

Retargeting of rAAV to distinct hematopoietic cells. To evaluate the retargeting of the rAAV-Z34C mutants, the hematopoietic cell lines M-07e (acute myeloid leukemia with megakaryocytic differentiation; M7) (1), Jurkat (T-cell leukemia), and Mec1 (chronic lymphatic leukemia; B-CLL) (24) were selected, because previous work had demonstrated that a specific and/or efficient transduction of these cells by AAV2-derived vectors was difficult (Table 2) (2). The transduction of target cells with unmutated rAAV-GFP vectors yielded titers of 2×10^4 to 2×10^5 GFP EFU/ml (Table 2).

The hematopoietic cell surface receptors CD29 (β_1-integrin), CD117 (c-kit stem cell factor receptor), and CXCR4 (coreceptor of human immunodeficiency virus) were chosen as potential targeting receptors. For this purpose, we used a mouse anti-CD29 MAb (IgG2a; Immunotec), a rabbit poly-

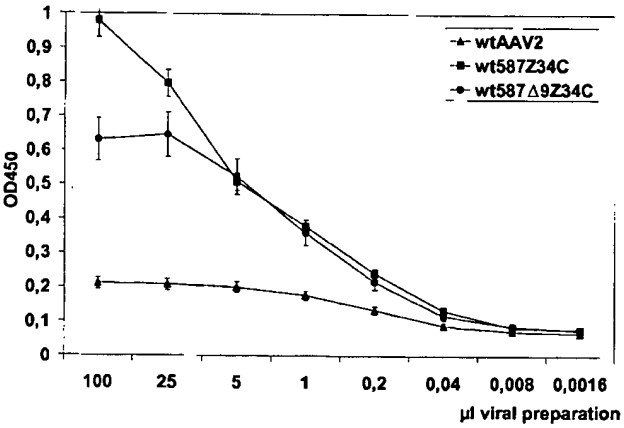

FIG. 3. Presentation and functionality of the Z34C ligand on AAV2 mutants. An ELISA was used to detect the Z34C ligand and its immunoglobulin binding affinity. The binding of rabbit IgG1 to wt587Z34C, wt587Δ9Z34C, and wild-type AAV2 (wtAAV2) is shown. Serial dilutions of viral preparations were used to coat 96-well plates overnight at 4°C and were blocked with PBS containing 2% BSA and 0.05% Tween. After a wash with PBS, biotinylated rabbit antibody was added (2.5 µg/ml in PBS), and the plates were incubated at room temperature for 1 h. Detection of Z34C-bound biotinylated antibody was performed as described in Material and Methods. Virus volumes are shown as titers in Table 1. OD450, optical density at 450 nm. Error bars show standard deviations.

TABLE 2. Retargeting to M-07e, Jurkat, and Mec1 cells by recombinant Z34C mutants and antibodies against CD29, CD117, and CXCR4[a]

Cells	Antibodies	Virus	Titer (GFP EFU/ml) under the following conditions[b]:				
			−/−/−	+/−/−	+/+/−	−/+/−	−/−/+
M-07e	CD117	rAAV-GFP	2×10^5	2×10^5	2×10^5	2×10^5	9×10^2
		rAAV-GFP587Z34C	<1	2×10^3	2×10^3	<1	<1
		rAAV-GFP587Δ9Z34C	<1	<1	ND	ND	ND
Jurkat	CD29	rAAV-GFP	2×10^4	2×10^4	2×10^4	2×10^4	<1
		rAAV-GFP587Z34C	<1	1×10^3	1×10^3	<1	<1
		rAAV-GFP587Δ9Z34C	<1	<1	ND	ND	ND
Jurkat	CXCR4	rAAV-GFP	2×10^4	2×10^4	2×10^4	2×10^4	<1
		rAAV-GFP587Z34C	<1	1×10^3	1×10^3	<1	<1
		rAAV-GFP587Δ9Z34C	<1	<1	ND	ND	ND
Mec1	CD29	rAAV-GFP	2×10^5	2×10^5	2×10^5	2×10^5	1×10^2
		rAAV-GFP587Z34C	<1	2×10^3	2×10^3	<1	<1
		rAAV-GFP587Δ9Z34C	<1	<1	ND	ND	ND
Mec1	CXCR4	rAAV-GFP	2×10^5	2×10^5	2×10^5	2×10^5	1×10^2
		rAAV-GFP587Z34C	<1	3×10^3	3×10^3	<1	<1
		rAAV-GFP587Δ9Z34C	<1	<1	ND	ND	ND
HeLa	—[c]	rAAV-GFP	5×10^7	5×10^7	5×10^7	5×10^7	8×10^2
		rAAV-GFP587Z34C	2×10^4	5×10^3	2×10^4	2×10^4	<1
		rAAV-GFP587Δ9Z34C	2×10^4	1×10^3	2×10^4	2×10^4	<1

[a] Control experiments were done with HeLa cells.

[b] Infections were done with (+) or without (−) targeting antibody/inhibitory protein A (10 μg/ml) or IgG (2 μg/ml)/AAV tropism-blocking heparin (100 μg/ml). No inhibition of transduction by the retargeting vectors was obtained with heparin. Inhibitory protein A or IgG was used independently and provided the same results. ND, not done.

[c] —, identical results were obtained with anti-CD29, anti-CXCR4, and anti-CD117 antibodies.

clonal anti-CD117 antiserum (ImoGenex), and a rabbit polyclonal anti-CXCR4 antiserum (N terminus specific; Chemicon). The expression of these target receptors on the surface of the target cell lines and the binding of the specific antibodies were confirmed by fluorescence-activated cell sorting analysis prior to testing in retargeting experiments (data not shown). All three receptors are known to mediate the uptake of their bound ligands and have already been used successfully for retargeting of other viruses (13, 32).

For transduction of hematopoietic cells, rAAV2-Z34C vectors (with GFP as a transgene) were loaded with the specific targeting antibodies and incubated for 24 h with irradiated target cells. Cells were analyzed for GFP gene expression 48 h after infection by fluorescence microscopy and flow cytometry. Specific retargeting was detected with mutant rAAV-GFP587Z34C on M-07e, Jurkat, and Mec1 cells. Different combinations of cells and antibodies against CD29, CD117, and CXCR4 were used to correspond to the different expression of these receptors on the different cell types, as shown in Table 2. Titers were estimated to be as high as 1×10^3 to 3×10^3 GFP EFU/ml. No retargeting or infection could be observed when the virus mutant was used without antibody (<1 GFP EFU/ml). rAAV2-Z34C transduction was specifically antibody mediated, because it could be blocked with soluble protein A or IgG molecules but not with heparin, which was used to block the natural receptor binding site of AAV2 (27).

Performing infection experiments by binding of virus-antibody complexes and inhibitory molecules at 4°C, washing, and shifting to 37°C did not affect or enhance transduction efficiency. In control experiments, antibodies against the targeted receptors did not enhance the infectivity of unmutated AAV2 vectors themselves (data not shown). No retargeting could be detected with mutant rAAV-GFP587Δ9Z34C. In addition, no retargeting was detected with antibodies against CD20, CD21, and HLA molecules. Infection of HeLa cells by AAV-Z34C mutants was reduced when the virus was loaded with any of the antibodies against targeting receptors not expressed on HeLa cells.

As an example, the retargeting and transduction of the B-CLL cell line Mec1 by the rAAV-GFP587Z34C vector conjugated to the anti-CXCR4 antibody are shown in Fig. 4. No transduction could be observed without the antibody (Fig. 4A), whereas the addition of the anti-CXCR4 antibody mediated specific, heparin-independent transduction of the cells (Fig. 4B).

DISCUSSION

This report presents a new AAV targeting strategy using a minimized domain of protein A and various antibodies binding to specific cell surface receptors. By insertion of an immunoglobulin binding domain into the capsid of AAV2, monoclonal or polyclonal antibodies were bound and allowed rAAV2 vectors expressing the GFP marker gene to be retargeted to specific hematopoietic cells.

The insertion size at AAV2 capsid position 578 is strictly limited (unpublished data). Therefore, we had to insert a relatively small coupling peptide into the AAV2 capsid. One possibility was the use of immunoglobulin binding proteins recognizing the Fc domain, since this would leave the variable

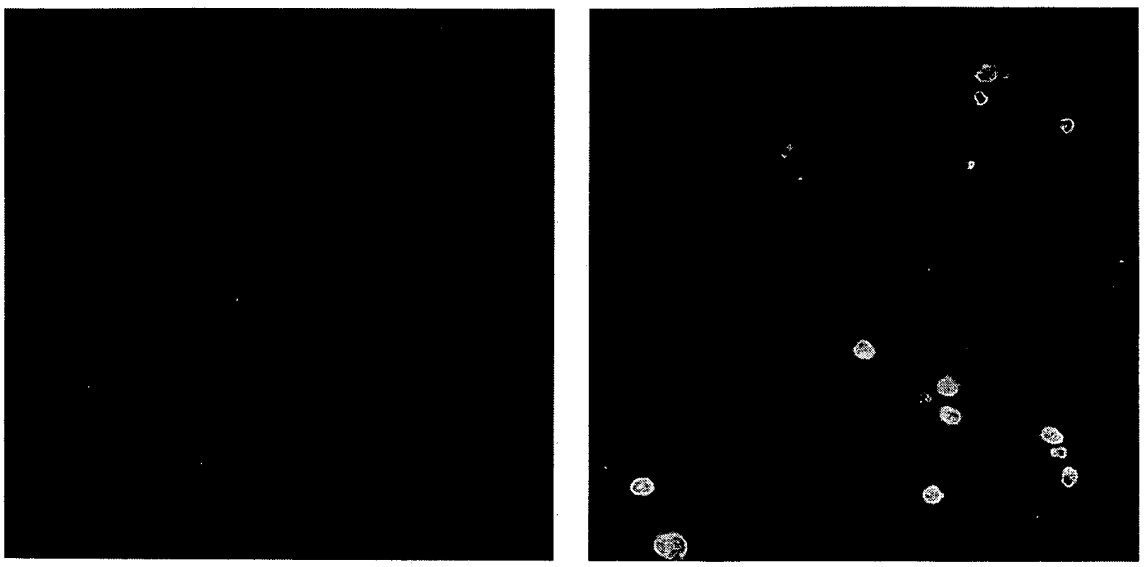

A B

FIG. 4. Transduction of Mec1 cells. Infection of Mec1 cells by rAAV-GFP587Z34C without (A) or with (B) anti-CXCR4 antibody was examined. Light microscopy was done with a confocal integrated GFP immunofluorescence overlay of infected cells.

domain of the immunoglobulin free for interacting with the specific cellular epitopes. Fortunately, a minimized binding motif of *S. aureus* protein A, Z34C, was described recently (25). Although the optimized Z34C domain of protein A shows a higher exchange rate, the binding affinity is reduced only twofold in comparison to that of the natural B domain. A large dimer of the Z domain of protein A was already used successfully for the retargeting of Sindbis virus (15, 16). The insertion of the Z34C ligand at position 587 resulted in a relatively modest reduction in packaging efficiency in comparison to that of the wild-type capsid (Table 1). The reduced packaging efficiency of the AAV2-Z34C mutants was explained at least in part by the generation of more empty capsids than were observed with the wild-type AAV2 capsid. This packaging efficiency also seemed to be affected by the size of the inserted ligand, because the combination of the insertion with a 9-aa deletion allowed packaging efficiency comparable to that of wild-type AAV2 to be maintained. Fortunately, the ligand insertion at position 587 did not affect the capsid morphology, as shown by electron microscopy and an ELISA specific for fully assembled capsids. Reduced packaging efficiency of mutants in combination with a transgene (GFP) was often observed with position 587 mutants (unpublished data). A hypothetical explanation of this observation is that the capsid stability of the position 587 mutants may be decreased.

Infection of HeLa cells, which was used to indicate the natural tropism of AAV2, was reduced up to 4 orders of magnitude. The explanation for this reduced infection via the wild-type AAV2 receptor is most likely disruption of the natural receptor binding site by the ligand insertion at position 587 (29). In heparin binding experiments, the affinity for heparin columns is reduced with all position 587 mutants (data not shown). However, in order to fully eliminate the natural host tropism, additional modifications of the viral capsid may be necessary. Infectivity for HeLa cells was reduced when Z34C mutants were loaded with targeting antibodies whose receptors were not expressed on HeLa cells. Epitopes on the viral capsid essential for natural receptor interactions probably were covered by the bound antibodies.

The insertion of Z34C at position 587 allowed functional expression of the immunoglobulin binding domain on the capsid surface. Both mutants wt587Z34C and wt587Δ9Z34C showed significant immunoglobulin binding. When added at comparable titers, wt587Z34C showed more effective antibody binding than wt587Δ9Z34C. Most likely, the reduced efficiency of antibody binding explained the failure of mutant wt587Δ9Z34C to transduce cells specifically.

The infection was specifically antibody mediated. No transduction could be detected with mutant rAAV2-GFP587Z34C without antibody, whereas the targeted infection could be blocked with soluble protein A or IgG molecules. In addition, no inhibition of transduction by the retargeting vectors was obtained with heparin, which blocks the natural receptor binding site of AAV2 (27). This result demonstrated that the interaction of the AAV2-Z34C mutants with the natural AAV receptor was not essential for infection or transduction and proved the altered infection profile and independence for HSPG (retargeting) (30). Although the transduction efficiency was reduced in comparison to that of the wild-type AAV2 capsid, the specificity of transduction was highly increased and could be targeted to specific receptors expressed on hematopoietic cells. This study provides the first demonstration that rAAV vectors can be targeted to specific cell receptors by use of a universal targeting approach.

Until now, targeting of viral vectors to hematopoietic cells has been tried by using retroviruses with short ligands or an-

tibody single-chain fragments inserted into the virus envelope (21). Engelstädter et al., who transduced Jurkat cells with a retrovirus targeted with antibody domains from a phage display library (5), achieved titers of up to 3×10^5 EFU/ml. The protein A targeting strategy used by Ohno et al. with the Z domain and Sindbis virus resulted in infectious titers of up to 2×10^5 infectious particles per ml with antibodies against CD4-positive cells (15, 16).

Different strategies were used in two recent studies to retarget AAV2 to hematopoietic cells. Yang et al. added the single-chain fragment variable region of an anti-CD34 MAb to the N terminus of the VP2 capsid protein (33). Although they obtained retargeted AAV2 virions, they achieved only low titers of up to 4×10^2 infectious virions per ml. A single-chain fragment variable region–VP2 fusion protein was used. Nonmutated capsid proteins were needed for virus assembly. This procedure made the composition of the viral capsid unpredictable. Another approach to retargeting of AAV2 is the use of bispecific antibodies recognizing the AAV2 capsid (through one Fab arm) and the alternative target cell surface receptor (through the other Fab arm) (2). This strategy allowed the transduction of the megakaryocytic leukemia cell line M-07e via the vector-bispecific antibody complex. However, it remains difficult and time-consuming to establish new bispecific antibodies for each cell type and targeting approach.

Recently, several groups tried to characterize the AAV2 capsid by random insertional mutagenesis or antibody epitope mapping (14, 19, 20, 30). Although these studies provided important insights into potential receptor binding sites and confirmed the relevance of position 587 as a virus receptor binding site (6, 29), no cell-type-specific retargeting was achieved. The results of this study may be a first step toward specific retargeting of rAAV2 to hematopoietic cells. Another practical application of this system may be the ability to rapidly and efficiently purify the rAAV587Z34C capsid on an affinity column. The insertion of immunoglobulin binding domains into the AAV2 capsid may provide a fast and universal targeting strategy for AAV2 vectors, in particular, for ex vivo gene transfer into hematopoietic cells. With these vectors, it may be possible to transduce specific hematopoietic cells. In addition, we will test different strategies for covalent coupling of antibodies to the viral capsid in order to use this system for an in vivo approach in the future. In addition, we will characterize the uptake mechanism for these specific targeting constructs by single virus tracing (23).

Taken together, this study provides the first demonstration that rAAV vectors can be targeted to specific cell surface receptors by use of a universal targeting approach with immunoglobulin binding domains. Given this proof of principle, our group is currently testing additional capsid mutants and immunoglobulin binding domains in order to combine high targeting specificity with higher transduction efficiency.

ACKNOWLEDGMENTS

We are grateful to Jürgen Kleinschmidt and Christiane Wobus (DKFZ) for providing AAV-specific antibodies and performing electron microscopy of AAV mutants.

This work was supported by a grant from the Deutsche Forschungsgemeinschaft (SFB 455) (to M.H.) and by stipends from the Studienstiftung des Deutschen Volkes and the Fond der Chemischen Industrie (BMBF) (to M.U.R.)

REFERENCES

1. **Avanzi, G. C., M. F. Brizzi, J. Giannotti, A. Ciarletta, Y. C. Yang, L. Pegoraro, and S. C. Clark.** 1990. M-07e human leukemic factor-dependent cell line provides a rapid and sensitive bioassay for the human cytokines GM-CSF and IL-3. J. Cell Physiol. **145**:458–464.
2. **Bartlett, J. S., J. Kleinschmidt, R. C. Boucher, and R. J. Samulski.** 1999. Targeted adeno-associated virus vector transduction of nonpermissive cells mediated by a bispecific $F(ab'\gamma)_2$ antibody. Nat. Biotechnol. **17**:181–186.
3. **Chiorini, J. A., C. M. Wendtner, E. Urcelay, B. Safer, M. Hallek, and R. M. Kotin.** 1995. High-efficiency transfer of the T cell co-stimulatory molecule B7-2 to lymphoid cells using high-titer recombinant adeno-associated virus vectors. Hum. Gene Ther. **6**:1531–1541.
4. **Conway, J. E., C. M. Rhys, I. Zolotukhin, S. Zolotukhin, N. Muzyczka, G. S. Hayward, and B. J. Byrne.** 1999. High-titer recombinant adeno-associated virus production utilizing a recombinant herpes simplex virus type I vector expressing AAV-2 Rep and Cap. Gene Ther. **6**:986–993.
5. **Engelstädter, M., M. Bobkova, M. Baier, J. Stitz, N. Holtkamp, T. H. Chu, R. Kurth, R. Dornburg, C. J. Buchholz, and K. Cichutek.** 2000. Targeting human T cells by retroviral vectors displaying antibody domains selected from a phage display library. Hum. Gene Ther. **11**:293–303.
6. **Girod, A., M. Ried, C. Wobus, H. Lahm, K. Leike, J. Kleinschmidt, G. Deleage, and M. Hallek.** 1999. Genetic capsid modifications allow efficient re-targeting of adeno-associated virus type 2. Nat. Med. **5**:1052–1056.
7. **Grimm, D., A. Kern, M. Pawlita, F. Ferrari, R. Samulski, and J. Kleinschmidt.** 1999. Titration of AAV-2 particles via a novel capsid ELISA: packaging of genomes can limit production of recombinant AAV-2. Gene Ther. **6**:1322–1330.
8. **Hacker, U. T., F. M. Gerner, H. Buning, M. Hutter, H. Reichenspurner, M. Stangl, and M. Hallek.** 2001. Standard heparin, low molecular weight heparin, low molecular weight heparinoid, and recombinant hirudin differ in their ability to inhibit transduction by recombinant adeno-associated virus type 2 vectors. Gene Ther. **8**:966–968.
9. **Hallek, M., and C. M. Wendtner.** 1996. Recombinant adeno-associated virus (rAAV) vectors for somatic gene therapy: recent advances and potential clinical applications. Cytokines Mol. Ther. **2**:69–79.
10. **Handa, A., S. Muramatsu, J. Qiu, H. Mizukami, and K. E. Brown.** 2000. Adeno-associated virus (AAV)-3-based vectors transduce haematopoietic cells not susceptible to transduction with AAV-2-based vectors. J. Gen. Virol. **81**:2077–2084.
11. **Kotin, R. M.** 1994. Prospects for the use of adeno-associated virus as a vector for human gene therapy. Hum. Gene Ther. **5**:793–801.
12. **Laughlin, C. A., J. D. Tratschin, H. Coon, and B. J. Carter.** 1983. Cloning of infectious adeno-associated virus genomes in bacterial plasmids. Gene **23**: 65–73.
13. **Mebatsion, T., S. Finke, F. Weiland, and K. K. Conzelmann.** 1997. A CXCR4/CD4 pseudotype rhabdovirus that selectively infects HIV-1 envelope protein-expressing cells. Cell **90**:841–847.
14. **Moskalenko, M., L. Chen, M. van Roey, B. A. Donahue, R. O. Snyder, J. G. McArthur, and S. D. Patel.** 2000. Epitope mapping of human anti-adeno-associated virus type 2 neutralizing antibodies: implications for gene therapy and virus structure. J. Virol. **74**:1761–1766.
15. **Ohno, K., and D. Meruelo.** 1997. Retrovirus vectors displaying the IgG-binding domain of protein A. Biochem. Mol. Med. **62**:123–127.
16. **Ohno, K., K. Sawai, Y. Iijima, B. Levin, and D. Meruelo.** 1997. Cell-specific targeting of Sindbis virus vectors displaying IgG-binding domains of protein A. Nat. Biotechnol. **15**:763–767.
17. **Ponnazhagan, S., P. Mukherjee, X. S. Wang, K. Qing, D. M. Kube, C. Mah, C. Kurpad, M. C. Yoder, E. F. Srour, and A. Srivastava.** 1997. Adeno-associated virus type 2-mediated transduction in primary human bone marrow-derived $CD34^+$ hematopoietic progenitor cells: donor variation and correlation of transgene expression with cellular differentiation. J. Virol. **71**:8262–8267.
18. **Qing, K., C. Mah, J. Hansen, S. Zhou, V. Dwarki, and A. Srivastava.** 1999. Human fibroblast growth factor receptor 1 is a co-receptor for infection by adeno-associated virus 2. Nat. Med. **5**:71–77.
19. **Rabinowitz, J. E., and R. J. Samulski.** 2000. Building a better vector: the manipulation of AAV virions. Virology **278**:301–308.
20. **Rabinowitz, J. E., W. Xiao, and R. J. Samulski.** 1999. Insertional mutagenesis of AAV2 capsid and the production of recombinant virus. Virology **265**:274–285.
21. **Russell, S. J., and F. L. Cosset.** 1999. Modifying the host range properties of retroviral vectors. J. Gene Med. **1**:300–311.
22. **Samulski, R. J., L. S. Chang, and T. Shenk.** 1987. A recombinant plasmid from which an infectious adeno-associated virus genome can be excised in vitro and its use to study viral replication. J. Virol. **61**:3096–3101.
23. **Seisenberger, G., M. U. Ried, T. Endress, H. Buning, M. Hallek, and C. Brauchle.** 2001. Real-time single-molecule imaging of the infection pathway of an adeno-associated virus. Science **294**:1929–1932.
24. **Stacchini, A., M. Aragno, A. Vallario, A. Alfarano, P. Circosta, D. Gottardi, A. Faldella, G. Rege-Cambrin, U. Thunberg, K. Nilsson, and F. Caligaris-Cappio.** 1999. MEC1 and MEC2: two new cell lines derived from B-chronic

lymphocytic leukaemia in prolymphocytoid transformation. Leuk. Res. **23:** 127–136.

25. **Starovasnik, M. A., A. C. Braisted, and J. A. Wells.** 1997. Structural mimicry of a native protein by a minimized binding domain. Proc. Natl. Acad. Sci. USA **94:**10080–10085.
26. **Summerford, C., J. S. Bartlett, and R. J. Samulski.** 1999. AlphaVbeta5 integrin: a co-receptor for adeno-associated virus type 2 infection. Nat. Med. **5:**78–82.
27. **Summerford, C., and R. J. Samulski.** 1998. Membrane-associated heparan sulfate proteoglycan is a receptor for adeno-associated virus type 2 virions. J. Virol. **72:**1438–1445.
28. **Wistuba, A., A. Kern, S. Weger, D. Grimm, and J. A. Kleinschmidt.** 1997. Subcellular compartmentalization of adeno-associated virus type 2 assembly. J. Virol. **71:**1341–1352.
29. **Wobus, C. E., B. Hugle-Dorr, A. Girod, G. Petersen, M. Hallek, and J. A. Kleinschmidt.** 2000. Monoclonal antibodies against the adeno-associated virus type 2 (AAV-2) capsid: epitope mapping and identification of capsid domains involved in AAV-2–cell interaction and neutralization of AAV-2 infection. J. Virol. **74:**9281–9293.
30. **Wu, P., W. Xiao, T. Conlon, J. Hughes, M. Agbandje-McKenna, T. Ferkol, T. Flotte, and N. Muzyczka.** 2000. Mutational analysis of the adeno-associated virus type 2 (AAV2) capsid gene and construction of AAV2 vectors with altered tropism. J. Virol. **74:**8635–8647.
31. **Xiao, X., J. Li, and R. J. Samulski.** 1998. Production of high-titer recombinant adeno-associated virus vectors in the absence of helper adenovirus. J. Virol. **72:**2224–2232.
32. **Yajima, T., T. Kanda, K. Yoshiike, and Y. Kitamura.** 1998. Retroviral vector targeting human cells via c-Kit–stem cell factor interaction. Hum. Gene Ther. **9:**779–787.
33. **Yang, Q., M. Mamounas, G. Yu, S. Kennedy, B. Leaker, J. Merson, F. Wong-Staal, M. Yu, and J. R. Barber.** 1998. Development of novel cell surface CD34-targeted recombinant adenoassociated virus vectors for gene therapy. Hum. Gene Ther. **9:**1929–1937.
34. **Zolotukhin, S., B. J. Byrne, E. Mason, I. Zolotukhin, M. Potter, K. Chesnut, C. Summerford, R. J. Samulski, and N. Muzyczka.** 1999. Recombinant adeno-associated virus purification using novel methods improves infectious titer and yield. Gene Ther. **6:**973–985.

ARTICLE

doi:10.1006/mthe.2001.0345, available online at http://www.idealibrary.com on IDEAL

Incorporation of Tumor-Targeting Peptides into Recombinant Adeno-associated Virus Capsids

Mirta Grifman,* Martin Trepel,†,[1] Paul Speece,*,‡ Luz Beatriz Gilbert,* Wadih Arap,† Renata Pasqualini,† and Matthew D. Weitzman*,[2]

*Laboratory of Genetics, The Salk Institute for Biological Studies, La Jolla, California 92186
†Department of GU Medical Oncology, University of Texas M. D. Anderson Center, Houston, Texas 77030
‡School of Medicine, University of California at San Diego, La Jolla, California 92093

Received for publication February 20, 2001; accepted in revised form May 7, 2001

The human parvovirus adeno-associated virus type 2 (AAV-2) possesses many features that make it an attractive vector for gene delivery *in vivo*. However, its broad host range may limit its usefulness and effectivity in several gene therapy applications in which transgene expression needs to be limited to a specific organ or cell type. In this study, we explored the possibility of directing recombinant AAV-2 transduction by incorporating targeting peptides previously isolated by *in vivo* phage display. Two putative loops within the AAV-2 capsid were examined as sites for incorporation of peptides. We tested the effects of deleting these loops and different strategies for the incorporation of several targeting peptides. The tumor-targeting sequence NGRAHA and a Myc epitope control were incorporated either as insertions or as replacements of the original capsid sequence. Viruses were assessed for packaging, accessibility of incorporated peptides, heparin binding, and transduction in a range of cell lines. Whereas recombinant viruses containing mutant capsid proteins were produced efficiently, transduction of several cell lines was significantly impaired for most modifications. However, certain mutants containing the peptide motif NGR, which binds CD13 (a receptor expressed in angiogenic vasculature and in many tumor cell lines), displayed an altered tropism toward cells expressing this receptor. Based on this work and previous studies, possible strategies for achieving *in vivo* targeting of recombinant AAV-2 are discussed.

INTRODUCTION

Adeno-associated virus type 2 (AAV-2) is a human parvovirus being developed into a promising delivery system for gene therapy applications. Recombinant adeno-associated virus (rAAV) vectors possess a number of attractive features, including lack of pathogenicity, ability to transduce both dividing and nondividing cells, and long-term transgene expression *in vitro* and *in vivo* (reviewed in 1, 2). rAAV vectors have been used to achieve expression of a large number of genes in a variety of cells and organs, including muscle, liver, brain, and lung (3–6). The wide host range of AAV may prove to be disadvantageous for systemic gene therapy, since it will result in transduction and possibly integration of the recombinant genome in unwanted cells and tissues. The ability to redirect rAAV infectivity and host range will circumvent these problems and may also enable the administration of lower doses of vector. Certain tissues and cell types are naturally resistant to rAAV transduction. These include human leukemia cell lines, airway epithelia, and $CD34^+$ cells (7–11). This may be due to the absence of receptors for AAV or other intracellular factors involved in infection. Heparan sulfate proteoglycan has been reported to be the primary attachment receptor for AAV-2 (12). In addition, human fibroblast growth factor receptor 1 (FGFR-1) and $\alpha_V\beta_5$ integrin have been proposed to act as secondary receptors (13, 14). Following receptor binding, AAV-2 particles enter the cell via receptor-mediated endocytosis through clathrin-coated pits, and dynamin is also involved in AAV-2 trafficking through the cytoplasm via microfilaments and microtubules (15–17). Most of the virus particles accumulate in a perinuclear pattern, with a slow entry of intact virions into the nucleus (17–19).

AAV particles have a diameter of 20–25 nm and contain a single-stranded genome of approximately 4700 nucleotides (20–22). The genome contains two open reading

[1] Present address: Department of Hematology and Oncology, The University of Freiburg Medical Center, Freiburg, Germany.

[2] To whom correspondence and reprint requests should be addressed at the Laboratory of Genetics, Salk Institute for Biological Studies, P.O. Box 85800, San Diego, CA 92186-5800. Fax: (858) 558 7454. E-mail: weitzman@salk.edu.

1525-0016/01 $35.00

frames, designated *rep* and *cap*, flanked by inverted terminal repeats which contain all the *cis* requirements for replication and packaging (23). Using alternate splicing and different translational initiation codons the virus generates three structural proteins, VP1, VP2, and VP3, from the cap gene (24). The small icosahedral capsid is composed of 60 subunits with a relative stoichiometry of 1:1:10 for VP1, VP2, and VP3. Although the three-dimensional structure of the AAV capsid has not yet been determined, those of some related parvoviruses have been solved by X-ray crystallography. The atomic structures are known for canine parvovirus (CPV) (25), feline panleukopenia virus (26), minute virus of mice (27), and the human parvovirus B19 (28). Parvoviral capsids contain a core structure comprising an eight-stranded β-barrel motif, similar to other icosahedral viruses. Between several strands of the β-barrel are large insertions that make up the majority of the capsid's surfaces. The surface features of the CPV capsid include a hollow cylinder at the fivefold axis of symmetry which is surrounded by a circular depression (canyon), a prominent protrusion at the threefold axis of symmetry (threefold spike), and a depression (dimple), spanning the twofold axis of symmetry. Alignments of parvoviral capsids reveal a high sequence conservation in the strands which make up the β-barrel motif (29). In contrast, sequence homologies in regions that code for the surface of the capsid are lower, consistent with an involvement in determining the different viral host ranges. Despite a divergence in sequence, antigenic sites are often located in analogous regions. Recently, several antigenic regions of AAV-2 have been mapped (30, 31) and their involvement in AAV-2-cell interaction and neutralization of AAV-2 infection was studied. Based on sequence alignments, most antigenic peptides in AAV correspond to similarly exposed regions in the different parvoviruses and they putatively map to the cylinder, the threefold spike loop, and the region between the twofold depression and the threefold spike (30, 31).

Strategies currently being explored for targeting viral vectors include bispecific conjugates and genetically modified capsids. Both of these approaches have recently been adapted for rAAV vectors (reviewed in 31a). In one study bispecific antibodies recognizing the AAV-2 viral capsid and a specific cell surface receptor were employed to retarget AAV-2 to human megakaryocytes that were nonpermissive for normal AAV infection (9). The use of bispecific conjugates is not always amenable to scale-up for clinical production and they also suffer from instability *in vivo*. Therefore a more attractive approach to vector retargeting is the genetic incorporation of targeting peptides into the rAAV capsid. The first attempt at expanding the tropism of AAV fused the single-chain variable fragment of a monoclonal antibody against human CD34 protein onto the N-terminus of the VP2 capsid protein and demonstrated improved infectivity of hematopoietic progenitor cells (32). Several recent reports have begun to address structural features of AAV capsids in order to identify sites amenable to incorporation of peptides. One study suggested six possible sites in the AAV capsid that were predicted to be within surface loops (33). A 14-amino-acid targeting peptide (L14) containing an RGD sequence was inserted into these sites and virus was produced. In three mutants the peptide was exposed on the capsid surface and one of these showed preferential transduction of integrin-expressing cells. Rabinowitz *et al.* employed linker insertional mutagenesis to place small peptide sequences (three to five amino acids) randomly across the entire capsid coding region (34). Mutants fell into three phenotypic groups, depending on their ability to assemble capsids, package DNA, and transduce cells. Recently, Wu *et al.* reported a broad mutational analysis of the AAV-2 capsid that identified several sites amenable to the incorporation of peptides (35). They also identified regions involved in heparin binding and were able to demonstrate altered tropism of viruses engineered to contain the serpin receptor ligand. It has been shown that the accessibility of incorporated peptides can also be affected by the composition of flanking residues (J. Bartlett, personal communication).

A combination of two important parameters will determine the success of genetically modified capsids for retargeting viral vectors *in vivo*. The first decision is to choose the location for insertions. The site must be such that (i) assembly and packaging of the virus capsid are not affected and (ii) peptides must be exposed on the surface of the virus. The second parameter is the choice of targeting peptide. In order for a rAAV vector to be directed to a specific tissue following intravenous administration it will require (i) that its natural tropism be diminished and (ii) that it contains a ligand that will recognize a receptor accessible through the circulation and selectively expressed in the organ or tissue of interest. The versatility of phage display technology has made it possible to screen for targeting peptides *in vivo*. The screening process involves injecting a phage library into an experimental animal and rescuing phage from the desired target by infecting host bacteria with tissue extract. Repeated selection yields phage that home preferentially to the target tissue (36, 37). Thus far, this method has been used to explore the vascular specificity of various peptides after their intravenous injection into mice and rats. Peptides capable of homing to the vasculature of organs and tumor tissues have been identified in this manner, attesting to the power of the method (36–38). Peptides targeting selective markers in the vasculature of specific organs or tissues are therefore attractive for incorporation into recombinant viral vectors for targeted gene delivery.

In this study we have explored genetic modification of the AAV-2 capsid by introducing a peptide motif, NGR, which targets a receptor, CD13 (39), that is specifically upregulated in angiogenic vasculature. CD13 is a key regulator of angiogenesis and functions as a vascular receptor for the NGR motif in activated blood vessels (39). The NGR motif has been successfully employed to enhance the antitumor properties of doxorubicin and tumor necrosis factor (TNF) (38, 40). Based on sequence homologies and on the results of previous studies, we chose two sites corresponding to CPV loops 3 and 4 (25). We eval-

uated the impact of deletions, replacements, and insertions within these loops. We inserted sequences coding for the motif NGR (38, 39), other organ-homing peptides (36, 37, 41), or a Myc epitope tag. Recombinant AAV vectors expressing reporter genes were generated with modified Cap proteins and analyzed for virus production, heparin binding, and transduction assays. We show by immunoprecipitation of epitope-tagged virions that these loops are presented on the surface of the capsid, although the degree of accessibility varied. Deletions, modifications, or insertions within the loops did not affect virus production. Deletion and large insertions at one of the loops abolished heparin binding. Transduction of several cell lines was significantly impaired for most deletions, mutations, and insertions. However, several mutants containing the NGR peptide displayed an altered tropism toward cells expressing CD13. These results are discussed in light of recently reported data, to suggest strategies for the incorporation of targeting peptides for systemic gene therapy.

MATERIALS AND METHODS

Plasmids. Plasmid pXX2 (42) was used as a template for the construction of all modified capsids. Plasmids with deletions of the loop regions (pXX2-ΔLoopIII and -ΔLoopIV) were generated by elongation PCR, introducing novel *MluI* and *SpeI* sites as shown in Fig. 2. The restriction sites were designed to allow for the in-frame insertion of oligonucleotides coding for foreign epitopes. All replacements and insertions were generated from these plasmids, except for insertions at the 588 site, which were cloned using a novel *SpeI* site introduced at nucleotide 3967 of AAV2 (GenBank Accession No. AF043303). All mutated plasmids were sequenced using an automated ABI Prism DNA sequencer 377 (PE Biosystems, Foster City, CA). Plasmid pXX6 supplies the adenovirus helper proteins for rAAV production (43) and pAAV-GFP contains a recombinant AAV genome with the green fluorescent protein flanked by viral inverted terminal repeats and expressed from a cytomegalovirus promoter.

Cell culture, transfection, and virus production. All cell lines were maintained in Dulbecco's modified Eagle's medium supplemented with 10% fetal bovine serum (FBS). Transfections were performed by calcium phosphate precipitation according to standard protocols and repeated multiple times. To produce rAAV with mutant capsid proteins, we transfected 293T cells with three plasmids: pXX2, which supplied wild-type or mutant capsid proteins; pXX6, which contained the adenovirus helper functions; and pAAV-GFP. For virus production 5 × 15-cm plates were transfected each with 6 μg pXX2, 25 μg pXX6, and 19 μg pAAV-GFP and incubated at 37°C for 72 h. Virus was purified using iodixanol gradients as described elsewhere (44). Wild-type adenovirus type 5 (Ad5) used for titration of transduction was propagated in 293 cells and purified by sequential rounds of ultracentrifugation in CsCl gradients. Titers of Ad5 were determined by plaque assays on 293 cells.

Virus titers, transduction assays, and FACS analysis. The titer of rAAV genome-containing particles per milliliter was determined by real-time PCR using SYBR Green I double-stranded DNA binding dye and an ABI Prism 7700 Sequence Detection System (PE Biosystems). Samples were prepared as previously described (45). The following primers were chosen to amplify eGFP: F1, CTGCTGCCCGACAACCA, and R2, CCATGTGATCGCGCTTCTC).

To assess transduction, cells grown in 24-well dishes were infected with rAAV (100–10,000 genomes/cell) and Ad5 (5 plaque forming units/cell) in fresh medium with 10% FBS. Ad5 co-infection was used to maximize transduction by rAAV by enhancement of second-strand synthesis as previously reported (54). Transduction by rAAV-GFP was determined by counting green cells using an Axiovert25 microscope (Carl Zeiss, Thornwood, NY) equipped with an OSRAM HBO mercury short arc lamp microscope or by FACS analysis using a Becton-Dickinson FACScan (San Jose, CA) with a 488-nm laser excitation. Transduction was measured 24–48 h following infection. Cells were photographed using a Nikon (Garden City, NY) microscope in conjunction with a charge-coupled device camera (Cooke Sensicam; Cooke Corp., Tonawanda, NY) and images were captured using SlideBook (Intelligent Imaging Innovation, Denver, CO). All transduction experiments were repeated at least three times. Expression of CD13 was measured by FACS using the antibody WM15 (Pharmingen, San Diego, CA). Each cell type was gated based on the fluorescence obtained when incubated with mouse IgG antibody. Mouse anti-β1 integrin, clone P4C10 (Life Technologies, Rockville, MD), was used as a positive control (100% gated).

Gel electrophoresis, Western blotting, immunoprecipitations, and heparin binding assays. An equal number of purified rAAV-GFP virions (10^9 genome-containing particles) were separated on 8% SDS-polyacrylamide gels and Western blotting was performed to detect capsid proteins. In all cases proteins were detected by enhanced chemiluminescence (NEN, Boston, MA, and Amersham, Buckinghamshire, UK) according to the manufacturer's instructions. AAV capsid proteins were detected with mAb B1 (American Research Products (ARP), Belmont, MA). Immunoprecipitations were performed from iodixanol-purified rAAV. Equivalent amounts of purified virus (10^{10} genome-containing particles) were precleared with protein G-Sepharose (Amersham/Pharmacia, Piscataway, NJ) for 1 h at 4°C in RIPA buffer (20 mM Tris, pH 8.0, 100 mM NaCl, 0.2% NP-40, 0.2% Triton X-100, and 0.2% deoxycholate). Samples were centrifuged and the supernatants containing the rAAV particles were incubated at 4°C overnight with antibodies A20 (ARP), A69 (ARP), or anti-Myc (Invitrogen, Carlsbad, CA) or a control antibody. Samples were washed four times in RIPA buffer. After being washed, pellets were boiled for 5 min in SDS-PAGE loading buffer. Proteins were separated on 8% SDS-polyacrylamide gels and capsid proteins detected by Western blotting with the B1 antibody.

Viruses with wild-type virions and deletions, insertions, or replacements (10^{10} genome-containing particles) were bound to 100 μl heparin agarose (Sigma, St. Louis, MO) in binding/washing buffer (20 mM Tris, pH 7.6, 150 mM NaCl, and 1 mM $MgCl_2$) for 1 h at 4°C. After six washes, bound virus was eluted with elution buffer (20 mM Tris, pH 7.6, 1 M NaCl). The fractions were detected by Western blotting using the B1 antibody.

RESULTS

Alignments of Parvovirus Cap Proteins

In order to identify suitable sites for insertion of targeting peptides, we aligned the amino acid sequences of several parvoviruses. We performed sequence alignments using the MacVector software package (Oxford Molecular Group, UK) and included recently reported sequences for AAV serotypes 1, 3, 5, and 6 (46–50). Antigenic sequences of AAV-2 are aligned to the corresponding regions of CPV in Fig. 1 and are shown as four domains, I, II, III, and IV, which contain loops 1–4 of CPV (25). We have marked on these alignments peptides previously identified as antigenic sites (see boxes 1–14).

An antigenic region in domain I of CPV (box 3) is the target of neutralizing antibodies (51, 52). Interestingly, a nonconserved amino acid sequence of B19, which is also the target for neutralizing antibodies (box 2) maps to the same site (53). A peptide containing sequences of AAV-2 which partially overlap with loop 1 of CPV based on sequence alignments has been shown to inhibit the binding of neutralizing antibodies to AAV in an ELISA (31). A minor component of the epitope recognized by the monoclonal antibody A20 (box 4) also aligns within this region (30), but this antibody does not inhibit cell binding. Mutations in either of these two epitopes have been

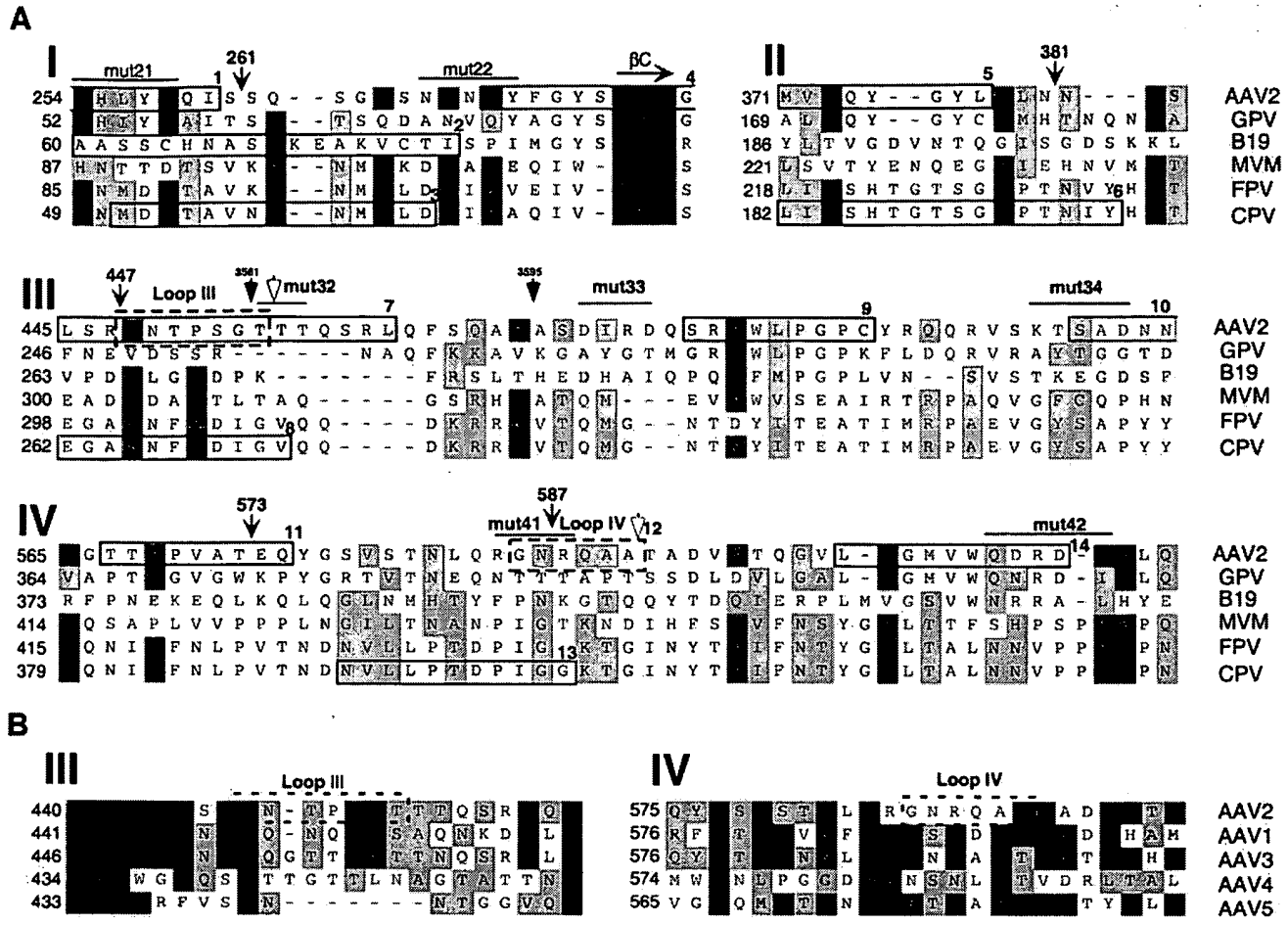

FIG. 1. Homology alignments of parvovirus Cap proteins. (A) The amino acid sequences of the capsid proteins of AAV-2, Genpept Accession No. (GP No.) 2906023; goose parvovirus (GPV), 9628653; B19, GP No. 4092542; minute virus of mice (MVM), GP No. 2982110; feline panleukopenia virus (FPV), GP No. 494031; and canine parvovirus (CPV), GP No. 494746, were aligned using the ClustalW alignment tool of the software program MacVector (Oxford Molecular Group, London). The alignments are shown for four domains (I–IV) within the capsid protein, which contain the antigenic loops of CPV. Identical sequences (dark blue) and similar sequences (light blue) are highlighted. Antigenic regions within the loops are enclosed by boxes that are numbered to the right (see text for details and references). Published mutations and their corresponding sites are indicated and part of the β-barrel is shown with a horizontal arrow. Sites of insertions are marked with an arrow (33), filled arrowhead (34), and open arrowhead (35). Numbering of mutations and sites match the corresponding papers. (B) Alignments of putative Loops III and IV of the AAV serotypes. The sequences of AAV serotypes 2, 1, 3, 4, and 5 are aligned, and regions modified in this study are shown enclosed by dashed boxes.

shown to severely impair transduction or destabilize the AAV capsid (35). A second major antigenic site of CPV lies within domain II (box 6) (25). An AAV-2 peptide (box 5) sequence forms an epitope, in conjunction with the peptide A-20 in domain I (box 4), that is recognized by a monoclonal neutralizing antibody. Taken together, these results imply that domains I and II are in close proximity in AAV-2. Moreover, the inability of the antibody that recognizes this region to inhibit receptor binding suggests that this region in AAV-2 is not involved in receptor recognition, but may have an important function in a later event in the infectious pathway. These putative loop regions are also well conserved between the different AAV serotypes (50). Therefore, it seems unlikely that insertion of targeting peptides at these loops would lead to targeted AAV transduction.

Several residues in antigenic loop 3 of CPV and the corresponding residues in related parvoviruses have been shown to be involved in viral tropism. One of the major neutralizing epitopes in CPV (box 8) is in the extended portion of loop 3 on the shoulder of the threefold spike (51). The AAV-2 sequence that aligns to this region (box 11) is also able to bind neutralizing antibodies; however, its involvement in receptor attachment is still not clear (31). All AAVs except serotype 5 contain an insertion at this site compared to other parvoviruses (Figs. 1A and 1B). Two monoclonal antibodies against AAV-2 recognize additional epitopes within domain III (boxes 9 and 10). Moreover, two charge-to-alanine mutations in this region resulted in the production of viruses defective in transduction (35). Rabinowitz *et al.* found that small insertions in this region also resulted in decreased transduction (34). However, insertion of the L14 peptide at residue 447 of the AAV-2 capsid protein resulted in exposure on the

surface of the capsid and increased binding to cells expressing integrins, but this virus did not retarget transduction.

Domain IV of AAV-2 contains two sequences which have been mapped as targets of neutralizing antibodies (boxes 11 and 14). Mutations in one of these epitopes resulted in an inability to assemble capsids (35). Mutations and insertions have also shown the involvement of an adjacent site (box 12) in heparin binding. Although both regions are variable between AAV serotypes (50), Fig. 1B shows that domain IV is more conserved. Based on the sequence alignments and previous findings, we decided to analyze different strategies for the incorporation of organ-targeting peptides into putative loops within domains III and IV of AAV-2. We have designated these Loop III and Loop IV (dotted boxes 7 and 12).

Effects of Deletions within Putative Loops III and IV of AAV-2

We first asked whether predicted Loops III and IV were essential for virus assembly and packaging by making deletions within these regions. Mutant plasmids were generated to encode capsid proteins with deletions of 7 or 6 amino acids within Loop III and Loop IV, respectively (Fig. 2A). These constructs were transfected together with a vector plasmid (pAAV-GFP) and an adenovirus helper plasmid (pXX6) into 293 cells to generate the mutant viruses rAAV-GFP-ΔIII and rAAV-GFP-ΔIV. Viruses were purified by iodixanol gradient ultracentrifugation and the amount of genome-containing particles was assessed by real-time PCR. The number of genome-containing particles for the viruses with the mutated Cap proteins was similar to that of those generated with wild-type Cap proteins (Fig. 2B). The protein composition of virions was determined by Western blotting of proteins from virus preparations having equivalent numbers of genome-containing virions. The stoichiometry of the three Cap proteins was similar to that of wild-type capsids. The ability of the viruses to transduce target cells was assessed by FACS analysis and fluorescence microscopy. As can be seen in Fig. 2C, transduction of 293 cells was significantly impaired for viruses with deletions in Loop III or IV, compared to virus generated with wild-type Cap proteins. These data suggest that the deleted portions of Loops III and IV are not essential for assembly or packaging of rAAV virions but that they have important roles in transduction.

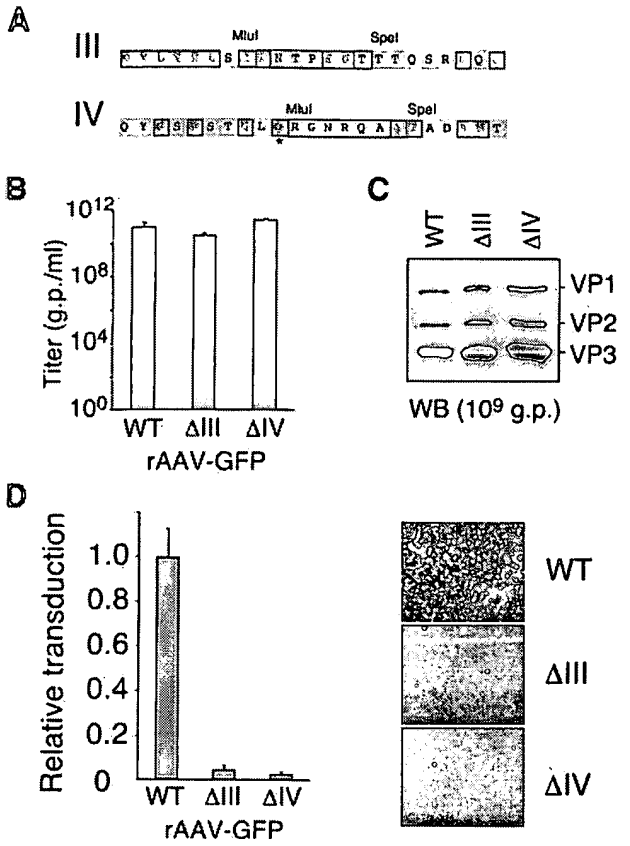

FIG. 2. Effects of deletions within putative Loops III and IV of AAV-2. (A) Constructs were generated with deletions in putative Loops III and IV. Sites of restriction enzymes *SpeI* and *MluI* used for cloning oligonucleotides are indicated. Sequences conserved between AAV serotypes are highlighted. Mutation of a single residue (Q), marked with an asterisk, prevented efficient transduction (see text for details). Enclosed boxes marked regions deleted. (B) Effect of deletions on number of genome-containing particles. Recombinant viruses with wild-type or mutant capsids were generated by transfections and purified by iodixanol gradients. Purified genome-containing rAAV vectors were quantified by real-time PCR against plasmid standards and are represented as genome-containing particles/ml (g.p./ml). (C) Virion composition of purified capsids. After iodixanol gradient purification an equal quantity of genome-containing virions as determined by real-time PCR (10^9 genomes) was analyzed by Western blotting with antibody B1. The positions of the capsid proteins VP1, VP2, and VP3 are indicated. (D) Deletions in Loops III and IV of AAV Cap proteins impair rAAV transduction. Transduction of 293 cells infected with rAAV-GFP at an m.o.i. of 1000 genomes/cell in the presence of Ad5 (m.o.i. 5 pfu) was assessed after 24–48 h by analyzing GFP expression by FACS analysis (left) or fluorescence (right).

Accessibility of Replacements or Insertions at Loops III and IV

Having shown that Loops III and IV were nonessential for assembly and packaging of AAV capsids we next assessed whether heterologous peptides inserted at these locations were presented on the surface of the virion. We first replaced the natural sequences of the loops with oligonucleotides encoding a Myc epitope. In addition to replacements of deleted sequences, we also selected two sites within Loops III and IV for insertion of targeting peptides. One of these sites was at amino acid 449 within Loop III and the second was at amino acid 588, which is in predicted Loop IV. The positions of these sites imposed on the CPV structure crystal structure are shown in Fig. 3A. Loop III is present in an extended conformation protruding from the virus, while Loop IV is in a pocket conformation, consistent with its putative function as a receptor anchor. These sites are similar but not identical to those recently used by others (33, 35).

In order for these sites to be useful in retargeting AAV vectors, it is necessary for inserted peptides to be presented on the surface of the virion. To determine the relative accessibility of peptides at these sites, we assessed the ability of

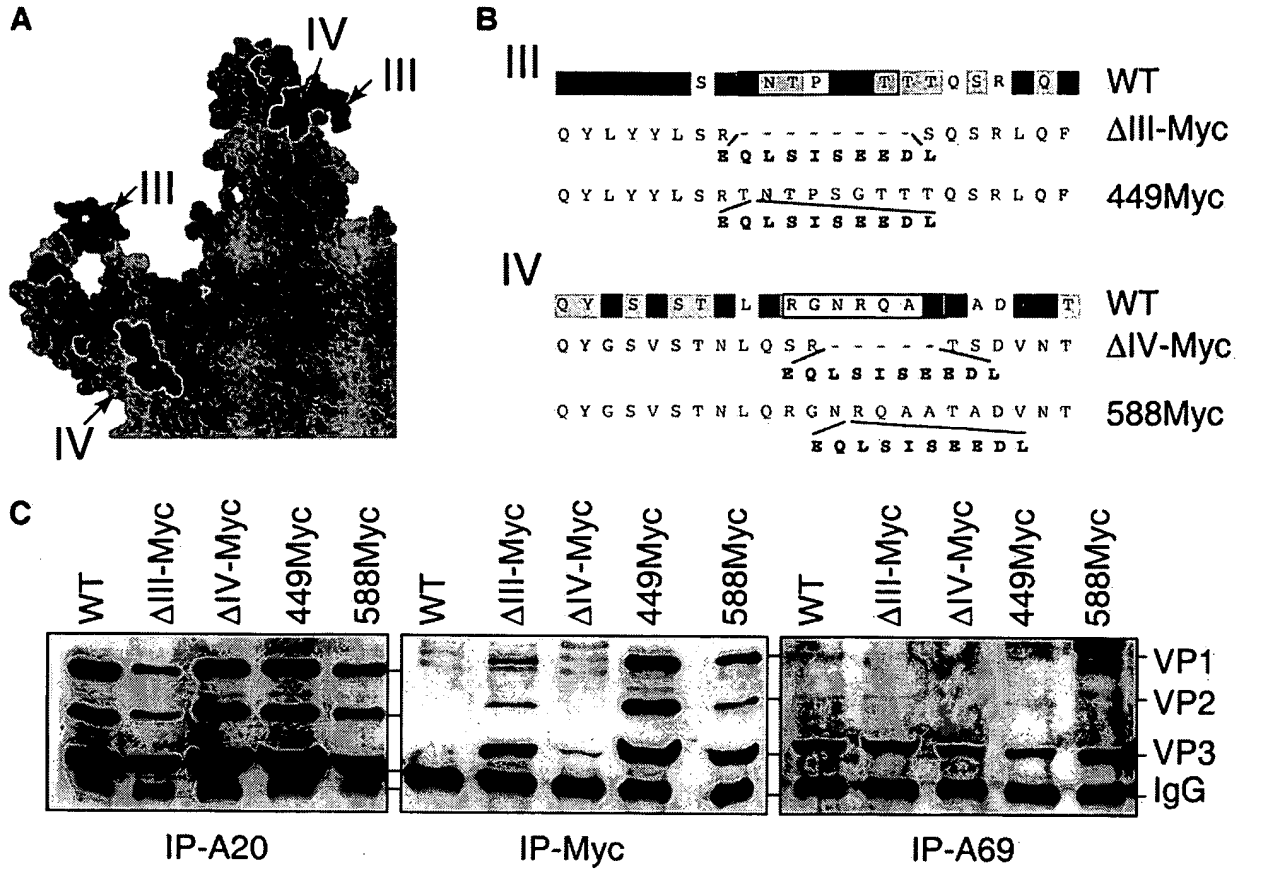

FIG. 3. Insertions or replacements in Loops III and IV are exposed on the capsid surface. (A) The positions of antigenic Loops III (green) and IV (blue) are shown as filled dots on the structure of the CPV Cap protein. (B) A peptide encoding the Myc epitope tag either replaced Loops III or IV or was inserted at residues 449 and 588. Sequences conserved between AAV serotypes are highlighted. (C) The accessibility of the Myc epitope in the fully assembled capsid was assessed by immunoprecipitation, followed by Western blotting. For each construct rAAV-GFP was generated by transfection and particles purified by iodixanol gradients. Similar numbers of genome-containing particles (10^{10}) were immunoprecipitated using antibodies that recognize intact AAV viral particles (A20), the Myc epitope, or VP2 capsid proteins (A69). Immunoprecipitated proteins were detected with an anti-Cap antibody (B1). The positions of VP1, VP2, and VP3 are indicated.

an anti-Myc antibody to immunoprecipitate epitope-tagged capsids (Fig. 3). Constructs for the mutant viruses were transfected into 293 cells together with the rAAV-GFP vector plasmid and the adenovirus helper plasmid. Cells were harvested and rAAV was purified by iodixanol gradients. The number of genome-containing particles was assessed by real-time PCR. Equal numbers of particles (10^{10} genome-containing particles) were immunoprecipitated using antibodies that recognize either intact AAV viral particles (A20) or the Myc epitope (Fig. 3C). Western blotting with an anti-Cap antibody (B1) demonstrated that the A20 antibody could isolate wild-type and mutant virions with equal efficiency. Control wild-type virus was not precipitated with the Myc antibody. In contrast, the Myc antibody was able to capture capsids containing the Myc epitope in Loops III and IV. The efficiency of capsid precipitation by the Myc antibody was higher for the insertions (rAAV-449Myc and rAAV-588Myc) compared to the loop replacements (rAAV-ΔIII-Myc or rAAV-ΔIV-Myc). We confirmed that the differences between viruses did not reflect immunoprecipitation of unassembled soluble proteins, by using an antibody to VP2 that also recognizes nonassembled Cap proteins (A69). Using this antibody similar levels of Cap proteins were detected with all viruses. No virus Cap proteins were detected using an antibody against a cellular protein as a negative control (data not shown). These experiments demonstrated that in most cases the Myc epitope was accessible to the antibody and was therefore presented on the surface of the assembled virions. These data confirm the findings of Girod *et al.* and Wu *et al.* (33, 35), who demonstrated surface exposure of the L14 peptide and HA tag, respectively, when inserted at adjacent sites. These results also highlight possible differences in the exposure of epitopes when present as replacements compared to insertions.

Effects of Replacing or Inserting Targeting Peptides into Putative Loop III or IV of AAV-2

Having established that sequences could be mutated or inserted in the putative Loops III and IV, we sought to assess the effects of incorporating targeting peptides at these sites. The tripeptide asparagine-glycine-arginine

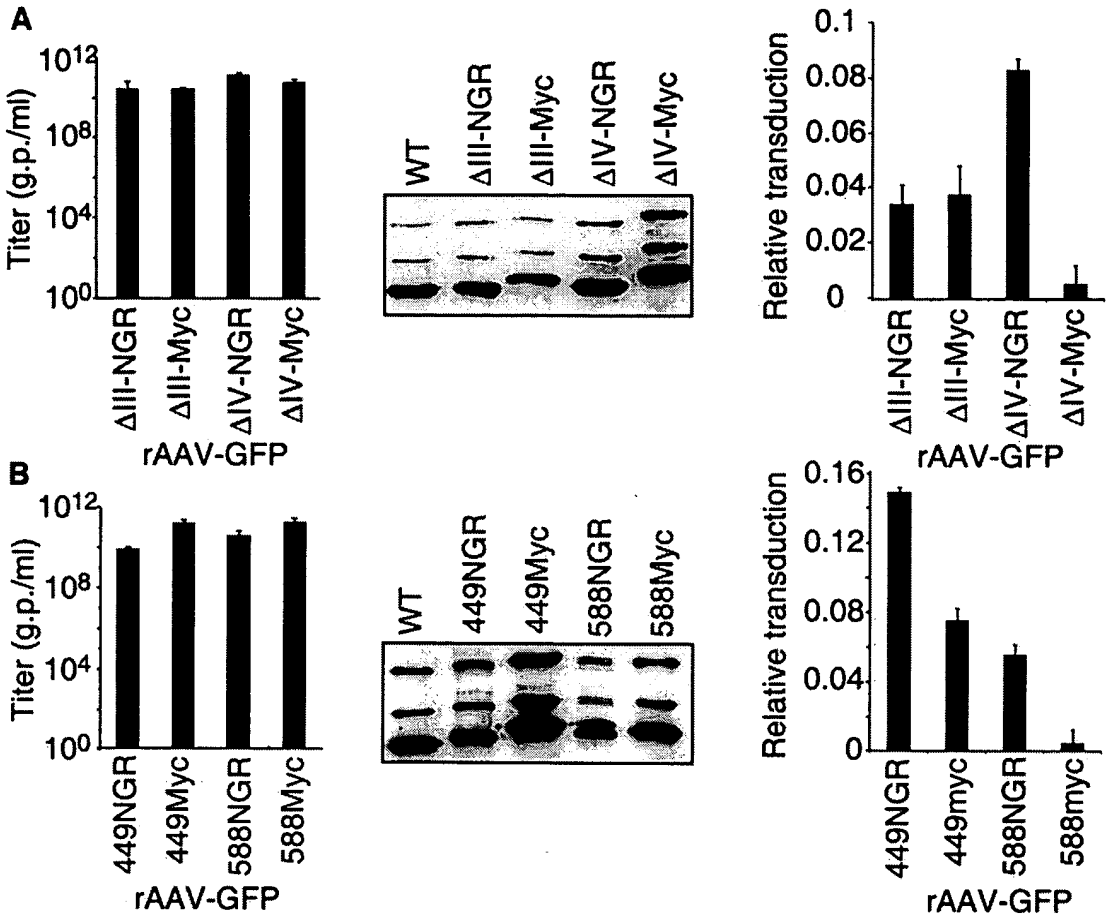

FIG. 4. Effects of replacements or insertions within the putative loops. Effects of loop replacements (A) or peptide insertions (B) on vector titers. Purified viruses were quantified by real-time PCR against plasmid standards and are represented as genome-containing particles/ml (g.p./ml) (left). Virion composition of wild-type and mutant viruses after iodixanol purification was assessed by Western blotting (center). Equal quantities of purified virions as determined by real-time PCR (10^9 genomes) were subjected to SDS–PAGE and Cap proteins detected by Western blotting with antibody B1. Replacements and insertions within regions of Loops III and IV of the AAV Cap impair rAAV transduction (right). Transduction of 293 cells infected with rAAV-GFP at an m.o.i. of 1000 in the presence of Ad5 (m.o.i. 5 pfu/cell) for 24–48 h was quantified by FACS analysis. Presented are transductions relative to wild-type capsids.

(NGR) was isolated using the *in vivo* phage selection system in which peptides capable of homing to tumor angiogenic vasculature were recovered from phage libraries. Peptides containing an NGR motif bind selectively to CD13 *in vivo* in tumor- and hypoxia-activated blood vessels (39). Oligonucleotides encoding this sequence were cloned into the putative loops, either as replacements of the original sequence or as insertions. Recombinant viruses for the replacements (rAAV-ΔIII-NGR or rAAV-ΔIV-NGR) or insertions (rAAV-449NGR and rAAV-588NGR) were generated by transfections and purified by iodixanol gradients. Control viruses contained the Myc epitope as a replacement (rAAV-ΔIII-Myc or rAAV-ΔIV-Myc) or insertion (rAAV-449Myc and rAAV-588Myc) at the same sites. The numbers of genome-containing particles were determined by real-time PCR and in all cases they were comparable to those obtained with wild-type capsid proteins (Fig. 4). The stoichiometry of these purified capsids was determined by Western blotting with a Cap antibody and remained the same with all modified capsids.

First, we tested the ability of the engineered viruses containing replacements or insertions to transduce 293T cells. Cells were transduced with 1000 genome-containing particles of rAAV per cell in the presence of adenovirus co-infection to maximize transduction (54). Despite their ability to assemble and package AAV particles, these mutant viruses were significantly impaired for transduction in 293T cells, with efficiencies ranging from 0.5 to 15% of wild-type (Fig. 4). Transduction was most severely impaired for viruses that contained the Myc epitope in Loop IV, either as a replacement or as an additional insertion. A titration of infections over a range of m.o.i. revealed that regardless of the amount of particles used, rAAV-ΔIV-Myc and rAAV-588Myc were unable to achieve more than 0.5% the transduction efficiency of wild-type virions (data not shown). These results confirm that targeting peptides can be inserted into the putative loops without affecting assembly and packaging but transduction is impaired.

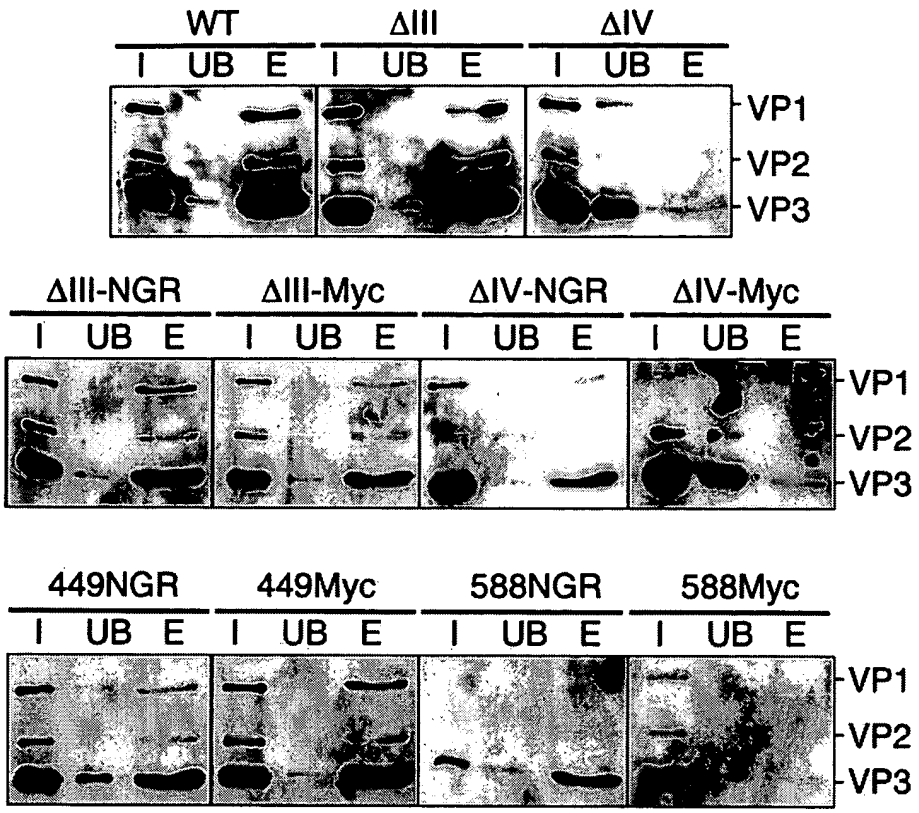

FIG. 5. Analysis of WT and mutant capsid virus binding to heparin. Iodixanol gradient-purified rAAV viruses were bound to heparin agarose for 1 h at 4°C. After extensive washing, bound virus was eluted with 1 M NaCl. The fractions were separated on SDS–8% acrylamide gels and analyzed by Western blotting using the B1 antibody. Shown are 5% of input virus (I), 5% of the unbound fraction (UB), and 20% of the eluted fraction (E). The positions of VP1, VP2, and VP3 are indicated.

Heparin Binding of AAV Capsids Containing Heterologous Peptide Sequences

One possible cause for the reduced infectivity of rAAV mutants containing foreign epitopes could be their inability to bind the viral cell surface receptors. A primary receptor for AAV-2 has been reported to be heparan sulfate proteoglycan (12). To test whether viruses with mutant capsids could bind heparin, we performed heparin batch binding experiments and detected the viruses by Western blotting using the B1 antibody (Fig. 5). Recombinant viruses purified by iodixanol gradient centrifugation were bound to heparin agarose for 1 h at 4°C. Following incubation of the viruses with heparin agarose, the unbound fraction was removed. After extensive washing of the heparin agarose, viruses were eluted in 1 M NaCl. As expected, viruses containing a wild-type capsid had a high affinity for the heparin agarose, and negligible amounts of virus were found in the unbound fraction. About 20% of the input virus was recovered in the elution from the beads. Most mutants had a binding and elution profile similar to that of the wild-type capsids. However, a deletion of 6 amino acids (GNRQAA) from Loop IV abolished binding to heparin. Interestingly, replacement of this sequence with the NGRAHA peptide sequence restored the ability of the mutant capsid to bind heparin (Fig. 5). Viruses with the Myc epitope tag in the Loop IV region were unable to bind heparin, which suggests that this region is important for attachment to the primary receptor. This is also consistent with their poor transduction efficiency (Fig. 4).

Altered Tropism of rAAV Containing the Tumor-Targeting Peptides

To determine whether incorporation of targeting peptides could alter the tropism of rAAV we tested transduction on a number of cell lines (Fig. 6). For this purpose we employed two highly tumorigenic cell lines. Kaposi sarcoma (KS1767) cells are derived from Kaposi sarcoma lesions (38). The second cell line tested was an embryonal rhabdomyosarcoma cell line (RD). Both cell lines express high levels of CD13, the NGR receptor, as assessed by FACS analysis (RD and KS1767 were 57 and 99% positive for CD13 compared to 8 or 3% positive for 293T and HeLa cells). Viruses were first titered on 293 cells and then equal transduction units of the different viruses were used to infect the other cells. An amount was chosen that resulted in 10% transduction of 293 cells as assessed by FACS analysis for GFP expression. Using these adjusted values, similar transduction efficiencies were seen for the viruses on HeLa cells (Figs. 6A and 6B). However, rAAV consisting

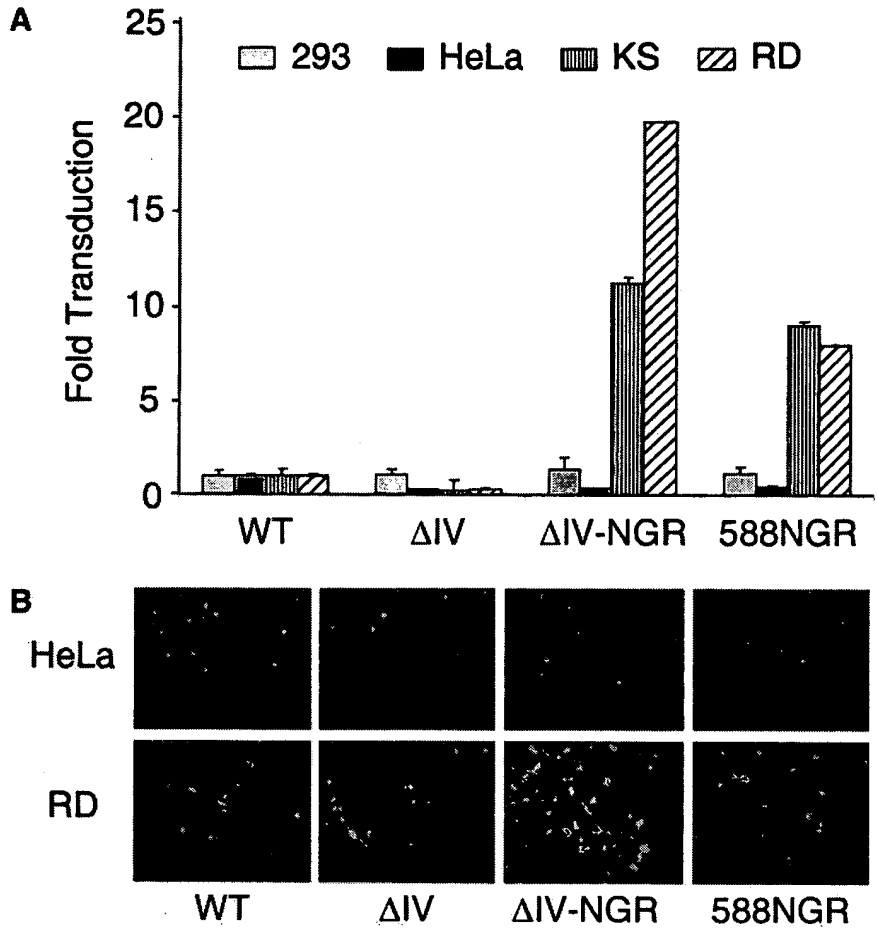

FIG. 6. Altered tropism of rAAV containing the NGRAHA sequence. Viruses were initially titered for transduction on 293 cells by FACS analysis of GFP expression. An equal amount of transduction units (able to achieve 10% transduction of 293 cells) was used to infect 293, HeLa, KS1767, and RD cells. These correspond to 1×10^7, 2×10^8, 5×10^8, and 4×10^8 genome-containing particles for WT, ΔIV, ΔIV-NGR, and 588NGR, respectively. Transduction was assessed at 24–72 h postinfection, by counting green cells under a fluorescence microscope or by FACS analysis. (A) Transduction efficiencies are shown relative to the wild-type capsid in the different cell lines. (B) Images of GFP expression captured by fluorescence microscopy. Transduction of HeLa cells was comparable for the different viruses but those containing NGR peptides showed preferential transduction of RD cells. There was a correlation between expression of CD13 (as measured by FACS analysis with the WM15 antibody) and altered tropism of NGR-containing viruses.

of wild-type capsids transduced the KS1767 and RD cell lines very poorly. In contrast, viruses containing the NGRAHA sequence at Loop IV, either as a replacement or as an insertion, were able to transduce these cell lines 10- to 20-fold better than wild type (Fig. 6A). This altered tropism was not observed for viruses with deletion of Loop IV or the Myc epitope at this site.

In the context of the phage coat protein or as a synthetic peptide, targeting was most efficient with cyclic peptides containing four cysteine residues (38). Based on the data from phage display libraries we included sequences containing the targeting NGR motif in the potentially cyclic (two cysteines) or double cyclic forms. Viruses containing the cyclic NGR sequences were less efficient than those with the linear peptide in transduction of 293 and HeLa cells but they also displayed enhanced tropism toward the tumorigenic, CD-13-positive cell lines RD and KS1767 (Table 1 and data not shown).

Several sequences have been isolated from phage display libraries and shown to home to different tissues *in vivo*. These include lung-, brain-, tumor-, and muscle-homing peptides (36, 55–57). We inserted a number of these targeting peptides into the 588 site, which we had defined as appropriate for accepting heterologous sequences (see Table 1). These included a GFE-containing peptide to target membrane dipeptidase expressed on lung vasculature (55), a muscle-homing peptide (56), and sequences identified in an *in vitro* phage display screen for NG2 proteoglycan binding sequences (57). Some of the viruses containing other targeting peptides were produced less efficiently and we were not able to observe altered tropism in the appropriate cell lines (Table 1). In general, we observed that smaller peptides were tolerated better than larger ones. Even at the same site we saw an effect of the sequence that was inserted, with linear peptides having fewer deleterious effects than sequences containing multiple cysteine residues.

TABLE 1

Properties of Recombinant AAV Viruses Containing Homing Peptides in Their Capsid Proteins

Virus[a]	Homing peptide[b]	Titer[c] (g.p./ml)	Transduction[d] (% of WT)	Cells[e]	Alt Trop[f]
588 GFE-4C	CGFECVRQCPERC	2.50×10^9	7.00	MBA-MBP[g]	–
588 NGR-2C	CNGRC	6.00×10^{10}	0.75	RD/KS1767	+
588 NGR-4C	CNGRCVSGCAGRC	4.30×10^9	0.75	RD/KS1767	+
588 L14	QAGTFALRGDNPQ	1.50×10^{10}	0.82	NA	ND
588 MH	ASSLNIA	7.70×10^{10}	1.12	NA	ND
588 NG2-1	TAASGVRSMH	1.00×10^{11}	1.3	B16F10NG2	–
588 NG2-2	LTLRWVGLMS	6.60×10^9	0.75	B16F10NG2	–

[a] Homing peptides were introduced into the AAV capsid at amino acid 588 and recombinant viruses were produced in 293T cells using pXX6 as a helper to package a GFP expression cassette.

[b] See text for details.

[c] Viruses were purified by iodixanol gradient centrifugation and titered by real-time PCR. Titers are presented in genome-containing particles (g.p./ml).

[d] Transduction was assessed in 293 cells by FACS analysis and is presented as a percentage of WT.

[e] Cell lines used to assess targeting of an equal amount of transduction units as assessed on 293 cells. NA, not applicable.

[f] Altered tropism was tested in the indicated cell lines. ND, not determined.

[g] MDA-MB-435-MBP (59).

Discussion

Homing peptides isolated by *in vivo* screening of phage display libraries provide novel tools for selective vascular targeting of therapies and are attractive for incorporation into viral vectors (36–38, 41, 58). It is unclear whether these peptides will be presented in the correct conformation on viral particles to enable targeting of modified vectors. We recently used targeting peptides to redirect adenoviral vectors to specific endothelial receptors using bispecific conjugates with antibodies recognizing adenovirus particles (59). Tumor-targeting peptides have also been successfully used to enhance the antitumor properties of doxorubicin and TNF (38, 40). In this study, we were able to generate modified AAV-2 capsids that contain targeting peptides, previously isolated by *in vivo* phage display. Peptides were incorporated as either replacements of native sequences or insertions. Modification of putative loops did not affect replication, assembly, and packaging of rAAV vectors. We show that the precise site of insertion and the choice of replacement of the original sequence can have an impact on the accessibility of the peptide at the capsid surface. We found that the transduction efficiency of rAAV-2 vectors bearing such peptides was severely compromised, but that in some cases we could demonstrate altered preference for transduction of tumor cells. This study represents the first attempt to target rAAV by genetic incorporation of tumor-targeting peptides previously isolated by phage display technologies. We were able to generate AAV viruses containing linear, cyclic, and double-cyclic versions of the NGR and these vectors showed altered tropism, with preferential transduction of cells that express the CD13 receptor.

Alignments of available sequences for all the parvovirus capsid proteins highlight large areas of sequence conservation (29). Sequences that make up the β-barrel are the most conserved. Consistent with this are genetic studies in which mutations within these regions result in noninfectious viruses, many of which do not make intact capsids (34, 35, and M.G. and M.D.W., unpublished data). A comparison of our alignment to the previously published ones (29, 33) reveals some differences, especially in variable regions where sequence similarity is low and insertions are present. We have also extended the alignments presented in Fig. 1 by including additional parvoviral sequences (e.g., Kilhamrat, porcine, and simian), which enhance the confidence of the alignment we show (data not shown). When the three-dimensional structure of the AAV-2 capsid is solved, the validity of these hypothetical alignments will be assessed by superimposing the actual structures. We were able to make deletions within the putative Loops III and IV of AAV-2 without causing any detrimental effects on virus assembly or packaging. This is in contrast to previous studies with CPV, in which deletions in loops 1, 3, and 4 affected capsid assembly and morphology (60). It should be noted, however, that in the CPV study the deletions were larger (12–16 amino acids) and the assay for assembly was the formation of virus-like particles after infection of insect cells with recombinant baculoviruses expressing the Cap proteins. Despite our ability to modify these loop regions we encountered some residues that were far more sensitive to alterations. For example a single point mutation within Loop IV (Q584S) completely abrogated rAAV transduction (data not shown). The dramatic effect of deletions in Loops III or IV on transduction by rAAV vectors suggests that these two regions are indeed involved in the infectious pathway. This may be at the level of attachment to cellular receptors or some additional step during internalization, cytoplasmic trafficking, or nuclear entry of the virus particle.

Three cellular receptors have been implicated in AAV infection (HSPG, FGFR-1, and $\alpha_V\beta_5$ integrin) although direct involvement of these proteins has recently been called into question (61–63). We could confirm that putative Loop IV is required for binding to heparin, which is consistent with its attachment to the proposed HSPG primary receptor (12) and recent mapping of two heparin-binding clusters (34, 35). We have not yet investigated binding of these mutants to the putative secondary receptors. It is interesting to note that while deleting a part of Loop IV abolishes heparin binding, replacing it with the NGR targeting peptide could restore binding. Replacement of the same sequence in Loop IV with the Myc epitope was unable to rescue heparin binding. The NGR peptide is similar to the sequence that has been deleted, suggesting that replacement of capsid epitopes with residues resembling the original sequence in size and charge may be well tolerated.

In order for rAAV vectors with altered tropism to be viable for clinical applications it is important that the production, packaging, and transduction efficiencies of the modified viruses are not severely compromised. One previous attempt to target AAV capsids required transfection of the modified capsid construct together with wild-type virus and gave a very low yield of virus (32). We found that our modified viruses were similar to wild type in their ability to replicate and package a vector genome but in almost every case the transduction of the modified capsid was suboptimal. This has been a common problem for all attempts so far to retarget rAAV vectors (33, 35). Our data suggest that this is due to a combination of size, sequence, and insertion site. We have found that larger peptides tend to have more detrimental effects on the properties of the modified virus particle. While some peptides such as the NGR and L14 (33) have been tolerated for insertion in Loops III and IV, others such as the serpin ligand resulted in no capsid formation (35). We have been able to show altered tropism for vectors containing targeting peptides but in all cases this was at the expense of transduction efficiency, which would not be acceptable for clinical applications.

Successful retargeting of rAAV vectors is likely to come from a delicate combination of the type of peptide inserted and the choice of insertion site. A number of studies have now described multiple sites that can be used for peptide insertions (32–35). In this study we have focussed on a limited number of sites and inserted multiple different sequences in two approaches, replacements or insertions. Our data suggest that the best approach may be to scan the AAV sequence for putative surface-exposed areas that contain nonconserved protein sequences matching the sequence to be inserted and replace these regions with the targeting ligand. Perhaps this may be best achieved through a combinatorial library approach, whereby rAAV vectors with modified capsids are selected directly for a given target. Libraries could also be used to select for viruses that have inserted peptides but also maintain transduction levels similar to those of wild-type capsids. One potential problem with a small virus such as AAV is that it is possible that receptor binding and other steps in the transduction process may be structurally linked, such as in CPV (64). Further studies of the pathways of AAV infection and rAAV transduction will reveal the role of different parts of the capsid in the infection entry process. The ability to restrict AAV-2 gene delivery to a specific organ or tissue will allow the use of smaller dosages of virus and will be important in limiting toxicity following systemic *in vivo* administration in a wide range of gene therapy applications.

ACKNOWLEDGMENTS

We thank David Chambers and Kelly Hardwicke for help with FACS analysis, Tom Hope for use of the fluorescence microscope and camera, Jude Samulski for plasmids, Sam Young for advice on heparin binding assays. We are grateful to Toni Cathomen, Travis Stracker, and Nik Somia for helpful discussions and for critically reading the manuscript. This work was supported by grants from the Department of Defense (DAMD 17-98-1-8041, to R.P. and M.D.W.) and the California Cancer Research Program (PF0071 to M.D.W.), an Innovation Grant from the Presidents' Club of the Salk Institute (M.D.W.), and the NIH. Martin Trepel was supported by the Deutsche Forschungsgemeinschaft (DFG) and by the Susan G. Komen Breast Cancer Foundation. Matthew D. Weitzman acknowledges gifts from the Mary H. Rumsey and Irving A. Hansen Foundations.

REFERENCES

[1] Monahan, P. E., and Samulski, R. J. (2000). AAV vectors: Is clinical success on the horizon? *Gene Ther.* **7**: 24–30.

[2] Klein, R. L., Mandel, R. J., and Muzyczka, N. (2000). Adeno-associated virus vector-mediated gene transfer to somatic cells in the central nervous system. *Adv. Virus Res.* **55**: 507–528.

[3] Xiao, X., Li, J., McCown, T. J., and Samulski, R. J. (1997). Gene transfer by adeno-associated virus vectors into the central nervous system. *Exp. Neurol.* **144**: 113–124.

[4] Snyder, R. O., *et al.* (1997). Persistent and therapeutic concentrations of human factor IX in mice after hepatic gene transfer of recombinant AAV vectors. *Nat. Genet.* **16**: 270–276.

[5] Flotte, T. R., *et al.* (1993). Stable in vivo expression of the cystic fibrosis transmembrane conductance regulator with an adeno-associated virus vector. *Proc. Natl. Acad. Sci. USA* **90**: 10613–10617.

[6] Fisher, K. J., *et al.* (1997). Recombinant adeno-associated virus for muscle directed gene therapy. *Nat. Med.* **3**: 306–312.

[7] Halbert, C. L., Standaert, T. A., Aitken, M. L., Alexander, I. E., Russell, D. W., and Miller, A. D. (1997). Transduction by adeno-associated virus vectors in the rabbit airway: Efficiency, persistence, and readministration. *J. Virol.* **71**: 5932–5941.

[8] Ponnazhagan, S., *et al.* (1997). Adeno-associated virus type 2-mediated transduction in primary human bone marrow-derived $CD34^+$ hematopoietic progenitor cells: Donor variation and correlation of transgene expression with cellular differentiation. *J. Virol.* **71**: 8262–8267.

[9] Bartlett, J. S., Kleinschmidt, J., Boucher, R. C., and Samulski, R. J. (1999). Targeted adeno-associated virus vector transduction of nonpermissive cells mediated by a bispecific F(ab'gamma)2 antibody. *Nat. Biotechnol.* **17**: 181–186.

[10] Mizukami, H., Young, N. S., and Brown, K. E. (1996). Adeno-associated virus type 2 binds to a 150-kilodalton cell membrane glycoprotein. *Virology* **217**: 124–130.

[11] Ponnazhagan, S., *et al.* (1996). Differential expression in human cells from the p6 promoter of human parvovirus B19 following plasmid transfection and recombinant adeno-associated virus 2 (AAV) infection: Human megakaryocytic leukaemia cells are non-permissive for AAV infection. *J. Gen. Virol.* **77**: 1111–1122.

[12] Summerford, C., and Samulski, R. J. (1998). Membrane-associated heparan sulfate proteoglycan is a receptor for adeno-associated virus type 2 virions. *J. Virol.* **72**: 1438–1445.

[13] Qing, K., Mah, C., Hansen, J., Zhou, S., Dwarki, V., and Srivastava, A. (1999). Human fibroblast growth factor receptor 1 is a co-receptor for infection by adeno-associated virus 2. *Nat. Med.* **5**: 71–77.

[14] Summerford, C., Bartlett, J. S., and Samulski, R. J. (1999). AlphaVbeta5 integrin: A co-receptor for adeno-associated virus type 2 infection. *Nat. Med.* **5**: 78–82.

[15] Sanlioglu, S., Benson, P. K., Yang, J., Atkinson, E. M., Reynolds, T., and Engelhardt, J. F. (2000). Endocytosis and nuclear trafficking of adeno-associated virus type 2 are controlled by rac1 and phosphatidylinositol-3 kinase activation. *J. Virol.* **74**: 9184–9196.

[16] Duan, D., Li, Q., Kao, A. W., Yue, Y., Pessin, J. E., and Engelhardt, J. F. (1999). Dynamin is required for recombinant adeno-associated virus type 2 infection. *J. Virol.* **73**: 10371–10376.

[17] Bartlett, J. S., Wilcher, R., and Samulski, R. J. (2000). Infectious entry pathway of adeno-associated virus and adeno-associated virus vectors. *J. Virol.* **74**: 2777–2785.

[18] Weitzman, M. D., Fisher, K. J., and Wilson, J. M. (1996). Recruitment of wild-type and recombinant adeno-associated virus into adenovirus replication centers. *J. Virol.* **70**: 1845–1854.

[19] Hansen, J., Qing, K., Kwon, H. J., Mah, C., and Srivastava, A. (2000). Impaired

intracellular trafficking of adeno-associated virus type 2 vectors limits efficient transduction of murine fibroblasts. *J. Virol.* **74:** 992–996.

[20] Berns, K. I. (1974). Molecular biology of the adeno-associated viruses. *Curr. Top. Microbiol. Immunol.* **65:** 1–20.

[21] Laughlin, C. A., Tratschin, J. D., Coon, H., and Carter, B. J. (1983). Cloning of infectious adeno-associated virus genomes in bacterial plasmids. *Gene* **23:** 65–73.

[22] Samulski, R. J., Berns, K. I., Tan, M., and Muzyczka, N. (1982). Cloning of adeno-associated virus into pBR322: Rescue of intact virus from the recombinant plasmid in human cells. *Proc. Natl. Acad. Sci. USA* **79:** 2077–2081.

[23] Berns, K. I. (1996). Parvoviridae: The viruses and their replication. In *Virology* (D. M. Knipe, B. N. Fields, P. M. Howley, Eds.), pp. 2173–2197. Lippincott–Raven, Philadelphia.

[24] Becerra, S. P., Koczot, F., Fabisch, P., and Rose, J. A. (1988). Synthesis of adeno-associated virus structural proteins requires both alternative mRNA splicing and alternative initiations from a single transcript. *J. Virol.* **62:** 2745–2754.

[25] Tsao, J., *et al.* (1991). The three-dimensional structure of canine parvovirus and its functional implications. *Science* **251:** 1456–1464.

[26] Agbandje, M., McKenna, R., Rossmann, M. G., Strassheim, M. L., and Parrish, C. R. (1993). Structure determination of feline panleukopenia virus empty particles. *Proteins* **16:** 155–171.

[27] Agbandje-McKenna, M., Llamas-Saiz, A. L., Wang, F., Tattersall, P., and Rossmann, M. G. (1998). Functional implications of the structure of the murine parvovirus, minute virus of mice. *Structure* **6:** 1369–1381.

[28] Agbandje, M., Kajigaya, S., McKenna, R., Young, N. S., and Rossmann, M. G. (1994). The structure of human parvovirus B19 at 8 A resolution. *Virology* **203:** 106–115.

[29] Chapman, M. S., and Rossmann, M. G. (1993). Structure, sequence, and function correlations among parvoviruses. *Virology* **194:** 491–508.

[30] Wobus, C. E., Hugle-Dorr, B., Girod, A., Petersen, G., Hallek, M., and Kleinschmidt, J. A. (2000). Monoclonal antibodies against the adeno-associated virus type 2 (AAV-2) capsid: Epitope mapping and identification of capsid domains involved in AAV-2-cell interaction and neutralization of AAV-2 infection. *J. Virol.* **74:** 9281–9293.

[31] Moskalenko, M., *et al.* (2000). Epitope mapping of human anti-adeno-associated virus type 2 neutralizing antibodies: Implications for gene therapy and virus structure. *J. Virol.* **74:** 1761–1766.

[31a] Rabinowitz, J. E., and Samulski, R. J. (2000). Building a better vector: The manipulations of AAV virions. *Virology* **278:** 301–308.

[32] Yang, Q., *et al.* (1998). Development of novel cell surface CD34-targeted recombinant adenoassociated virus vectors for gene therapy. *Hum. Gene Ther.* **9:** 1929–1937.

[33] Girod, A., *et al.* (1999). Genetic capsid modifications allow efficient re-targeting of adeno-associated virus type 2. *Nat. Med.* **5:** 1438.

[34] Rabinowitz, J. E., Xiao, W., and Samulski, R. J. (1999). Insertional mutagenesis of AAV2 capsid and the production of recombinant virus. *Virology* **265:** 274–285.

[35] Wu, P., *et al.* (2000). Mutational analysis of the adeno-associated virus type 2 (AAV2) capsid gene and construction of AAV2 vectors with altered tropism. *J. Virol.* **74:** 8635–8647.

[36] Pasqualini, R., and Ruoslahti, E. (1996). Organ targeting in vivo using phage display peptide libraries. *Nature* **380:** 364–366.

[37] Rajotte, D., Arap, W., Hagedorn, M., Koivunen, E., Pasqualini, R., and Ruoslahti, E. (1998). Molecular heterogeneity of the vascular endothelium revealed by in vivo phage display. *J. Clin. Invest.* **102:** 430–437.

[38] Arap, W., Pasqualini, R., and Ruoslahti, E. (1998). Cancer treatment by targeted drug delivery to tumor vasculature in a mouse model. *Science* **279:** 377–380.

[39] Pasqualini, R., *et al.* (2000). Aminopeptidase N is a receptor for tumor-homing peptides and a target for inhibiting angiogenesis. *Cancer Res.* **60:** 722–727.

[40] Curnis, F., Sacchi, A., Borgna, L., Magni, F., Gasparri, A., and Corti, A. (2000). Enhancement of tumor necrosis factor alpha antitumor immunotherapeutic properties by targeted delivery to aminopeptidase N (CD13). *Nat. Biotechnol.* **18:** 1185–1190.

[41] Koivunen, E., *et al.* (1999). Tumor targeting with a selective gelatinase inhibitor. *Nat. Biotechnol.* **17:** 768–774.

[42] Li, J., Samulski, R. J., and Xiao, X. (1997). Role for highly regulated rep gene expression in adeno-associated virus vector production. *J. Virol.* **71:** 5236–5243.

[43] Xiao, X., Li, J., and Samulski, R. J. (1998). Production of high-titer recombinant adeno-associated virus vectors in the absence of helper adenovirus. *J. Virol.* **72:** 2224–2232.

[44] Zolotukhin, S., *et al.* (1999). Recombinant adeno-associated virus purification using novel methods improves infectious titer and yield. *Gene Ther.* **6:** 973–985.

[45] Clark, K. R., Liu, X., McGrath, J. P., and Johnson, P. R. (1999). Highly purified recombinant adeno-associated virus vectors are biologically active and free of detectable helper and wild-type viruses. *Hum. Gene Ther.* **10:** 1031–1039.

[46] Muramatsu, S., Mizukami, H., Young, N. S., and Brown, K. E. (1996). Nucleotide sequencing and generation of an infectious clone of adeno-associated virus 3. *Virology* **221:** 208–217.

[47] Bantel-Schaal, U., Delius, H., Schmidt, R., and zur Hausen, H. (1999). Human adeno-associated virus type 5 is only distantly related to other known primate helper-dependent parvoviruses. *J. Virol.* **73:** 939–947.

[48] Xiao, W., Chirmule, N., Berta, S. C., McCullough, B., Gao, G., and Wilson, J. M. (1999). Gene therapy vectors based on adeno-associated virus type 1. *J. Virol.* **73:** 3994–4003.

[49] Chiorini, J. A., Kim, F., Yang, L., and Kotin, R. M. (1999). Cloning and characterization of adeno-associated virus type 5. *J. Virol.* **73:** 1309–1319.

[50] Rutledge, E. A., Halbert, C. L., and Russell, D. W. (1998). Infectious clones and vectors derived from adeno-associated virus (AAV) serotypes other than AAV type 2. *J. Virol.* **72:** 309–319.

[51] Langeveld, J. P., *et al.* (1993). B-cell epitopes of canine parvovirus: Distribution on the primary structure and exposure on the viral surface. *J. Virol.* **67:** 765–772.

[52] Strassheim, M. L., Gruenberg, A., Veijalainen, P., Sgro, J. Y., and Parrish, C. R. (1994). Two dominant neutralizing antigenic determinants of canine parvovirus are found on the threefold spike of the virus capsid. *Virology* **198:** 175–184.

[53] Yoshimoto, K., *et al.* (1991). A second neutralizing epitope of B19 parvovirus implicates the spike region in the immune response. *J. Virol.* **65:** 7056–7060.

[54] Fisher, K. J., Gao, G.-P., Weitzman, M. D., DeMatteo, R., Burda, J. F., and Wilson, J. M. (1996). Transduction with recombinant adeno-associated virus for gene therapy is limited by leading strand synthesis. *J. Virol.* **70:** 520–532.

[55] Rajotte, D., and Ruoslahti, E. (1999). Membrane dipeptidase is the receptor for a lung-targeting peptide identified by in vivo phage display. *J. Biol. Chem.* **274:** 11593–11598.

[56] Samoylova, T. I., and Smith, B. F. (1999). Elucidation of muscle-binding peptides by phage display screening. *Muscle Nerve* **22:** 460–466.

[57] Burg, M. A., Pasqualini, R., Arap, W., Ruoslahti, E., and Stallcup, W. B. (1999). NG2 proteoglycan-binding peptides target tumor neovasculature. *Cancer Res.* **59:** 2869–2874.

[58] Arap, W., Pasqualini, R., and Ruoslahti, E. (1998). Chemotherapy targeted to tumor vasculature. *Curr. Opin. Oncol.* **10:** 560–565.

[59] Trepel, M., Grifman, M., Weitzman, M. D., and Pasqualini, R. (2000). Molecular adaptors for vascular-targeted adenoviral gene delivery. *Hum. Gene Ther.* **11:** 1971–1981.

[60] Hurtado, A., Rueda, P., Nowicky, J., Sarraseca, J., and Casal, J. I. (1996). Identification of domains in canine parvovirus VP2 essential for the assembly of virus-like particles. *J. Virol.* **70:** 5422–5429.

[61] Qiu, J., Handa, A., Kirby, M., and Brown, K. E. (2000). The interaction of heparin sulfate and adeno-associated virus 2. *Virology* **269:** 137–147.

[62] Qiu, J., and Brown, K. E. (1999). Integrin alphaVbeta5 is not involved in adeno-associated virus type 2 (AAV2) infection. *Virology* **264:** 436–440.

[63] Qiu, J., Mizukami, H., and Brown, K. E. (1999). Adeno-associated virus 2 co-receptors? *Nat. Med.* **5:** 467–468.

[64] Simpson, A. A., Chandrasekar, V., Hebert, B., Sullivan, G. M., Rossmann, M. G., and Parrish, C. R. (2000). Host range and variability of calcium binding by surface loops in the capsids of canine and feline parvoviruses. *J. Mol. Biol.* **300:** 597–610.

APPENDIX D

Abstract: Nicklin SA et al (2001) Mol Ther. 4, 174-81
Efficient and selective AAV2-mediated gene transfer directed to human vascular endothelial cells.

Gene therapy vectors based on adeno-associated virus-2 (AAV2) offer considerable promise for human gene therapy. Applications for AAV vectors are limited to tissues efficiently transduced by the vector due to its natural tropism, which is predominantly skeletal muscle, neurons, and hepatocytes. Tropism modification to elevate efficiency and/or selectivity to individual cell types would enhance the scope of AAV for disease therapies. The vascular endothelium is implicitly important in cardiovascular diseases and cancer, but is relatively poorly transduced by AAV vectors. We therefore genetically incorporated the peptide SIGYPLP, which targets endothelial cells (EC), into position I-587 of AAV capsids. SIGYPLP-modified AAV (AAVsig) showed enhanced transduction of human EC compared with AAV with a wild-type capsid (AAVwt), a phenotype independent of heparan sulphate proteoglycan (HSPG) binding. In contrast, AAVsig did not enhance transduction of primary human vascular smooth muscle cells or human hepatocytes, principal targets for AAV vectors in local or systemic gene delivery applications, respectively. Furthermore, infection of EC in the presence of bafilomycin A(2) indicated that intracellular trafficking of AAV particles was altered by targeting AAV by means of SIGYPLP. AAV vectors with enhanced tropism for EC will be useful for diverse gene therapeutics targeted at the vasculature.